

# Functional Analysis of the D- and E- subunits of photosystem I in *Arabidopsis thaliana*

Inaugural - Dissertation  
zur  
Erlangung des Doktorgrades  
der Mathematisch-Naturwissenschaftlichen Fakultät  
der Universität zu Köln

vorgelegt von

**Anna Ihnatowicz**

aus Danzig, Polen  
Köln  
2005

Die vorliegende Arbeit wurde am Max-Planck-Institut für Züchtungsforschung, Köln-Vogelsang, in der Abteilung Pflanzenzüchtung und Ertragsphysiologie (Prof. Dr. F. Salamini) in der Arbeitsgruppe von PD Dr. D. Leister angefertigt.

Berichterstatter: Prof. Dr. Francesco Salamini  
Prof. Dr. Ulf-Ingo Flügge

Tag der mündlichen Prüfung: 11. 07. 2005

## ABBREVIATIONS

<b><i>A. thaliana</i></b>	<i>Arabidopsis thaliana</i>
<b>ATP</b>	Adenosine triphosphate
<b>bp</b>	basepair(s)
<b>BLAST</b>	basic local alignment search tool
<b>cDNA</b>	complementary deoxyribonucleic acid
<b>Chl</b>	chlorophyll
<b>Ci</b>	curie
<b>Col-0</b>	Columbia 0
<b>cTP</b>	chloroplast transit peptide
<b>d</b>	day
<b>DNA</b>	deoxyribonucleic acid
<b>dNTP</b>	deoxynucleotide triphosphate
<b>dSpm</b>	defective <i>Suppressor-mutator</i>
<b>F</b>	fluorescence
<b>h</b>	hour
<b>hcf</b>	high chlorophyll fluorescence
<b>LHCI</b>	light harvesting complex I
<b>LHCII</b>	light harvesting complex II
<b>MALDI-TOF</b>	matrix-assisted laser desorption ionization-time of flight
<b>M</b>	molarity
<b>min</b>	minute
<b>mol</b>	mole
<b>mRNA</b>	messenger ribonucleic acid
<b>MS</b>	mass spectrometry
<b>NADP(H/+)</b>	nicotinamide adenine dinucleotide phosphate (reduced/oxidised)
<b>°C</b>	degree Celsius
<b>PAGE</b>	polyacrylamide gel electrophoresis
<b>pam</b>	photosynthesis affected mutant
<b>PAM</b>	pulse amplitude modulation
<b>PCR</b>	polymerase chain reaction
<b>PFD</b>	photon flux density
<b>PSI</b>	photosystem I
<b>PSII</b>	photosystem II
<b>qT</b>	state transition quenching
<b>RNA</b>	ribonucleic acid
<b>RT-PCR</b>	reverse transcription-polymerase chain reaction
<b>rpm</b>	rounds per minute
<b>s</b>	second
<b>SDS</b>	sodium dodecyl sulphate
<b>w/v</b>	weight per volume
<b>WT</b>	wild-type

---

## **CONTENTS**

<b>1. <u>INTRODUCTION</u></b>	<b>1</b>
1.1 Composition of thylakoid membranes	2
1.2 Structure and function of photosystem I	5
1.3 Overview of electron transport	7
1.4 Chlorophyll fluorescence parameters	8
1.5 Redox-controlled thylakoid protein phosphorylation	11
1.6 Functional genomics	14
Forward Genetics	15
Reverse Genetics	16
<b><u>AIM OF THE THESIS</u></b>	<b>17</b>
<b>2. <u>MATERIALS AND METHODS</u></b>	<b>18</b>
2.1 Plant propagation and growth measurement	18
2.2 Automatic screening for photosynthetic mutants of <i>A. thaliana</i>	18
2.3 Isolation of <i>dSpm</i> insertion-flanking sequences	19
2.4 Isolation of T-DNA insertion mutants	19
2.5 Sequence analysis	20
2.6 Analysis of nucleic acids	21
2.6.1 Nucleic acids preparation	21
2.6.2 cDNA single strand synthesis	21
2.6.3 Reverse-transcription PCR (RT-PCR)	21
2.6.4 Northern analysis	21
2.7 Complementation of <i>Arabidopsis</i> mutants	22
2.7.1 Complementation of the <i>psad1-1</i> mutant	22

---

2.7.2 <i>Agrobacterium</i> strain	24
2.7.3 <i>Agrobacterium</i> -mediated transformation	24
2.7.4 Selection of transformed plants	24
2.8 Biochemical Analysis	25
2.8.1 Total protein isolation	25
2.8.2 Preparation of thylakoid membranes	25
2.8.3 Native and 2D PAGE	25
2.8.4 Immunoblot analysis	26
2.8.5 PSI complex isolation	26
2.8.6 Phosphorylation analysis	26
<i>In vivo</i> phosphorylation	26
Detection of phosphoproteins in polyacrylamide gels	27
2.9 Mass spectrometry	27
LC-ESI MS/MS	27
Protein Identification	28
2.10 Chlorophyll fluorescence measurements	28
2.11 Pigment analysis	29
2.12 Expression profiling	29
<b>3. <u>CHARACTERIZATION OF PSI-D MUTANTS</u></b>	<b>31</b>
<b>RESULTS</b>	<b>31</b>
3.1 Identification and phenotype of PSI-D mutants	31
3.2 Expression of <i>PsaD</i> in wild-type, single and double mutant plants	35
3.3 Increased dosage of the <i>PsaD2</i> gene can complement the <i>psad1-1</i> mutation	37
3.4 PSI composition, accumulation of other thylakoid proteins and leaf pigments	39
3.5 Photosynthetic electron flow	46
3.6 Expression of mRNAs for nucleus-encoded chloroplast proteins in <i>psad1-1</i>	48
<b>DISCUSSION</b>	<b>50</b>

---

<b>4. <u>FUNCTIONAL ANALYSIS OF PSI-D1 PHOSPHORYLATION</u></b>	<b>53</b>
<b>RESULTS</b>	<b>53</b>
4.1 Detection of PSI-D1 phosphorylation by mass spectrometry	53
4.2 Complementation of <i>psad1-1</i> mutant plants with the mutated <i>PsaD1</i> gene	55
<b>DISCUSSION</b>	<b>60</b>
<b>5. <u>EFFECTS OF <i>psad1-1</i> AND <i>psae1-3</i> MUTATIONS ON THE LEVEL OF THYLAKOID PROTEIN PHOSPHORYLATION</u></b>	<b>63</b>
<b>RESULTS</b>	<b>63</b>
5.1 The level of thylakoid protein phosphorylation is significantly higher in <i>psad1-1</i> and <i>psae1-3</i> mutants	63
5.2 Identification of Lhca4 phosphorylation	65
<b>DISCUSSION</b>	<b>72</b>
<b>6. <u>FUNCTIONAL ANALYSIS OF PSI-E</u></b>	<b>77</b>
<b>RESULTS</b>	<b>77</b>
6.1 Generation of <i>psae1-3 psae2-1</i> double mutant	77
6.2 Growth of the <i>psae1-3 psae2-1</i> double mutant is significantly reduced	79
6.3 Accumulation of both <i>PsaE</i> transcripts is completely suppressed in <i>psae1-3 psae2-1</i> double mutant	81
6.4 PSI-E does not accumulate in <i>psae1-3 psae2-1</i> double mutant	82
<b>DISCUSSION</b>	<b>83</b>

<b>Summary</b>	86
<b>Zusammenfassung</b>	88
<b>References</b>	90
<b>Appendix</b>	105
<b>Erklärung</b>	105
<b>Lebenslauf</b>	106
<b>Acknowledgements</b>	107

## **1. INTRODUCTION**

Life on earth depends on photosynthesis. This is the process, by which light energy is captured and subsequently converted to chemical energy. Oxygenic photosynthesis is carried out by plants and some algae as well as by cyanobacteria and their relatives. In plants and algae the photosynthetic processes are performed in a specialized organelle called chloroplast. It is commonly accepted that chloroplasts originated from an ancestral cyanobacterium living in symbiosis with a primitive eukaryotic cells (Douglas, 1998). In addition to photosynthesis chloroplasts also carry out other functions such as the synthesis of amino acids, fatty acids and lipids, plant hormones, nucleotides, vitamins and secondary metabolites. Moreover, chloroplasts are involved in the assimilation of nitrogen and sulphur as well as hosting the transcriptional and translational machinery necessary for the expression of their own genome (Pesaresi *et al.*, 2001). It can be estimated that about 10 percent of genes in plants are involved in photosynthesis (Scheller *et al.*, 2004). Many of these genes have originated from cyanobacteria, but plants have also recruited a number of additional proteins for chloroplast functions (Abdallah *et al.*, 2000).



## 1.1 Composition of thylakoid membranes

The primary reactions of the oxygen-evolving photosynthesis are performed by four large protein complexes: photosystem I (PSI), photosystem II (PSII), ATPase and cytochrome  $b_6/f$  (Figure 1.1).

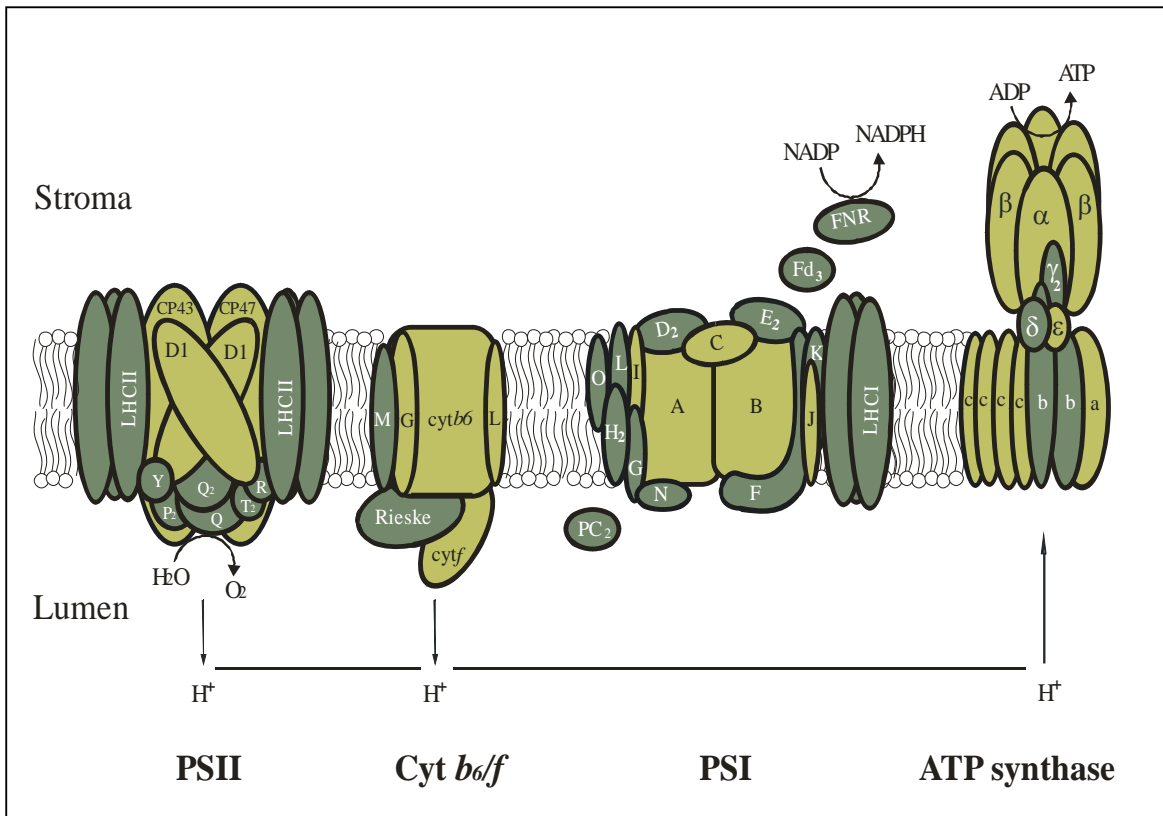
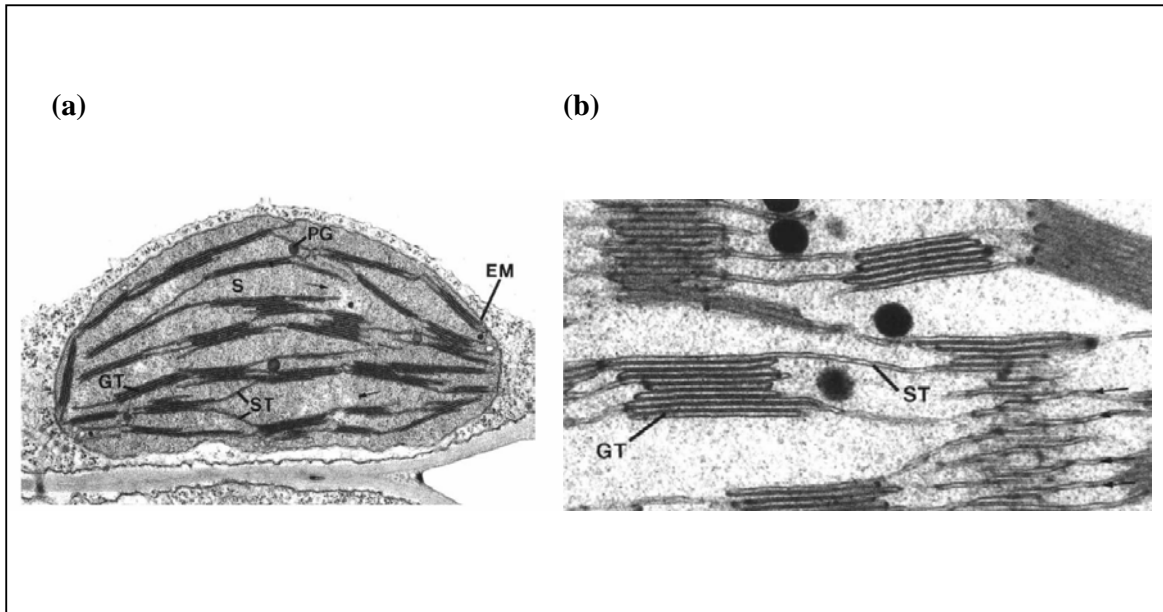


**Figure 1.1**

Composition of the thylakoid membrane complexes: Photosystem II (PSII), cytochrome  $b_6/f$  (Cyt  $b_6/f$ ), Photosystem I (PSI), ATP Synthase complex and the soluble electron carriers (plastocyanin, PC; ferredoxin, Fd) involved in the light-driven production of ATP and NADPH. The formation of a proton ( $H^+$ ) gradient is also shown. Nuclear-encoded subunits are indicated in dark-green, while subunits encoded by plastome are indicated in light-green color.

In plants and some green algae, these complexes are integrated into the thylakoid membrane of the chloroplast. The thylakoid membranes are structurally inhomogeneous. They consist of two main domains: the grana, which are stacks of thylakoids, and the stroma lamellae, which are unstacked thylakoids and connect the grana stacks (Dekker and Boekema, 2005) (Figure 1.2).

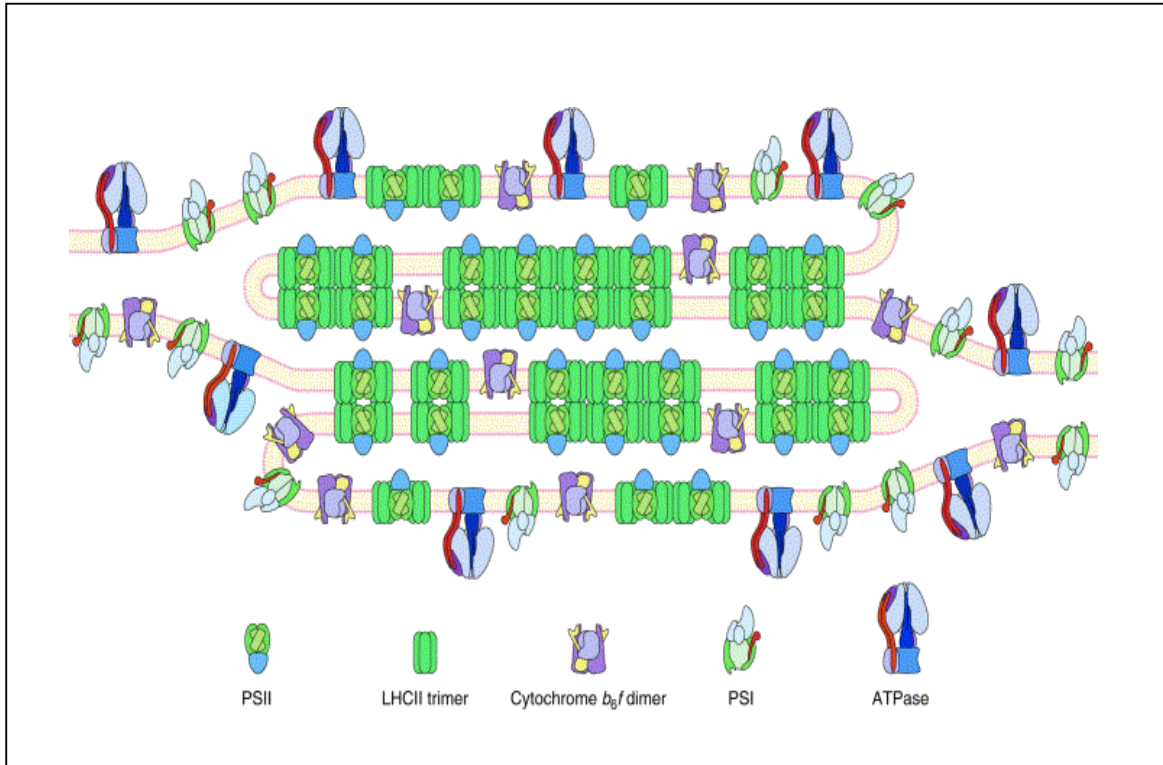


Reproduced from Staehelin and Arntzen (1986)

**Figure 1.2**

(a) Ultrastructure of young tobacco chloroplast. Two envelope membranes (EM) surround the chloroplast stroma (S), where the stacks of thylakoids (grana) (GT) and the stroma lamellae (ST), can be recognized. (PG) plastoglobuli are also indicated. (b) Grana (GT) and the stroma lamellae (ST) of a spinach thylakoid membranes.

The two domains differ in protein composition and biochemical properties (Albertson, 1995). The grana are enriched in photosystem II (PSII) (Figure 1.3), which uses light energy to drive two chemical reactions - the oxidation of water and the reduction of plastoquinone. The photosystem II complex is composed of more than 25 structurally and functionally distinct subunits organized hierarchically (Hankamer *et al.*, 1997 and 1998). Most of the PSII subunits are encoded in the chloroplast genome, including the core D1/D2 heterodimer, the chlorophyll-containing CP43 and CP47 proteins, as well as Cyt  $b_{559}$ . PSII is closely associated with six chlorophyll a/b binding proteins which form the light harvesting antenna of PSII (Lhcb1-6) and are encoded by the nuclear *CAB* genes (Jansson, 1994 and 1999). The major light-harvesting complex II (LHCII) is trimeric and consists of the Lhcb1-3 proteins containing chlorophyll a/b and carotenoids. The minor Lhcb proteins, Lhcb4 (CP29), Lhcb5 (CP26), and Lhcb6 (CP24) are monomeric and also contain chlorophyll a/b and carotenoids. Their function is transfer of excitation energy from LHCII trimers to the PSII core complex (Yakushevskaya *et al.*, 2001).



Reproduced from Trends Plant Sci. 6, 317-26 (2001)

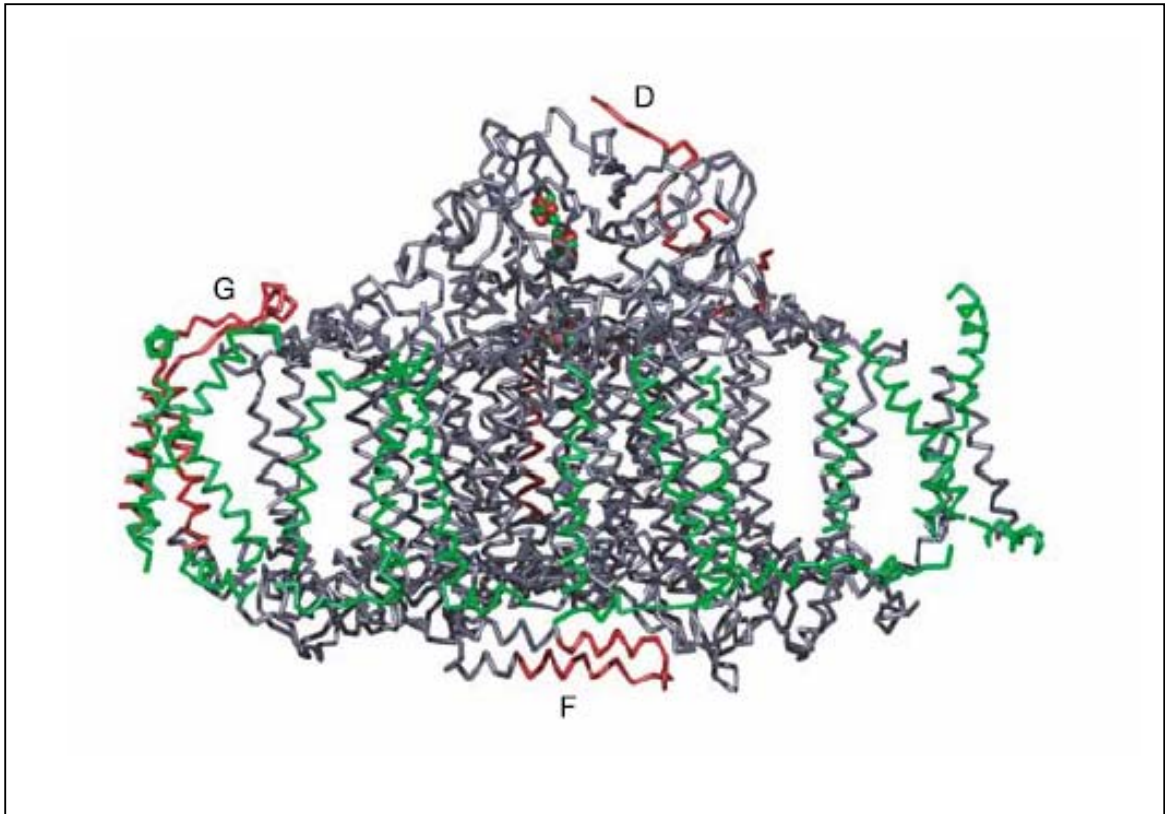
**Figure 1.3**

The topography of thylakoid stacks and heterogeneity in the distribution of photosynthetic complexes. LHCII-rich regions of thylakoid are tightly appressed, forming grana. The lateral separation of PSI and PSII arises from the interaction of PSII with the membrane-'adhesive' antenna complex, LHCII. The *cyt b<sub>6</sub>/f* complex is present in all parts of the thylakoid membrane (Allen and Forsberg, 2001).

Protein complexes which contain extended, stromal-phase projections into the aqueous phase are excluded from the interior of grana stacks: these are photosystem I (PSI) and ATPase (Allen and Forsberg, 2001) (Figure 1.3). The composition of plant PSI is described more in details in Chapter 1.2. Most components of the chloroplast ATP synthase (cpATPase) are plastome-encoded, in *Arabidopsis*, only subunits *b'*,  $\delta$ , and  $\gamma$  are encoded by nuclear genes (Maiwald *et al.*, 2003). ATP synthase produces ATP from adenosine diphosphate (ADP) and inorganic phosphate using energy from a transmembrane proton-motive force. Location of PSI and ATPase in the stroma lamellae and the surface exposed grana membranes allows NADPH and ATP to be immediately released into the stroma. Cytochrome *b<sub>6</sub>/f* complex (*cyt b<sub>6</sub>/f*) is mediating electron transport between the two photosystems by transferring electrons from plastoquinol to plastocyanin. In *Arabidopsis*, *cyt b<sub>6</sub>/f* contains at least eight subunits, of which six are plastome-encoded.

## 1.2 Structure and function of photosystem I

Photosystem I (PSI) catalyzes the light-induced transfer of electrons from plastocyanin on the luminal side to ferredoxin (Fd) on the stromal side. The further electron transfer from Fd to  $\text{NADP}^+$ , generating NADPH, is catalysed by the Fd:  $\text{NADP}^+$ -oxidoreductase (Haldrup *et al.*, 2003). The PSI complexes of cyanobacteria and plants are functionally and structurally similar. The crystal structures of cyanobacterial (Jordan *et al.*, 2001) and plant PSI (Ben-Shem *et al.*, 2003) (Figure 1.4) have recently been established. Plant PSI is slightly larger than its cyanobacterial pendant (Kitmitto *et al.*, 1997), and trimer formation has been observed only in cyanobacteria (Chitnis and Chitnis, 1993).



Reproduced from Nature 426, 630-5 (2003)

**Figure 1.4**

The structural model of plant PSI at 4.4 Å. A view from the LHCI side. Subunits F, G and D are indicated. The helix-loop-helix N-terminal domain of subunit F and the N terminus of subunit D unique to plant photosystem I are coloured red (Ben-Shem *et al.*, 2003).

Eukaryotic PSI is composed of a core complex and a light-harvesting complex (LHC). The light-harvesting complex I (LHCI) in plants is composed of four different subunits denoted Lhca1 to Lhca4 (Jansson, 1999). However, in the sequenced genome of *Arabidopsis thaliana* there are additional open reading frames coding for two more LHC type proteins (Lhca5-6) that are presumably associated with PSI (Ganeteg *et al.*, 2004).

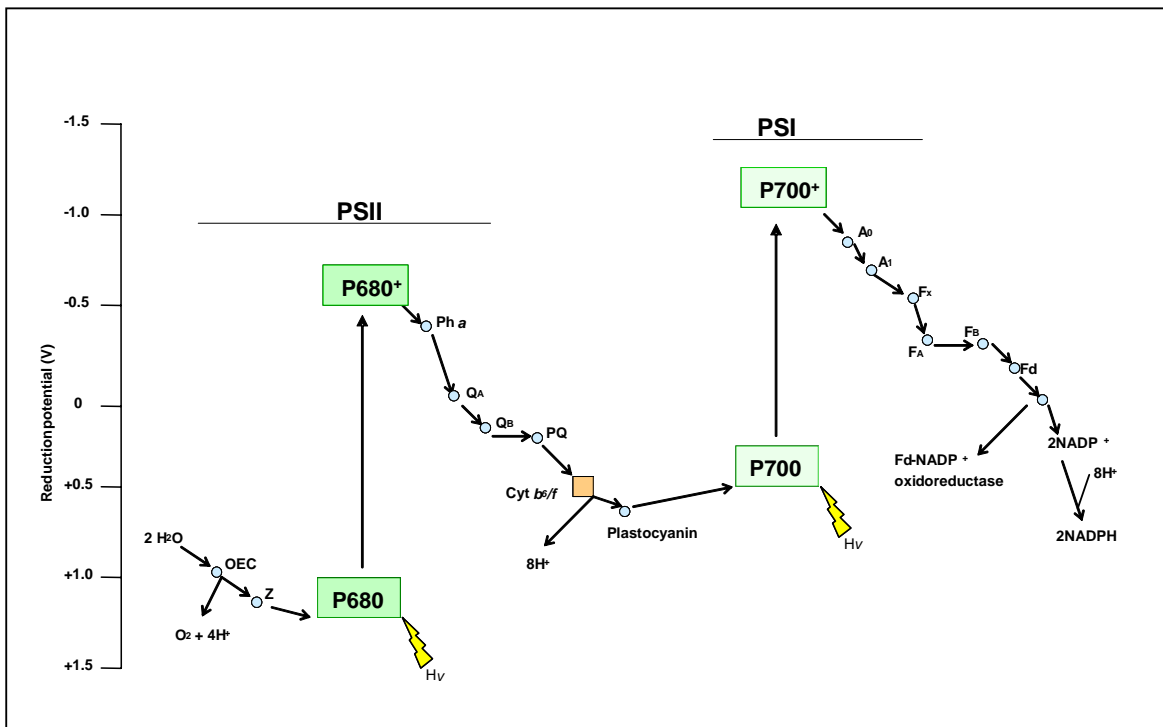
In plants, the PSI core complex is formed by 14 different subunits denoted PSI-A to -L and PSI-N to -O (Knoetzel *et al.*, 2002; Scheller *et al.*, 2001). Four of them (G, H, N and O) have no counterpart in cyanobacteria. In flowering plants, no homologue of the cyanobacterial PSI-M has yet been discovered. The three subunits PSI-A, -B and -C, which bind the electron acceptors, are crucial for PSI function. In *Arabidopsis*, these proteins together with PSI-I and -J are encoded by plastid DNA, whereas all other subunits are encoded by the nuclear genome.

The stromal ridge of PSI, on which emphasis was put in this thesis, is composed of the PSI-D, -E and -F subunits. As it was shown by Varotto *et al.* (2000) *Arabidopsis* plants lacking one of the two *PsaE* genes show a general decrease in the polypeptide level of the whole stromal ridge of PSI, a marked increase in light sensitivity and photoinhibition, as well as significant reduction in size. Cyanobacterial mutants lacking PSI-E are deficient in ferredoxin-mediated NADP<sup>+</sup> photoreduction but interestingly they do not differ from wild type when grown under normal photoautotrophic conditions (Chitnis *et al.*, 1989). The growth rate of cyanobacterial mutants lacking PSI-E is reduced as compared to wild type strain only when grown under low-light or low-CO<sub>2</sub> conditions (Zhao *et al.*, 1993). In contrast, the growth of cyanobacterial mutants lacking PSI-D is significantly affected (Xu *et al.*, 1994). In *Arabidopsis*, both PSI-E and PSI-D subunits together with PSI-H are encoded by two functional genes. Interestingly, there are three subunits in the PSI complex PSI-D, -E and -F, which contain the N-terminal extensions specific only for eukaryotes (Figure 1.4).

Downregulation of individual PSI subunits by antisense or co-suppression strategies together combined with the identification of insertion mutants, have provided the basis for the functional analysis of almost all nucleus-encoded PSI polypeptides (Haldrup *et al.*, 1999 and 2000; Jensen *et al.*, 2000 and 2002; Lunde *et al.*, 2000; Naver *et al.*, 1999; Varotto *et al.*, 2000a and 2002b).

### 1.3 Overview of electron transport

In higher plants, photosynthesis is driven by light-induced electron transfer from the water-oxidising photosystem II (PSII) to the ferredoxin-reducing photosystem I (PSI). Light energy utilized in the primary reactions of the oxygen-evolving photosynthesis is absorbed by a number of different chlorophyll-containing proteins. Most of the light energy is absorbed by the light harvesting complexes (LHC), which contain the majority of the chlorophylls. The antenna pigments transfer excitation energy to the reaction centers that are special chlorophyll cofactors, at which a photochemical reaction traps the energy (Heathcote *et al.*, 2002). The resulting electrons are transferred through a series of redox reactions to acceptors at progressively lower electrochemical potential (Figure 1.5).



Based on Horton (2003)

**Figure 1.5**

Z-scheme, showing the reduction potentials and electron flow during photosynthesis. Z, electron donor to P680; Ph<sub>a</sub>, pheophytin a, electron acceptor of P680; Q<sub>A</sub>, plastoquinone tightly bound to PSII; Q<sub>B</sub>, pool made up of PQ and PQH<sub>2</sub>; A<sub>0</sub>, chlorophyll a, the primary electron acceptor of PSI; A<sub>1</sub>, phylloquinone; F<sub>x</sub>, F<sub>B</sub> and F<sub>A</sub>, iron sulfur clusters; F<sub>d</sub>, soluble ferredoxin; Fd-NADP<sup>+</sup>, ferredoxin-NADP<sup>+</sup> oxidoreductase; NADP<sup>+</sup>, oxidised nicotinamide adenine dinucleotide phosphate.

In the PSII reaction centre, electrons are transferred from the photo-excited primary electron donor, chlorophyll P680, to the electron-stabilizing acceptor, plastoquinone  $Q_A$  via a rapid oxidoreduction of a phaeophytin molecule. Plastoquinone (PQ) is a small molecule, which functions as a mobile electron carrier within the hydrophobic core of the thylakoid membrane. The electron of  $Q_A$  is then transferred to a further plastoquinone molecule named  $Q_B$ . The reduction of plastoquinone by PSII requires two electrons and two protons creating  $PQH_2$ . The reduced plastoquinone molecule transfers the electrons to the cytochrome  $b_6/f$  complex, which is a membrane-bound protein complex containing four electron carriers. It is made up of 6 polypeptides which do not bind any chlorophyll. In this complex, electrons are then passed to plastocyanin, a small copper-containing protein. The photo-oxidized  $P680^+$  species is re-reduced by an electron coming from the oxidized molecules of water in a reaction that as a by-product sets free molecular oxygen (Durrant *et al.*, 1995).

In the PS I reaction center the absorbed photon induces charge separation of the primary donor of PSI, P700, and the primary chlorophyll A acceptor defined as  $A_0$  (Rutherford and Heathcote, 1985). Each electron is then transported by a series of secondary electron acceptors (the phylloquinone molecule named  $A_1$  and the (4Fe-4S) center named  $A_2$ ) to the stromal surface, where soluble ferredoxin (an Fe-S protein) transfers the electron to FAD and finally to  $NADP^+$ . The oxidised PSI reaction center ( $P700^+$ ) is subsequently re-reduced by plastocyanin (Gross, 1993). As a net result of the light reaction molecules of NADPH and ATP are synthesized, which subsequently provide the energy for the dark reactions of photosynthesis, known as the Calvin cycle.

## 1.4 Chlorophyll fluorescence parameters

The measurement of chlorophyll fluorescence kinetics provides an important and useful tool, as to gain information on the organization and function of the photosynthetic apparatus. Light energy absorbed by chlorophyll molecules in a leaf can be lost by a number of different mechanisms. First of all, it can drive photosynthesis (photochemistry) and excess energy can be

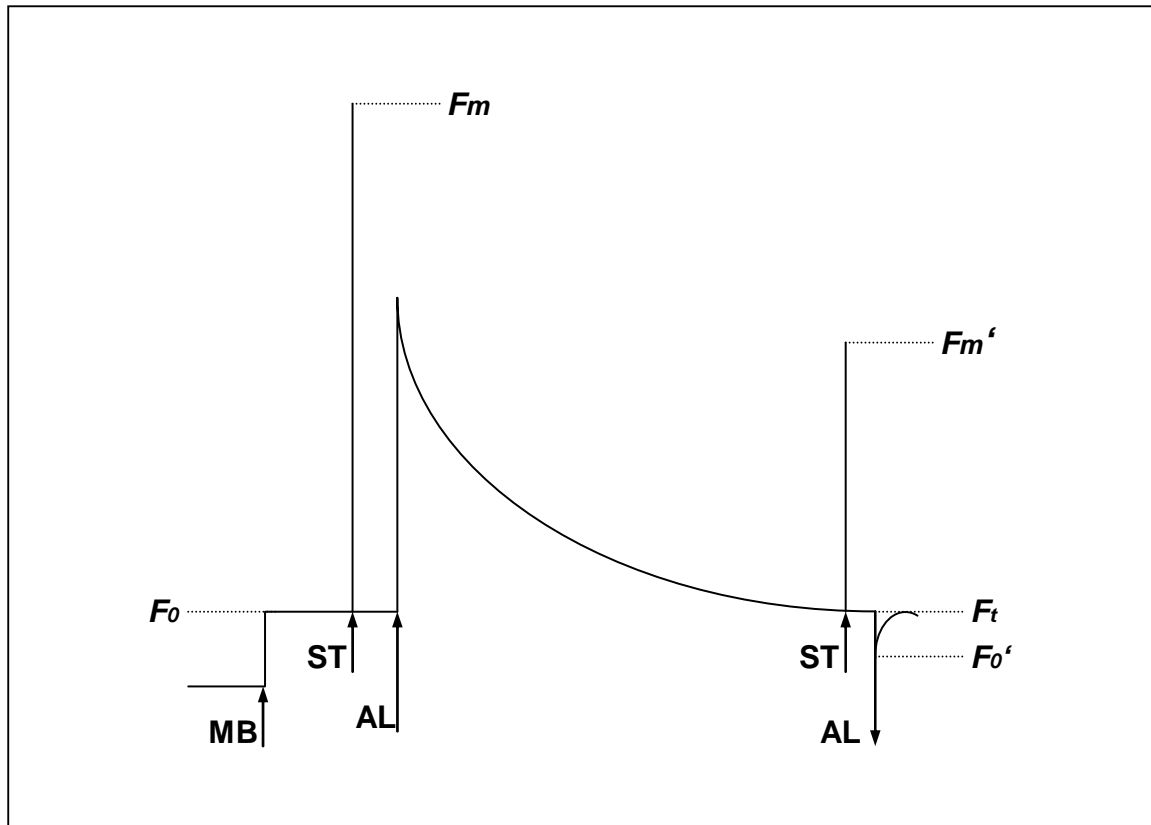
dissipated as heat or it can be re-emitted as light-chlorophyll fluorescence. All these processes occur in competition, in a way that any increase in the efficiency of one will result in a decrease in the yield of the other two (Maxwell and Johnson, 2000). Generally, fluorescence yield is highest when photochemistry and heat dissipation are lowest. But under normal conditions, dissipation as heat represents only a minor contribution to chlorophyll de-excitation. Therefore, changes in the fluorescence yield reflect mainly changes in photochemical efficiency.

The spectrum of fluorescence is different than the spectrum of absorbed light. Therefore, fluorescence yield can be quantified by exposing leaves to light of a defined wavelength and measuring the amount of light re-emitted at longer wavelengths than that of the absorbed light. To quantify chlorophyll fluorescence, the Pulse Amplitude Modulation (PAM) fluorometer system has been developed (Schreiber *et al.*, 1986). In this system, the measuring light is modulated (high frequency pulses of light) and the detector is tuned in a way that it detects fluorescence excited only by the measuring light.

If the plant is dark-adapted, all functionally competent PSII reaction centers are able to trap excitation energy; the reaction centers are in their open state. Under these conditions, the energy is transferred from the antennae system to the reaction centers and the fluorescence emission is quenched due to the photochemical reactions. This process is called photochemical quenching (qP).

The measurement of chlorophyll fluorescence is started by switching on the measuring light and the minimal level of fluorescence ( $F_0$ ) is measured. This light ( $\uparrow$ MB, Figure 1.5) is sufficiently weak not to drive photosynthetic electron transport. A saturating flash of light is then applied ( $\uparrow$ ST) which allows measuring the maximum fluorescence level in the dark-adapted state ( $F_m$ ). After that the actinic light ( $\uparrow$ AL) is switch on in order to drive photosynthesis, and at appropriate intervals, further saturating flashes are applied. Values for the fluorescence maximum in the light ( $F_m'$ ) can be measured. The level of fluorescence which is measured immediately before the next saturating flash is ( $F_t$ ). At the end of the measurement turning off the actinic light ( $\uparrow$ AL) allows to measure the minimal fluorescence level ( $F_0'$ ) in the presence of far-red light.



**Figure 1.6**

Fluorescence parameters measured by the Pulse Amplitude Modulation fluorometer system (PAM).  $\uparrow$ MB: measuring light;  $\uparrow$ ST: saturating flash of light;  $\uparrow$ AL: actinic light. Fluorescence levels and parameters are defined more in details in Table 1, Table 2 and in the text.

**Table 1.1**

Fluorescence levels	
$F_0$	the minimal fluorescence level of a dark-adapted leaf
$F_m$	the maximum fluorescence level of a dark-adapted leaf
$F_m'$	the maximum fluorescence level of a light-adapted leaf
$F_t$	the transient fluorescence of light-adapted leaf
$F_0'$	the minimal fluorescence level in the presence of far-red light

Table 1.2

Commonly used fluorescence parameters		
$\Phi_{II}$	Quantum yield of PSII	$(F_m' - F_0')/F_m'$
<b>qP</b>	Photochemical quenching	$(F_m' - F_t)/(F_m' - F_0')$
$F_v/F_m$	Maximum quantum yield of PSII	$(F_m - F_0)/F_m$
<b>qN</b>	Non-photochemical quenching	$1 - (F_m' - F_0')/(F_m - F_0)$

Photochemical quenching parameters always relate to the relative value of  $F_m'$  and  $F_t$  (Maxwell and Johnson, 2000). One of the most useful parameter in plant physiology research is  $\Phi_{II}$ . This parameter is the quantum yield of PSII that measures the efficiency of PSII and represent the fraction of photons used to perform photochemistry. Therefore, it can be used in the research as an indicator of the photosynthetic efficiency.

### 1.5 Redox-controlled thylakoid protein phosphorylation

The thylakoid membranes contain several polypeptides that are reversibly phosphorylated. Chloroplast phosphoproteins were first found in thylakoid membranes by Bennett (1977, 1980). Later, presence of protein phosphorylation was also identified in the soluble stroma (Foyer, 1985), in the lumen between the inner and outer envelopes of chloroplast (Soll and Bennett, 1988), in the envelope membranes (Sveshnikova *et al.*, 2000) and recently in soluble plastid proteins (Carlberg *et al.*, 2003).

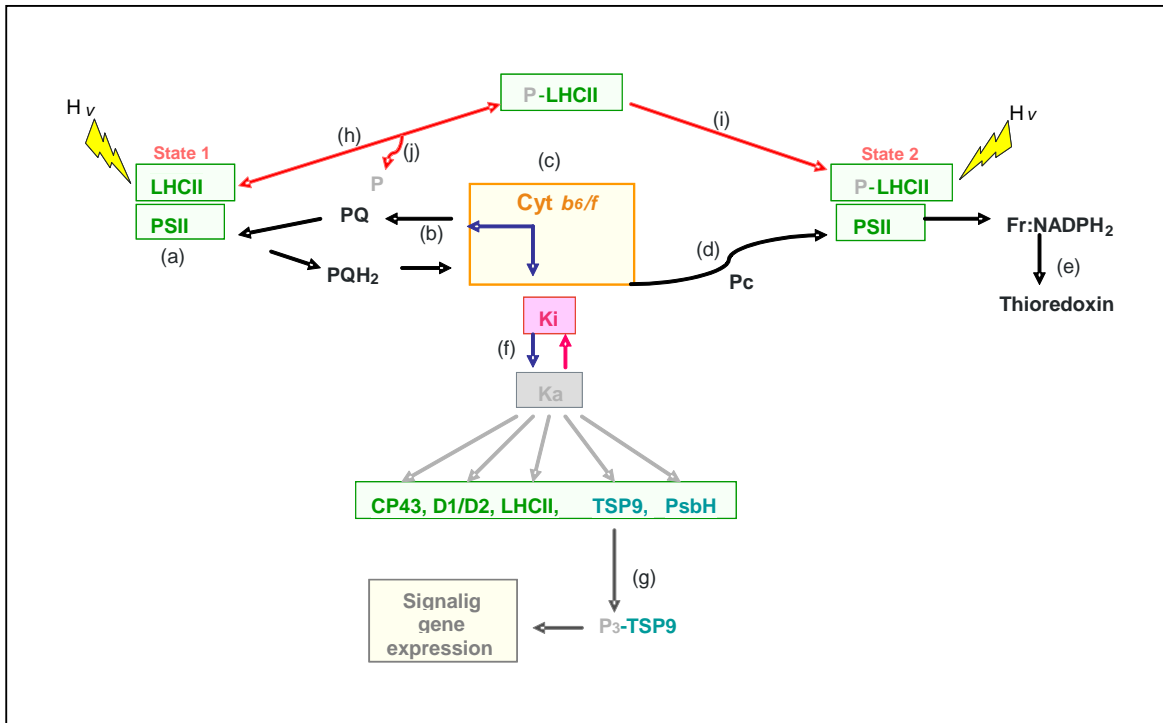
Phosphorylation of thylakoid membrane proteins is caused by a unique light-induced and redox-controlled system (Allen and Bennett, 1981). This redox-dependent thylakoid protein

phosphorylation regulates both short- and long-term acclimation of the photosynthetic apparatus to changes in environmental conditions.

On the one hand, plants have to acclimate to long-term light changes by altering the ratio of PSII to PSI. The reducing power produced by photosynthetic electron transfer controls the translation of main chloroplast-encoded proteins (Danon and Mayfield, 1994). On the other hand, short-term changes in light intensity create an imbalance between the excitation and electron flow of PSI and PSII. This imbalance results in rapid changes in the redox state of the plastoquinone pool and as a consequence the photosynthetic apparatus might be damaged. Reduced PQ promotes back electron flow to PSII resulting in the generation of the harmful singlet oxygen and causing photo-inactivation and degradation of its D1 core protein (Rutherford and Faller, 2001). Oxygen-evolving organisms have overcome this problem by a short-term response called state transition. This mechanism allows plants to balance the distribution of absorbed light energy between the two photosystems by moving a mobile pool of light harvesting complex from photosystem II (PSII) to photosystem I (PSI) (Haldrup *et al.*, 2001). LHCII is phosphorylated by thylakoid-bound protein kinase(s) (Bennett, 1991; Depege, 2003; Bellafiore, 2005) and in its phosphorylated form dissociates from PSII, migrates towards the stroma membranes and then finally associates with PSI. After dephosphorylation LHCII returns to PSII.

Several studies have been performed in order to identify the redox sensor regulating protein phosphorylation in the thylakoid membranes. It was shown that light regulates thylakoid protein phosphorylation in at least three different ways. Firstly, several studies which have been conducted on the redox-controlled protein phosphorylation of PSII and LHCII proposed that plastoquinone functions as a key regulator of thylakoid protein kinase(s) (Bennett, 1991; Allen, 1992). These studies demonstrated that the membrane protein kinases are activated upon reduction of the plastoquinol and its binding to the quinol-oxidation site of a cytochrome *b<sub>6</sub>/f* complex, which serves as a redox sensor (Vener *et al.*, 1995 and 1997) (Figure 1.7). Secondly, also the thiol disulfide redox state has been shown to influence strongly phosphorylation of the thylakoid protein, via the chloroplast ferredoxin-thioredoxin system (Carlberg *et al.*, 1999; Rintamäki *et al.*, 2000). Thirdly, regulation of thylakoid protein phosphorylation occurs at the substrate level. The light-induced conformational changes in the chlorophyll-binding membrane proteins expose their respective sites for phosphorylation as it was shown by Zer

*et al.* (1999, 2003). Up to now all of the phosphopeptides in thylakoid membranes were shown to be involved either in the regulation of the light energy distribution between the two photosystems or in the light-induced turnover of PSII reaction center subunits (Figure 1.7).



Based on Trends Biochem Sci. 28, 467-70 (2003)

**Figure 1.7**

Redox control of kinase(s) activation, thylakoid protein phosphorylation, state transition and signaling gene expression. **(a)** In state 1 LHCII bound to photosystem II. **(b)** Kinase activation is related to the plastoquinol (PQH<sub>2</sub>): plastoquinone (PQ) ratio. **(c)** The dimeric cytochrome *b<sub>6</sub>/f* complex. Blue arrows indicate protein kinase activation [inactivated form (Ki) to activated form (Ka)] via conformational changes of the complex during PQH<sub>2</sub> oxidation. **(d)** Plastocyanin (Pc) is reduced by cytochrome *b<sub>6</sub>/f* and is oxidized by photosystem I (PSI). PSI reduces ferredoxin (Fr). **(e)** Thioredoxins reduced by electron flow from PSI. **(f)** Activated protein kinase(s) (Ka) phosphorylate (light-gray arrows) thylakoid-bound proteins: chlorophyll-protein complexes (green) and membrane-bound or extrinsic proteins (cyan). Ka reverts back to Ki. **(g)** Thylakoid-bound protein TSP9 is released from the thylakoid membrane when its three threonine sites are phosphorylated (P<sub>3</sub>-TSP9) and might signal for gene expression. **(h)** Dissociation of phosphorylated LHCII (P-LHCII) from PSII. **(i)** P-LHCII binds to PSI (state 2). **(j)** Dephosphorylation of P-LHCII and release of inorganic phosphate (P) allows return and binding of LHCII to PSII (state 1). Red arrows indicate the state-transition process. Black arrows indicate electron flow (Zer and Ohad, 2003).

Recently, protein phosphorylation was found in PSI for the first time. The phosphorylation site identified *in vivo* in thylakoid membranes of *Arabidopsis thaliana* by mass spectrometry, is localized to the first threonine in the N-terminus of PSI-D1 protein (Hansson and Vener, 2003).

In the same study two other phosphorylation sites were identified: one in the acetylated N-terminus of the minor chlorophyll *a*-binding protein CP29 and a second, previously uncharacterized, nuclear encoded protein, named thylakoid membrane phosphoprotein of 14 kDa (TMP14). These results extend involvement of the protein phosphorylation in thylakoid membranes beyond the photosystem II and LHCII and open a new direction in studies of possible PSI regulation by the redox-controlled protein phosphorylation (Hansson and Vener, 2003).

## 1.6 Functional genomics

The commonly used term ‘functional genomics’ represents a new phase of genome analysis, in which the fundamental strategy is to expand the scope of biological investigation from studying single genes or proteins to studying all genes or proteins at once in a systematic fashion (Hieter and Boguski, 1997). It involves several modern, high throughput and large-scale techniques combined with statistical and computational analysis of the results.

There is the whole range of current strategies which can be used and which cover the fields of genomics, transcriptomics and proteomics (Figure 1.8). The most important procedures are: forward genetics, reverse genetics, microarray-based measurements of gene expression, two-dimensional electrophoresis of proteins, mass spectrometry and bioinformatics (Richmond and Somerville, 2000; Somerville and Somerville, 1999).

The small mustard species *Arabidopsis thaliana* was the first plant to be completely sequenced (Arabidopsis Genome Initiative, 2000). *Arabidopsis thaliana* has been adopted as a model organism in the study of plant biology because of many advantages like: small size, short generation time, and high efficiency of transformation (Meinke *et al.*, 1998). It was also chosen for sequencing, because it has a highly compact genome of about 130 Mb with little interspersed repetitive DNA. It is closely related to many food plants such as canola, cabbage, cauliflower, broccoli, turnip, rutabaga, kale, Brussels sprouts, kohlrabi, and radish (Somerville and Somerville, 1999). With continued progress in the area of genomics, new molecular technologies, and database management, the model plant *Arabidopsis thaliana* is becoming an

important tool for the comparison of conserved processes in eukaryotes and the identification of plant specific genes, which might be important for crop improvement.

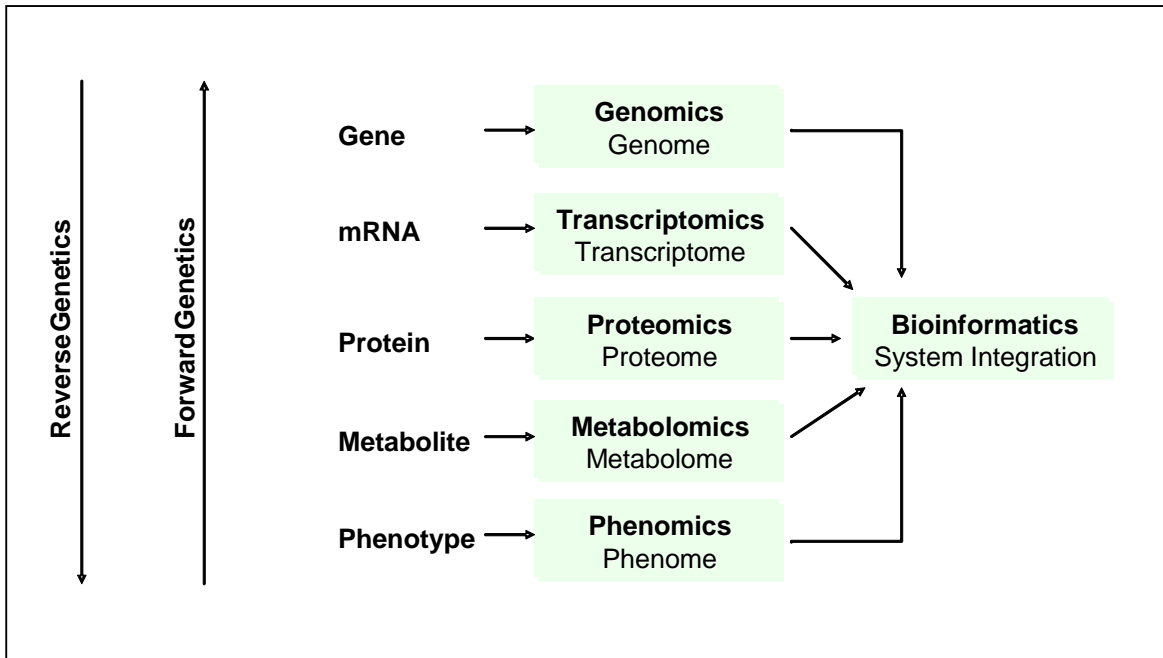


**Figure 1.8**

Overview of methods and steps involved in functional genomics analysis. Methods for forward and reverse genetics, which link phenotypes with genes, or vice versa, are also indicated.

There are several collections of mutagenised *Arabidopsis* populations, which are available through public stock centers. The isolation of *Arabidopsis* mutants via forward and reverse genetics linking phenotypes with genes, and vice versa (Figure 1.8), has become the common strategy to investigate the biological processes in higher plants.

### Forward Genetics

The functional analysis of photosynthesis can be carried out by isolating mutants with alteration in photosynthetic performance. Identification of photosynthetic mutants can be performed in several ways. The most common are based on alteration in pigmentation and chlorophyll fluorescence parameters, preferentially on photochemical quenching (Meurer *et al.*, 1998). Nevertheless it is known that mutation affecting photosynthesis do not necessarily have to

show strong and obvious phenotypes. For this class of mutants, other basic parameters of chlorophyll fluorescence were used, like non-photochemical quenching (Bradbury and Baker, 1981) and the effective quantum yield of PSII (Genty *et al.*, 1989).

### **Reverse Genetics**

Photosynthetic mutants can be also identified by screening large collections of *Arabidopsis* lines mutagenised by random insertions of transposons (Speulman *et al.*, 1999; Tissier *et al.*, 1999; Meissner *et al.*, 1999) or T-DNA (Krisan *et al.*, 1999). Their screening in order to obtain an insertion in a particular gene of interest is usually performed using PCR-based approaches; in which one of the primers is complementary to the target gene and the other to the insertional mutagen (Parinov and Sundaresan, 2000).

## **AIM OF THE THESIS**

The aim of this thesis was to understand the function of PSI-D and PSI-E subunits, which are located on the stromal face of photosystem I, as well as to uncover the biological significance of duplication of genes coding for these subunits. For this purpose knock-out alleles for each gene have been identified and approaches of forward and reverse genetics have been used.

In algae and cyanobacteria both PSI-D and PSI-E have been shown to play an important role during photosynthesis. Consequences of the corresponding mutations in *Arabidopsis* on general thylakoid composition and protein regulation have been investigated by using different biochemical techniques, like proteomics and mass spectrometry.

The impact of each *PsaD* gene, as well as the effect of a complete lack of PSI-D on PSI-D function, is characterized in detail in Chapter 3. The structural and functional alterations of PSI caused by these mutations are described.

Possible function of PSI-D1 phosphorylation is discussed in Chapter 4. Effects of *psad1-1* and *psae1-3* mutations on protein phosphorylation are described in Chapter 5. The sixth chapter describes the effect of a complete lack of PSI-E subunit on growth and fitness of plants.



## **2. MATERIALS AND METHODS**

### **2.1 Plant propagation and growth measurement**

Seeds of *Arabidopsis thaliana* lines were placed on wet Whatman paper in Petri dishes and incubated for 3 d at 2-5°C in the dark. This stratification was done in order to break dormancy and improve germination rate and synchrony. After cold treatment, seeds were sown in plastic trays with *Minitray* soil (Gebr. Patzer GmbH & co. KG, Sinntal-Jossa, Germany). Plants were grown in the greenhouse under following conditions: day period of 16 h with 20°C and PFD of 80  $\mu\text{mol photons m}^{-2} \text{ s}^{-1}$ ; night period of 8 h with 15°C. Fertilisation with “Osmocote plus” (15% N, 11% P2 O5, 13% K2O, 2% MgO; Scotts Deutschland GmbH, Nordhorn, Germany) was performed according to the manufacturer’s instructions.

For the analysis of plants after transformation and of *psad1-1 psad2-2* double mutants, plants were grown on Murashige and Skoog medium containing 2% (for double mutant) or 1% (for transformant plants) sucrose in a culture chamber on a 16-h-day period (PFD = 15  $\mu\text{mol photons m}^{-2} \text{ sec}^{-1}$  for double mutants, and PFD = 80  $\mu\text{mol photons m}^{-2} \text{ sec}^{-1}$  for transformant plants) at 22°C.

Plant growth was measured by using an integrated digital video image analysis system (Abington Partners, Bath, UK) as reported in Leister *et al.* (1999).

For the mutant screening, plant trays were transferred 3-4 weeks after germination into a climate chamber under short day conditions (day period of 10.5 h with 20°C and constant PAR of 200  $\mu\text{mol sec}^{-1} \text{ m}^{-2}$ ; night period of 13.5 h with 15°C). Plants stayed under these conditions for at least 2 d and then the effective quantum yield of PSII was measured.

### **2.2 Automatic screening for photosynthetic mutants of *Arabidopsis thaliana***

Screening of a collection of *Arabidopsis* lines carrying independent insertions of the *dSpm* transposon (the Sainsbury Laboratory *Arabidopsis* Transposants (SLAT) collection (Tissier *et al.*, 1999)) for alterations in the effective quantum yield of PSII ( $\Phi_{II}$ ) was performed by Erik Richly as described previously (Varotto *et al.* 2000b). This screening resulted in the identification of the mutant line *photosynthesis-affected mutant 62* (*pam62*).

### 2.3 Isolation of *dSpm* insertion-flanking sequences

Isolation of genomic sequences flanking the termini of the *dSpm* insertion was achieved by inverse PCR as described by Tissier *et al.* 1999 and the insertion site was identified by Erik Richly. To amplify regions flanking the *dSpm* insertions, the primer pair *dspm1* and *dspm11* (Tissier *et al.* 1999) was used. On the basis of this screening the insertion site in *psad1-1* was identified.

### 2.4 Isolation of T-DNA insertion mutants

The T-DNA insertion lines for *PsaD2*, *PsaE1* and *PsaE2* were identified by screening the T-DNA populations by PCR using gene specific primers in combination with different T-DNA specific primers. Amplifications were performed with *Taq* polymerase (Roche) and the following cycling conditions: initial denaturation for 3 min at 93°C, followed by 35 cycles of 15 sec denaturation at 93°C, 45 sec annealing at 55°C and 1 min 30 sec elongation at 72°C. The PCR products were then separated by a 1% agarose gel. Positive lines were confirmed by sequencing the PCR-amplified T-DNA flanking regions and homozygous plants were obtained in the T3 progeny also using this PCR based approach. T-DNA populations and primers used for screening are listed below; for primers sequences (5'-3' orientation) see Table 2.1.

The mutant *psad2-1* was identified in the SALK collection, (<http://signal.salk.edu/>; Alonso *et al.*, 2003) which is consist of flank-tagged *ROK2* T-DNA lines (ecotype Col-0), by using the insertion flanking database signal (<http://signal.salk.edu/cgi-bin/tdnaexpress>). The *psad2-2* mutant was identified in the SALK collection by PCR-screening of the hierarchically pooled plant DNA with following primers: *PsaD2-226s*, *PsaD2-185as* and for T-DNA: *pROK2/pBIN19-460as*.

The T-DNA insertion line for *PsaE2* was obtained by screening the AFGC population (*Arabidopsis* Functional Genomics Consortium; <http://afgc.stanford.edu/>), performed by Claudio Varotto according to the guidelines described at: <http://www.biotech.wisc.edu/NewServicesAndResearch/Arabidopsis/GuidelinesIndex.html>. The primers used for this screening of the AFGC collection in order to obtain *psae2-1* mutants were: *E2--923s*, *E2-1556as* and for T-DNA left border: *JL-202*.

Insertions within the *PsaE1* gene were identified in UWBC collection (<http://www.biotech.wisc.edu/NewServicesandResearch/Arabidopsis/>) by using following primers: E1-51539s, E1-53150as, *T-DNA right border*: Taq3.

**Table 2.1**

Primer Name	Sequence (5'–3' orientation)
PsaD2-226s	GTGGCATGTGGGAAACATATCC
PsaD2-185as	CACGTAAAATTCCTCTACTTGTGCT
pROK2/pBIN19-460as	GTGCCCAGTCATAGCCGAATAGC
E2--923s	AATCCAGGGGAAAGCCAAGCAAACACTAT
E2-1556as	TTAGCC ACTACATTTGCTATGACCATCAC
JL-202	CATTTTATAATAACGCTGCGGACATCTAC
E1-51539s	TTTTCGGTAGAAATTTGCACAGA
E1-53150as	CAACGTTCTTGAACCAATAGGA
Taq3	CTGATACCAGACGTTGCCCGCATAA

## 2.5 Sequence analysis

Sequence data were analysed with the Wisconsin Package Version 10.0, Genetics Computer Group, Madison, Wisconsin (GCG; Devereux *et al.*, 1984) and amino acid sequences were aligned using *ClustalW* (Thompson *et al.*, 1994). Chloroplast import sequence predictions were carried out using the *TargetP* program (Emanuelsson *et al.*, 2000).

For the protein and nucleotide sequence comparison the databases at NCBI (<http://www.ncbi.nlm.nih.gov>) and MIPS (<http://mips.gsf.de>) were employed.

## 2.6 Analysis of nucleic acids

### 2.6.1 Nucleic acids preparation

Isolation of *Arabidopsis* DNA was performed as described in Liu *et al.*, 1995. For RT-PCR analysis total plant RNA was extracted from 100 mg of fresh tissues using the RNeasy Plant System (Qiagen). Total plant RNA used in Northern analyses was extracted with the TRIzol method (Invitrogen™, life technologies).

### 2.6.2 cDNA single strand synthesis

First-strand cDNA was synthesized, with oligo (dT) 12-18 primers, using the SuperScript Pre-amplification System (Invitrogen, Karlsruhe, Germany).

### 2.6.3 Reverse-transcription PCR (RT-PCR)

Two microliters of first-strand cDNA mixture in a total volume of 20 µl were used for RT-PCR amplification. Products obtained by a PCR of 30 cycles with the *PsaD1/PsaD2* and *PsaE1/PsaE2*-specific primers as well as control primers for the *ACTIN1* gene were analyzed on either 4.5% (w/v) polyacrylamide gel or 2% agarose gel. The polyacrylamide gels were visualized by silver staining. *PsaD* gene specific primers used for RT-PCR were: PsaD1/2-22/22s and PsaD1/2-230/218as. For amplification of *PsaE*-specific regions the following primers were used: PsaE1/2-248/257s, PsaE1/2-395/404as, and PsaE1-53499as. As a control primers for the *ACTIN1* gene were used: ACTIN1-33s, ACTIN1-994as. See Table 2.2 for the sequences of the primers.

### 2.6.4 Northern analysis

RNA gel blot analysis was performed under stringent conditions (Sambrook *et al.*, 1989) using a <sup>32</sup>P-labelled *PsaD1/PsaD2*-specific probe and control probe for the *ACTIN1* gene. Signals were quantified by using a phosphorimager (Storm 860; Molecular Dynamics, Sunnyvale, CA,

USA) and the program image quant for Macintosh (version 1.2; Molecular Dynamics). Following primers that anneal to both *PsaD* genes were used for amplification of the *PsaD1/PsaD2*-specific Northern probe: PsaD1/2-22/22s and PsaD1/2-441/429-as. The *ACTIN1*-specific primers: ACTIN1-33s and ACTIN1-994as were used to obtain control probe. See Table 2.2 for the sequences of the primers.

**Table 2.2**

<b>Primer Name</b>	<b>Sequence (5'–3' orientation)</b>
PsaD1/2-22/22s	ATCTTCA(A/G)C(C/T)CCGCCATAACAACC
PsaD1/2-230/218as	GGTGTGTTTGGGTCTAGCTGCGG
PsaD1/2-441/429-as	CACTCTGTAAAACCTGGTAAGTGATC
PsaE1/2-248/257s	GAGG(G/A)TC(T/C)AAGGTCAAGATTCTA
PsaE1/2-395/404as	ACTA(T/C)GCATTGGA(T/C)GAGGT(C/G)GAAGA
PsaE1-53499as	CCTCATCTGAATCTCGAGCC
ACTIN1-33s	TGCGACAATGGAACCTGGAATG
ACTIN1-994as	GGATAGCATGTGGAAGTGCATACC

## **2.7 Complementation of *Arabidopsis* mutants**

The GATEWAY Technology based on the bacteriophage lambda site-specific recombination system was used for cloning and subcloning DNA fragments into an Entry and Destination Vectors (<http://www.invitrogen.com/content.cfm?pageid=4072&e=452,440>).

### **2.7.1 Complementation of the *psad1* mutants**

The binary expression vector pJAN33 (MPIZ) was used to perform the complementation tests with *PsaD1* and *PsaD2* sequences. The vector carries the cauliflower mosaic virus 35S

promoter, a  $\beta$ -lactamase gene providing ampicillin and carbenicillin resistance for selection in *E.coli* and *Agrobacterium*, and a kanamycin resistance gene as plant selectable marker. To amplify full length cDNAs for subcloning, the following primers with 5'-terminal *attB* sites were used: PsaD1-GATEs, PsaD1-GATEas for *PsaD1* gene and PsaD2-GATEs, PsaD2-GATEas for *PsaD2* gene (Table 2.3).

Table 2.3

Primer Name	Sequence (5'–3' orientation)
PsaD1-GATEs	GGGGACAAGTTTGTACAAAAAAGCAGGCTATG GCAACTCAAGCCGCGGGATCT
PsaD1-GATEas	GGGGACCACTTTGTACAAGAAAGCTGGGTTTAC AAATCATAACTTTGTTTGCCA
PsaD2-GATEs	GGGGACAAGTTTGTACAAAAAAGCAGGCTATG GCAACTCAAGCCGCGGAATCT
PsaD2-GATEas	GGGGACCACTTTGTACAAGAAAGCTGGGTTTAC AAATCATAAGATTGTTTCCCA

Table 2.4

Primer Name	Sequence (5'–3' orientation)
PsaD1_ala	GCAATCCGCGCCGAGAAAGCTGATTCCTCCGCCG
PsaD1_asp	GCAATCCGCGCCGAGCCCGATGATTCCTCCGCCG
PsaD1_mutag_as	TTTCTCGGCGCGGATTGCGGTTTTGGTGAA

In vitro site-directed mutagenesis was performed by using GeneTailor™ Site-Directed Mutagenesis System (Invitrogen™, Life technologies). For generation of the mutated version of the entry clones the following primers were used: PsaD1\_ala, PsaD1\_asp, and PsaD1\_mutag\_as (Table 2.4).

### **2.7.2 *Agrobacterium* strain**

*Agrobacterium tumefaciens* genotype GV3101, carrying the helper plasmid pMP90RK, was used for *Arabidopsis* transformation. This strain contains a chromosomal rifampicillin resistance gene. The pMP90RK helper plasmid carries a kanamycin resistance gene for selection and the *vir* (virulence) genes, which act in trans to mediate gene transfer into plants (Koncz *et al.*, 1990).

### **2.7.3 *Agrobacterium*-mediated transformation**

*Arabidopsis thaliana* plants were transformed according to Clough and Bent (1998). Flowers were immersed in *Agrobacterium* suspension containing 5% sucrose and the surfactant Silwet-77 (0.0005% v/v) for 20 sec. After this dipping, plants were transferred to the greenhouse and seeds were collected after 3 weeks.

### **2.7.4 Selection of transformed plants**

After transformation plants were grown on Murashige and Skoog medium containing 1% sucrose in a culture chamber under 16-h-day conditions (PFD = 80  $\mu\text{mol photons m}^{-2} \text{sec}^{-1}$ ) at 22°C. Transgenic plants were selected on the basis of their resistance to kanamycin or hygromycin and then transferred to soil. Successful complementation was confirmed by the measurement of chlorophyll fluorescence and plant growth. In addition, the presence and overexpression of the transgene in the complemented mutant plants were confirmed by PCR and RT-PCR.

## 2.8 Biochemical Analysis

### 2.8.1 Total protein isolation

Leaves were harvested in eppendorf tubes, frozen immediately in liquid nitrogen and ground. Total proteins were isolated by subsequently grinding in extraction buffer (100 mM Tris pH 8.0, 50 mM EDTA pH 8.0, 0.25 M NaCl, and 1 mM DTT, 0.75% SDS). Samples were vortexed for 10 sec, incubated at 68°C for 10 min and after centrifugation at 15000g for 10 min frozen in -80°C. Protein concentration was determined using BIORAD Protein Assay.

### 2.8.2 Preparation of thylakoid membranes

Leaves from 4-week-old plants were harvested in the middle of the light period and thylakoids were prepared as described by Bassi *et al.* (1985). Leaf material was homogenized in blender in cold T1 buffer (0.5% milk powder, 0.4 M Sorbitol, 0.1 M Tricine pH 7.8), sieved through nylon membrane into glass beaker and centrifuged at 4°C, 4500 rpm for 10 min. Subsequently, pellet was resuspended with a brush in cold T2 buffer (20 mM HEPES pH 7.8, 10 mM EDTA pH 8.0) and sample was centrifuged at 10000 rpm for 10 min. Pellet was resuspended in small volume of T3 buffer (50% glycerol, 10 mM HEPES pH 7.5, 1 mM EDTA pH 8.0) and the thylakoid membrane concentration amount was calculated according to the total chlorophyll content as described in Porra *et al.* (1989).

### 2.8.3 Native and 2D PAGE

Thylakoid membranes extracted from WT and *psad1-1* plants, corresponding to 30 µg of chlorophyll, were first fractionated on a non-denaturing lithium dodecyl sulfate polyacrylamide (LDS-PA) gradient gels and then on a denaturing SDS-PA gradient (10-16% gel) as a second dimension, as described by Pesaresi *et al.*, 2001 and 2002). Proteins were visualized by Coomassie staining, and densitometric analyses of the protein gels were performed by using the Lumi Analyst 3.0 (Boehringer Mannheim/Roche). Because of the limited amount of *psad1-1*



*psad2-1* samples, 2-D gel analysis was performed by using thylakoid membrane samples corresponding to 20 µg of chlorophyll. Proteins were visualized by silver staining.

#### **2.8.4 Immunoblot analysis**

Protein amounts equivalent to 5 µg of chlorophyll (for *psad* single-gene mutants; and *psae* single and double mutants), or to 40 µg of total protein (for *psad1 psad2* double mutants) were loaded for each genotype. Decreasing amounts of WT proteins were loaded in parallel lanes (0.8x WT, 0.6x WT and 0.4x WT for *psad1-1*, *psad2-1*, and *psae* single and double mutants; 0.75x WT, 0.5x WT and 0.25x WT for *psad1-1 psad2-1*). For immunoblot analyses, proteins were transferred to Immobilon-P membranes (Millipore, Eschborn, Germany) and incubated with antibodies specific for individual polypeptides of PSI, PSII and LHCI. Phosphorylated threonine residues were identified using a phosphothreonine-specific antibody raised in rabbits (Cell Signaling Technology Inc.). Signals were detected using the Enhanced Chemiluminescence Western Blotting Kit (Amersham Biosciences, Sunnyvale, CA, USA) and quantified using the Lumi Analyst 3.0 (Boehringer Mannheim/Roche, Basel, Switzerland).

#### **2.8.5 PSI complex isolation**

Thylakoid membranes prepared according to Bassi *et al.* (1985) were washed twice with 5 mM EDTA pH 7.8, spun down at 12000 rpm for 5 min and resuspended in ddH<sub>2</sub>O. Thylakoids were diluted to 2mg/ml with ddH<sub>2</sub>O, stirred for 10 min at 0°C with an equal volume of 2% β-Dodecyl maltoside, spun down at 13000 rpm for 5 min and loaded on a 0.4 M sucrose gradient (20 mM Tricine-NaOH pH 7.5, 0.06% β-DM, 0.4 M sucrose). After centrifugation at 39000 rpm for 22 h fractions from the sucrose gradient were collected, frozen and stored at -80°C.

#### **2.8.6 Phosphorylation analysis**

##### ***In vivo* phosphorylation**

For the determination of thylakoid proteins phosphorylation *in vivo*, WT and *psad1-1* plants were dark-adapted for 16 h. Single leaves were harvested from plants and then placed in Micro

plates with 5  $\mu\text{l}$  of 1mM Tricine-NaOH (pH 10.0  $\rightarrow$  final pH 7.8) and 10  $\mu\text{Ci}$  of [ $\text{P}^{33}$ ] orthophosphoric acid. Then leaves were left in the dark for 30 min to incorporate radioactivity. Following the incorporation, leaves were exposed to varying light conditions (80  $\mu\text{mol photons m}^{-2} \text{ s}^{-1}$ , 2 h for low light adaptation, 800  $\mu\text{mol photons m}^{-2} \text{ s}^{-1}$ , 2 h for high-light stress and dark adaptation). Thylakoids were prepared as described by Haldrup *et al.* (1999) in the presence of the phosphatase inhibitor NaF (10 mM) and separated on SDS-PAGE. Incorporation of radioactivity was detected by phosphoimager (Storm 860, Molecular Dynamics).

### **Detection of phosphoproteins in polyacrylamide gels**

PSI complexes from WT, *psad1-1* and *psae1-3* mutant leaves were isolated in the presence of 10 mM NaF (see 2.8.5). Proteins corresponding to 5 $\mu\text{g}$  of chlorophyll were separated by a 16-23% gradient SDS-PAGE as reported by Knoetzel *et al.* (2002). Proteins were visualized by Coomassie staining and Pro-Q<sup>®</sup> Diamond Phosphoprotein Gel Stain (Molecular Probes). Stained gels were visualized using phosphoimager (Storm 860, Molecular Dynamics).

## **2.9 Mass spectrometry**

### **LC-ESI MS/MS**

A Dual Gradient System HPLC pump (Dionex, Amsterdam) including a Famos auto sampler and Switchos was connected to a Finnigan LTQ (linear quadrupole ion trap) mass spectrometer (Thermo Electron Corp., San Jose, CA). The LTQ was operated via Instrument Method files of Xcalibur to acquire a full MS scan between 350 and 2000  $m/z$  followed by full MS/MS scans of the three most intensive ions from the preceding MS scan. The heated desolvation capillary was set to 180°C. The relative collision energy for collision induced dissociation was set to 35%, dynamic exclusion was enabled with a repeat count of 2, a repeat duration of 0.5 min, and a 3 minutes exclusion duration window. Samples were loaded onto a 15 cm fused silica column. The fritless 100  $\mu\text{m}$  capillary was packed in house with Eclipse XDB C<sub>18</sub> (Hewlett Packard, Palo Alto, CA). The column flow rate was set to 0.15-0.25  $\mu\text{L} / \text{min}$  and a spray voltage of 1.8 kV was used.

The buffer solutions used for the chromatography were 5% ACN (acetonitrile); 0.012% HFBA (heptafluorobutyric acid); 0.5% acetic acid (buffer A), 80% ACN; 0.012% HFBA; 0.5% acetic acid (buffer B). After equilibration for 5 min with buffer A, a linear gradient was generated within 60 min.

### Protein Identification

The SEQUEST algorithm was used to interpret MS/MS spectra. Results were interpreted on the basis of a conservative criteria set, *i.e.* only results with DCn (delta normalized correlation) scores greater than 0.1 were accepted, all fragments had to be at least partially tryptic and the cross-correlation scores (Xcorr) of single charged, double charged or triple charged ions had to be greater than 1.8, 2.5, or 3.5. Spectra were manually evaluated to match the following criteria: Distinct peaks with signals clearly above noise levels, differences of fragment ion masses in the mass range of amino acids, and fulfilment of consecutive b and y ion series.

## 2.10 Chlorophyll fluorescence measurements

The procedure used to identify mutants that showed a change in  $\Phi_{II}$ , the effective quantum yield of PSII ( $\Phi_{II} = (F_m' - F_o')/F_m'$ ), has been described before by Varotto *et al.* (2000a and 2000b). *In vivo* Chl a fluorescence of single leaves was measured using PAM 101/103 (Walz, Effeltrich, Germany) as described by Varotto *et al.* (2000a). To determine the maximum fluorescence ( $F_m$ ) and the  $(F_m - F_o)/F_m$  ratio ( $=F_v/F_m$ ) 0.8-sec pulses of white light ( $6000 \mu\text{mol photons m}^{-2} \text{sec}^{-1}$ ) were used. A 15-min illumination with actinic light ( $65 \mu\text{mol photons m}^{-2} \text{sec}^{-1}$  for single-gene mutants and WT grown on soil;  $15 \mu\text{mol photons m}^{-2} \text{sec}^{-1}$  for double mutants and WT grown in sterile culture) was used to drive electron transport between PSII and PSI before measuring  $\Phi_{II}$ , qN (non-photochemical quenching =  $1 - (F_m' - F_o')/(F_m - F_o)$ ), and qP (photochemical quenching =  $(F_m' - F_s)/(F_m' - F_o')$ ).

State transitions were also measured with the PAM 101/103 fluorometer (Walz, Effeltrich, Germany). After 30-min incubation in the dark, the maximum fluorescence ( $F_m$ ) of leaves was measured by using a saturating light pulse (0.8 sec,  $6000 \mu\text{mol photons m}^{-2} \text{sec}^{-1}$ ). Leaves were subsequently illuminated for 20 min with blue light ( $80 \mu\text{mol photons m}^{-2} \text{sec}^{-1}$ ) from a Schott KL-1500 lamp equipped with a Walz BG39 filter. The maximum fluorescence in state 2 ( $F_m^2$ ),

was then measured. Next, state 1 was induced by switching to far-red light (Walz 102-FR; peak emission 730 nm,  $90 \mu\text{mol photons m}^{-2} \text{sec}^{-1}$ ), and  $F_m^1$  was recorded 20 min later.  $qT$  was calculated according to the equation:  $qT = (F_m^1 - F_m^2) / F_m^2$  (Jensen *et al.*, 2000).

A dual-wavelength pulse-modulation system (ED-P700DW; Walz, Effeltrich, Germany) was used to record changes in the absorbance of P700<sup>+</sup>. Leaves were illuminated with background far-red light, and immediately after full oxidation of P700, a saturating blue-light pulse (50 msec) was applied (XMT-103; Walz, Effeltrich, Germany) to reduce P700<sup>+</sup>. Parameters  $t_{1/2\text{red}}$  and  $t_{1/2\text{ox}}$  were calculated from the recorded kinetics of P700 reduction and re-oxidation.

## 2.11 Pigment analyses

Pigments analyses performed by Dr. Peter Jahns were analyzed by reversed-phase HPLC as described previously by Färber *et al.* (1997). For pigment extraction, leaf discs were frozen in liquid nitrogen and disrupted in a mortar in the presence of acetone. After a short centrifugation, pigment extracts were filtered through a 0.2- $\mu\text{m}$  membrane filter and either used directly for HPLC analysis or stored for up to 2 d at  $-20^\circ\text{C}$ .

## 2.12 Expression profiling

The 3292-GST array, representing genes known or predicted to encode proteins featuring a chloroplast transit peptide (cTP), has been described previously by Richly *et al.* (2003). At least three experiments with different filters and independent cDNA probes derived from plant material corresponding to pools of at least 50 individuals were performed for each condition or genotype tested, thus minimizing variation between individual plants, filters or probes. cDNA probes were synthesized by using a mixture of oligonucleotides matching the 3292 genes in antisense orientation as primer, and hybridized to the GST array as described by Kurth *et al.* (2002) and Richly *et al.* (2003). Images were read using the Storm phosphorimager (Molecular Dynamics). Hybridization images were imported into the arrayvision program (version 6; Imaging Research Inc.), where artefacts were removed, background correction was performed and resulting values were normalized with reference to intensity of all spots on the array (Kurth

*et al.*, 2002; Richly *et al.*, 2003). In the next step, those data were imported into the arraystat program (version 1.0 Rev. 2.0; Imaging Research Inc.) and a  $z$ -test (nominal  $\alpha$  set to 0.05) was performed to identify statistically significant differential expression values as described by Pesaresi *et al.* (2003a). The above DNA array analyses were performed by Angela Dietzmann, Alexander Biehl and Erik Richly.

### **3. CHARACTERIZATION OF PSI-D MUTANTS**

In *Arabidopsis thaliana*, the D-subunit of photosystem I (PSI-D) is encoded by two functional genes, *PsaD1* and *PsaD2*, which are highly homologous. Knock-out alleles for each locus have been identified by a combination of forward and reverse genetics. The impacts of each *PsaD* gene, as well as the effect of a complete lack of PSI-D, on PSI-D function have been characterized in detail on the basis of the molecular, physiological and biochemical approaches. The structural and functional alterations of PSI caused by these mutations are described.

## **RESULTS**

### **3.1 Identification and phenotype of PSI-D mutants**

A mutant line for the *PsaD1* gene was identified by screening the SLAT collection of T-DNA insertion lines (the Sainsbury Laboratory Arabidopsis Transposants collection; Tissier *et al.*, 1999) for alterations in the effective quantum yield of PSII ( $\Phi_{II}$ ; Varotto *et al.*, 2000b). This line carrying independent insertion of the *dSpm* transposon was named *photosynthesis-affected mutant 62* (*pam62*). The photosynthetic lesion was inherited as a recessive trait, which was confirmed by segregation analysis. Isolation of genomic sequences flanking the termini of the *dSpm* insertion was achieved by inverse PCR as described by Tissier *et al.* (1999), and the insertion site was identified. The *dSpm* transposon insertion is located in the unique exon of the *PsaD1* gene (At4g02770) coding for PSI-D (Figure 3.1a). Accordingly the mutant *pam62* was designated *psad1-1*.

In *Arabidopsis thaliana* there is second gene coding for PSI-D (*PsaD2*, At1g03130), which is highly homologous to *PsaD1*. The amino acid sequences of two *Arabidopsis* proteins, PSI-D1 and -D2, share 96% of similarity and 95% identity (Figure 3.2). The N-terminal chloroplast transit peptide of higher plant and *Chlamydomonas* PSI-D, which is shown in Figure 3.2 (domain I) was either experimentally determined (spinach, tomato, barley, *Chlamydomonas*) or predicted by the *TargetP* program (*Arabidopsis*, rice). After cleavage of predicted chloroplast transit peptides the proteins PSI-D1 and -D2 differ only in the highly variable plant-specific N-

terminal extension (domain II in Figure 3.2). This N-terminal extension of the higher-plant proteins is rich in alanine and proline and highly diversified. The C-terminal domain of PSI-D from higher plants is highly similar to the corresponding segment of algal and cyanobacterial PSI-D proteins (domain III in Figure 3.2).

In order to establish the photosynthetic functions of both *PsaD* genes, the database signal (<http://signal.salk.edu/cgi-bin/tdnaexpress>; Alonso *et al.*, 2003) was searched for insertions in the *PsaD2* gene. Firstly, a line was identified that carried a copy of the 5.2-kbp ROK2 T-DNA inserted 36 bp 5' to the ATG of the *PsaD2* gene, and this mutant line was designated *psad2-1* (Figure 3.1b). During the screening of the SALK collection of T-DNA lines for insertions in the *PsaD2* locus, using the PCR approach described in Materials and Methods, a second *psad2* mutant allele was identified. This line was isolated from the pool CS61661, and designated *psad2-2*. This second mutation also derived from a ROK2 T-DNA inserted 107 bp 5' to the ATG of the *PsaD2* gene (Figure 3.1b).

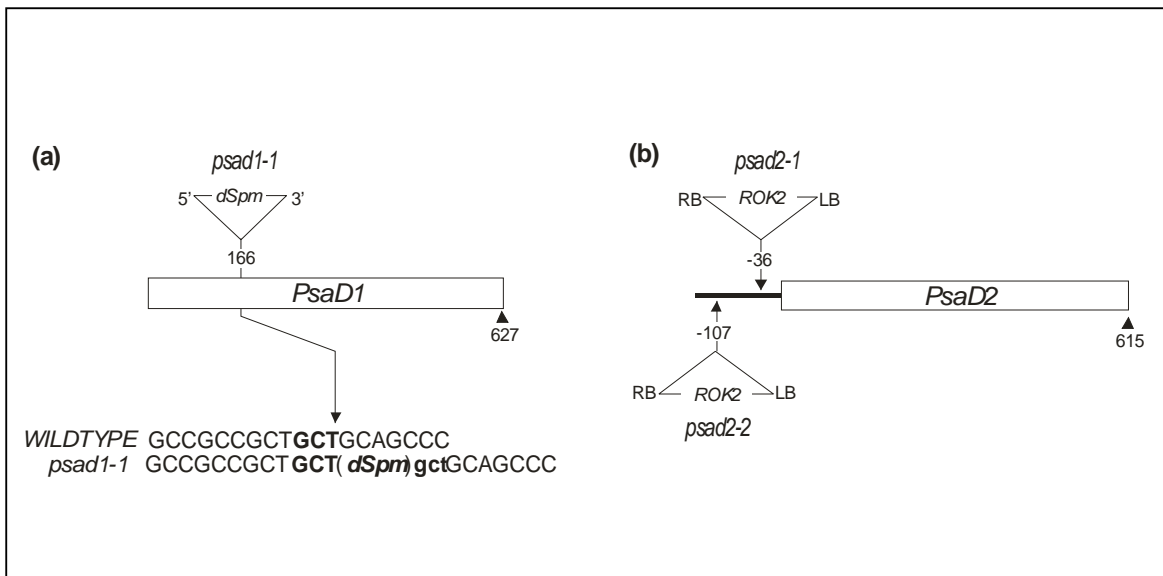


**Figure 3.1**

Tagging of the *PsaD1* and *PsaD2* genes. (a) In *psad1-1*, the *PsaD1* gene (At4g02770) is disrupted by an insertion of the non-autonomous *dSpm* element (Tissier *et al.*, 1999). Upper case letters indicate plant DNA sequences flanking the *dSpm* element, bold uppercase letters indicate the transposon target site in WT and the duplicated target site is indicated by bold lowercase letters. (b) The *psad2-1* and *psad2-2* mutants carry insertions of the 5.2-kbp pROK2 T-DNA (<http://www.signal.salk.edu>) in the promoter region of the *PsaD2* gene (At1g03130). The *dSpm* and T-DNA insertions are not drawn to scale.

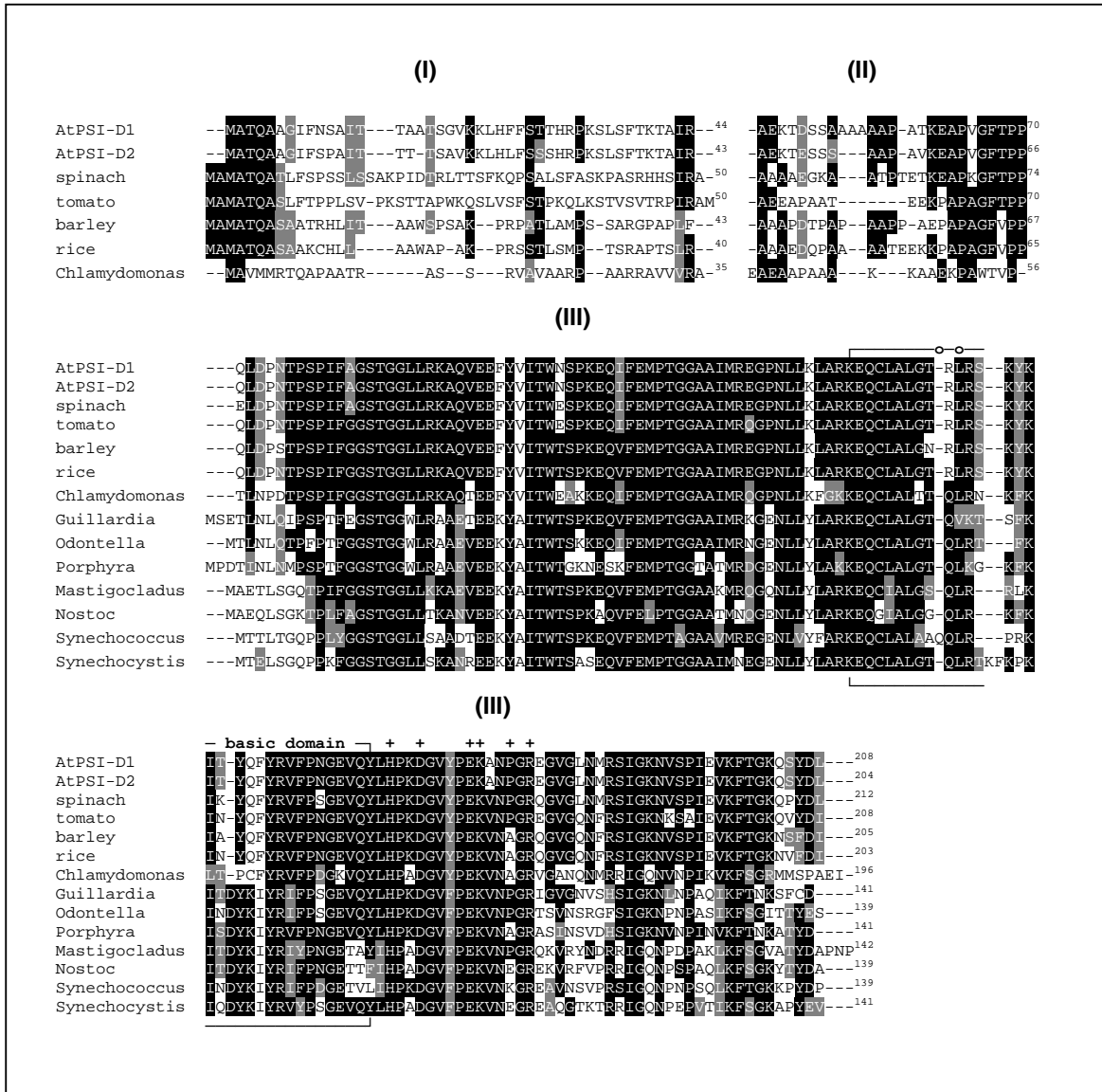


**Figure 3.2**

Comparison of PSI-D protein sequences from higher plants, algae and prokaryotes. The amino acid sequences of the *Arabidopsis* PSI-D1 and -D2 proteins (Accession numbers: At4g02770 and At1g03130) were compared with those of PSI-D from spinach (GI:19855891), tomato (GI:82100), barley (GI:478404), rice (GI:29367391) and with PSI-D sequences from the green alga *Chlamydomonas reinhardtii* (GI:498824), the red alga *Porphyra purpurea* (GI:2147918), the cryptophyte alga *Guillardia theta* (GI:3603032), the chlorophyll *a/c* containing alga *Odontella sinensis* (GI:7443141) and from four cyanobacterial species: *Nostoc* sp. PCC 8009 (GI:5052771), *Synechocystis* sp. PCC 6803 (GI:16329280), *Synechococcus* sp. (GI:47576) and *Mastigocladus laminosus* PCC 7605 (GI:2160762). Black boxes indicate strictly conserved amino acids; shaded boxes closely related amino acids. The symbol '+' refers to amino acid residues involved in the binding of ferredoxin (Bottin *et al.*, 2001; Hanley *et al.*, 1996; Lagoutte *et al.*, 2001); circles highlight lysine residues of the basic domain, which are important for the interaction of PSI-D with other PSI subunits (Chitnis *et al.*, 1997).



Under greenhouse conditions, *psad1-1* plants had light-green leaves and were notably reduced in size compared to wild type (WT) plants; in contrast, both *psad2* lines showed WT-like growth and leaf coloration (Figure 3.3a). When the growth rates of the two single-gene mutants *psad1-1* and *psad2-1* were compared to that of WT plants (Leister *et al.*, 1999), growth of *psad1-1* plants was found to be substantially reduced compared to the mutants *psad2-1* and *psad2-2* (data not shown), and WT plants (Figure 3.3b).

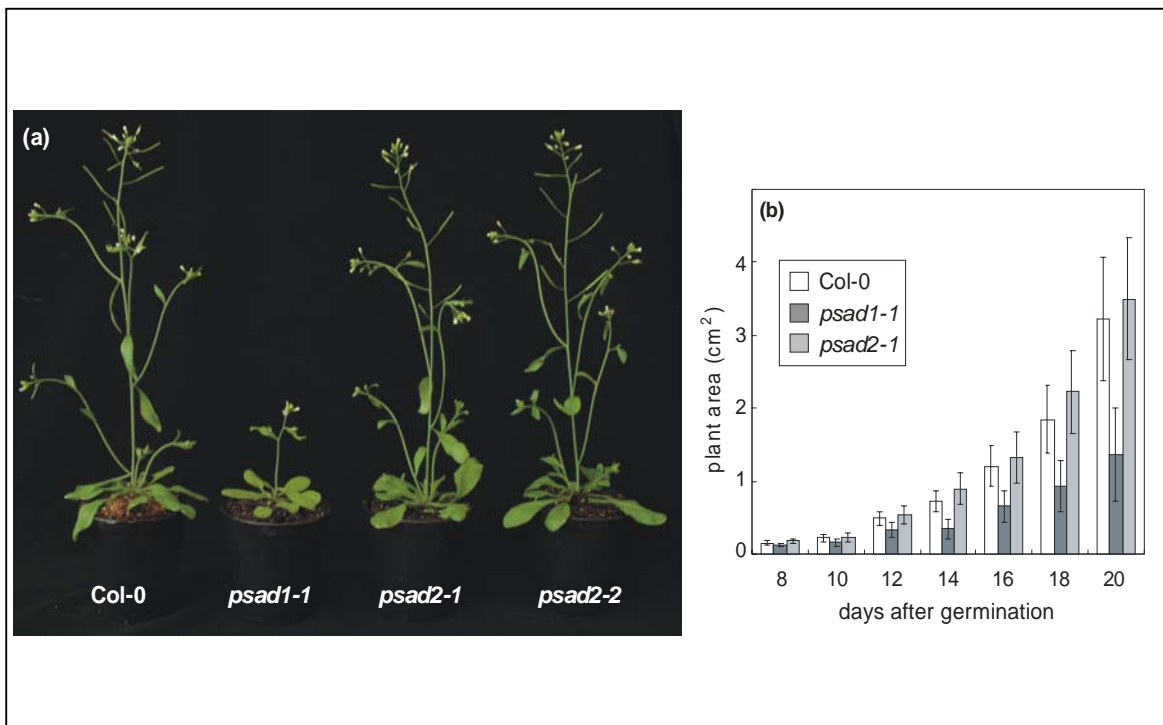


**Figure 3.3**

Phenotypes of *psad1-1* and *psad2-1*, *psad2-2*. **(a)** WT, *psad1-1*, *psad2-1* and *psad2-2* plants (4 weeks old) were grown in the greenhouse under long-day conditions. **(b)** Growth kinetics of *psad1-1* and *psad2-1* mutants compared to WT. Thirty-six plants of each genotype were measured during the period from 8 to 20 days after germination. Mean values  $\pm$  SDs (bars) are shown.

Crosses were carried out between *psad1-1* and *psad2-1* and homozygous F<sub>2</sub> double-mutant plants were identified. The *psad1-1 psad2-1* double mutants were lethal when grown on soil, but could be propagated in axenic culture on medium supplemented with sucrose (Figure 3.4a). Heterotrophically grown double mutants had yellowish leaves, remained very small and exhibited a high-chlorophyll-fluorescence (hcf) phenotype, similar to the mutant phenotypes

previously observed by Meurer *et al.* (1996). This indicates that the absence of PSI-D causes a block in photosynthetic electron flow (Figure 3.4b). In addition, double mutants were highly photosensitive and could only be propagated under low-light conditions (photon flux density, PFD = 15  $\mu\text{mol photons m}^{-2}\text{sec}^{-1}$ ).

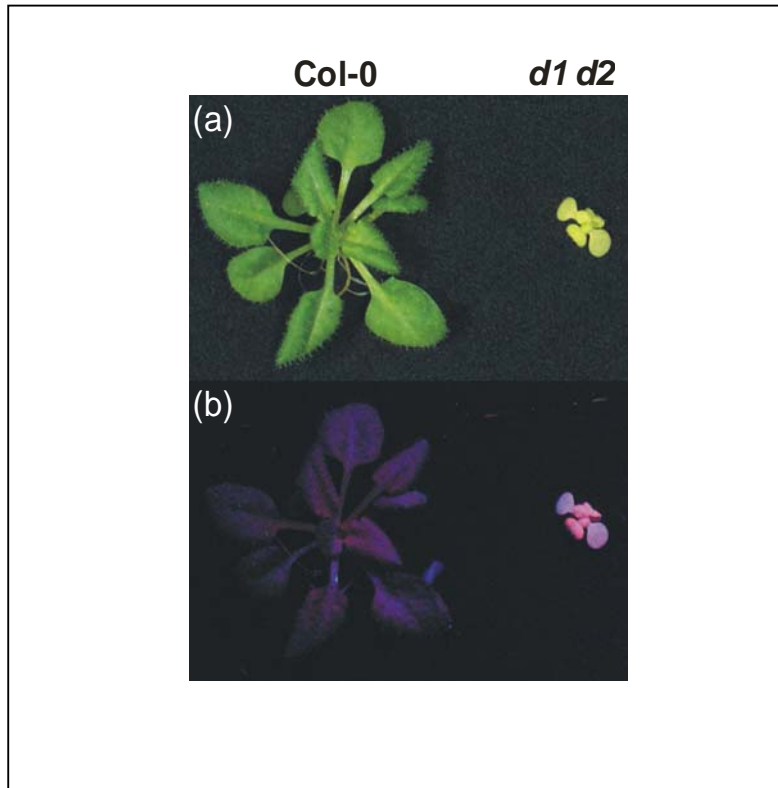


**Figure 3.4**  
WT and *psad1-1 psad2-1* double mutant plants (*d1 d2*) grown on sucrose-containing MS medium and illuminated with white light (a) or UV light (b).

### 3.2 Expression of *PsaD* in wild-type, single and double mutant plants

Northern analysis using a *PsaD* specific probe revealed a marked decrease in the level of *PsaD* mRNA in *psad1-1*, and a slighter decrease in *psad2-1* (Figure 3.5a). In order to discriminate between *PsaD1* and *PsaD2* transcripts reverse-transcription PCR (RT-PCR) analyses were performed. Products obtained after PCR for 30 cycles with *PsaD1/PsaD2* specific primers and control primers for the *ACTIN1* gene in the same reactions were analysed on a 4.5% (w/v) polyacrylamide gel. The products derived from transcripts of the two *PsaD* genes differ in size

by 12 bp. After visualization by silver staining it have been shown that in *psad1-1* mutant, *PsaD1* transcript accumulation was completely suppressed, and that in *psad2-1* and *psad2-2*, the transcript of *PsaD2* was not detectable (Figure 3.5b). In the *psad1-1 psad2-1* double mutant, the accumulation of both forms of *PsaD* transcripts was completely suppressed (Figure 3.5c). As a control, PCR with genomic WT-DNA was performed. The difference in size of the *ACTIN1* WT (DNA) band is because of the presence of two introns in the genomic amplicon.

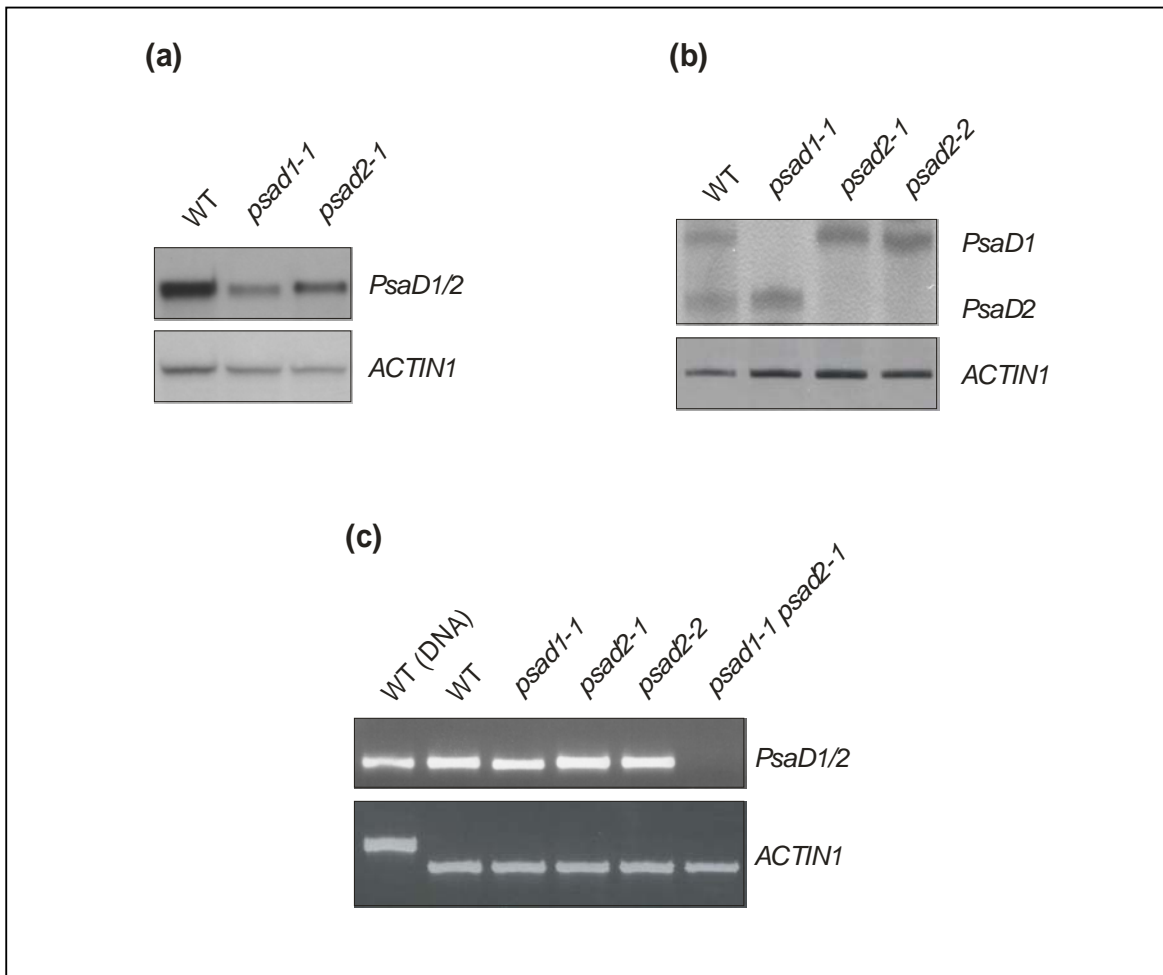


**Figure 3.5**

Expression of *PsaD* mRNA in mutant and WT plants. (a) Northern analysis of *PsaD* transcripts. Aliquots (20  $\mu$ g) of total RNA were hybridized with a mixture of *PsaD1* and *PsaD2* cDNA fragments. To control for variation in loading, the blots were probed with a cDNA fragment derived from the *ACTIN1* gene. (b) Detection of *PsaD1* and *PsaD2* transcripts by RT-PCR. WT and mutants single strand cDNA were amplified with *PsaD1/D2* specific primers and analysed on a 4.5% (w/v) polyacrylamide gel. (c) Detection of *PsaD* transcripts by RT-PCR. Products amplified with primers recognizing both *PsaD* transcripts were analysed on a 2.0% agarose gel. As a control, PCR with genomic WT-DNA was performed.

### 3.3 Increased dosage of the *PsaD2* gene can complement the *psad1-1* mutation

The almost identical sequence of the two mature PSI-D proteins suggested that PSI-D1 and -D2 have redundant functions. An experiment was carried out to complement the *psad1-1* mutation by introducing into the mutant background either the *PsaD2* (Figure 3.6) or the *PsaD1* (Figure 3.7) gene under transcriptional control of the 35S promoter.

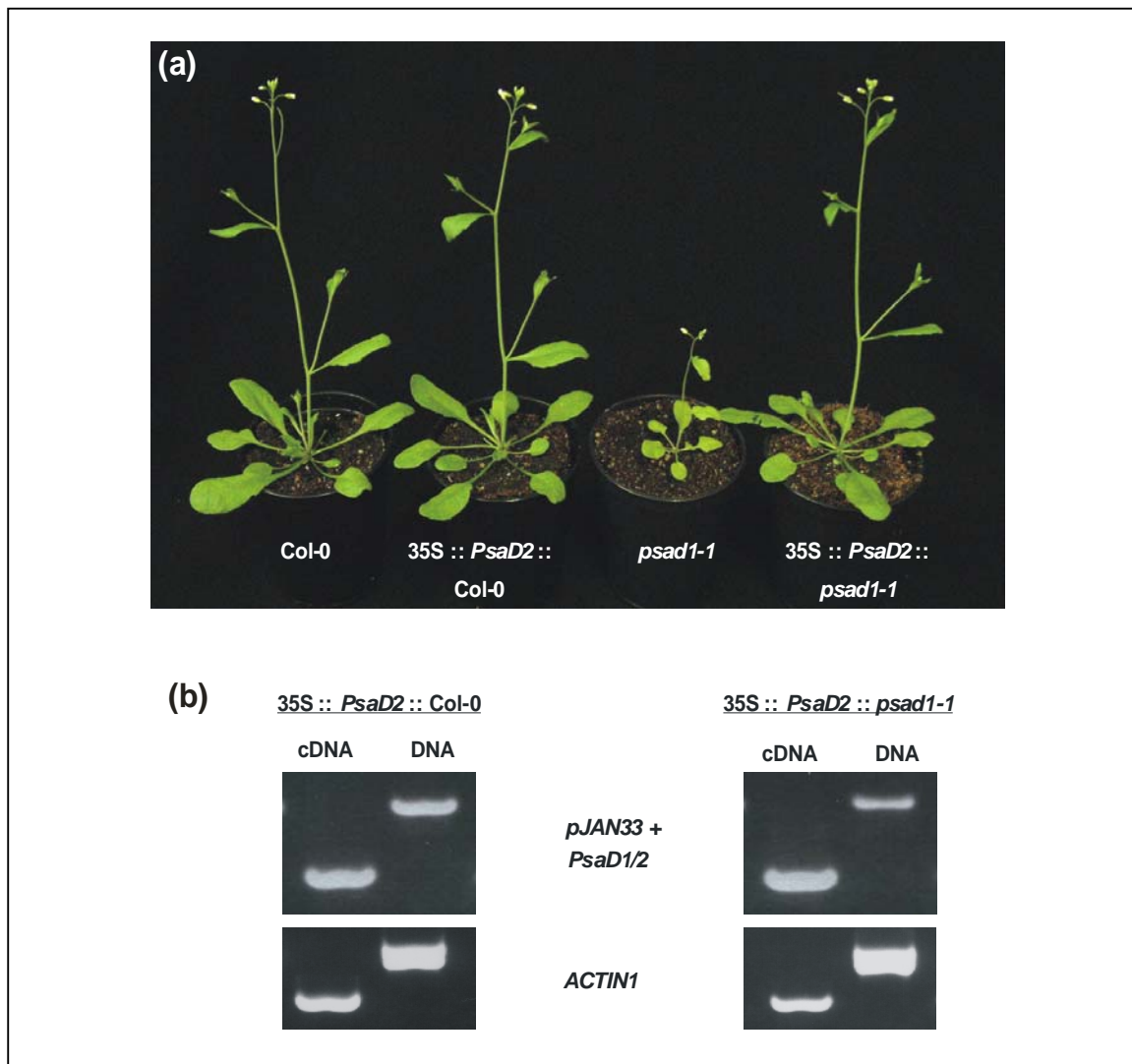


**Figure 3.6**

Complementation test. **(a)** 4-week-old WT plants, *psad1-1* mutants and T2 generation of WT control and *psad1-1* mutant plants transformed with *PsaD2*-cDNA fused to the 35S promoter. **(b)** Presence and overexpression of the transgene in the complemented mutant and WT control plants was confirmed by PCR and RT-PCR. Products obtained after PCR for 30 cycles with primers specific for transgene (*PsaD1/2*-441as and pJAN33) were analysed on a 2.0% agarose gel. The differences in size between cDNA and DNA are because of the presence of one intron in the vector which was used for complementation test. As a control, PCR with control primers for the *ACTIN1* gene were performed.

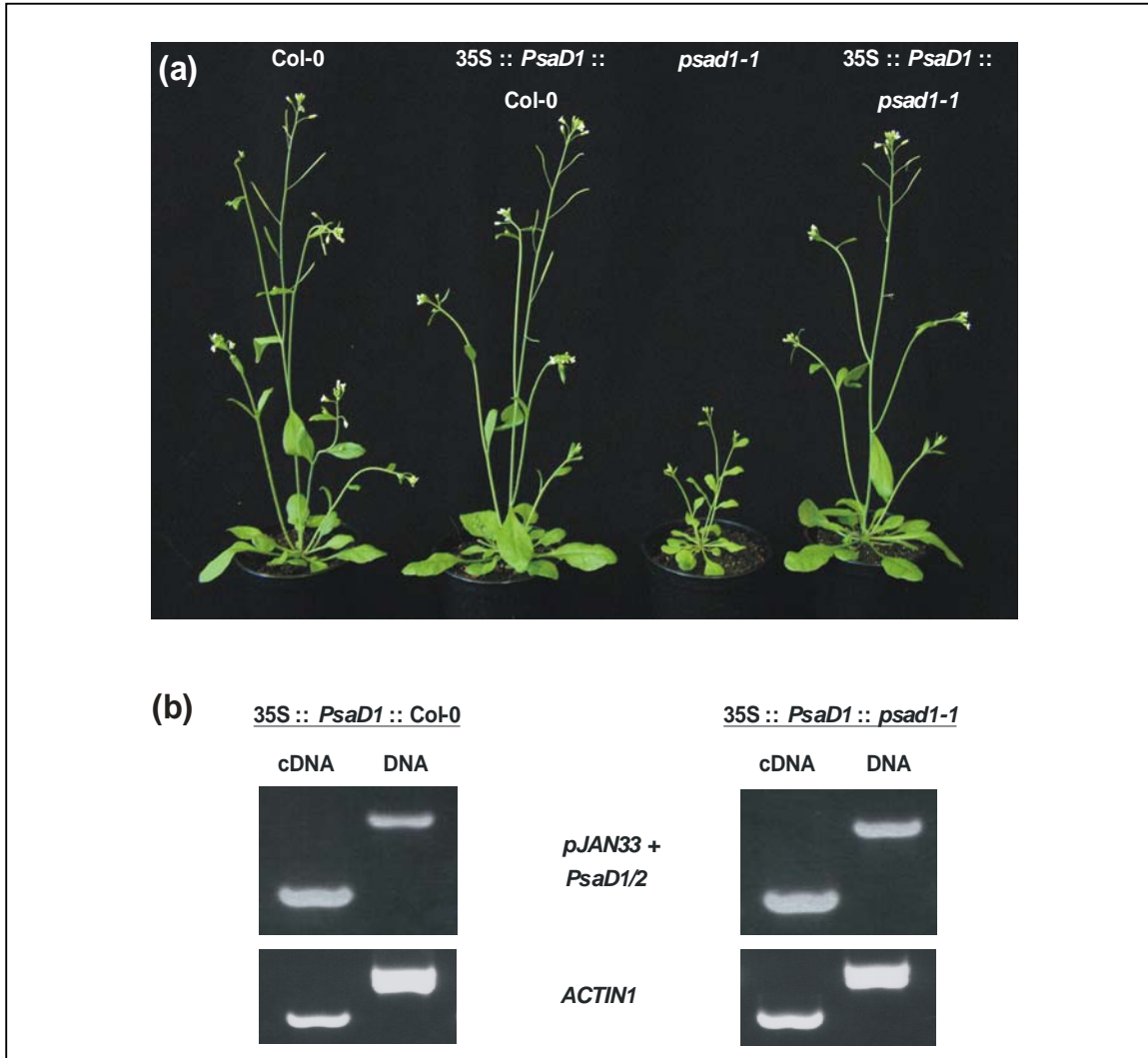


**Figure 3.7**

Complementation test. **(a)** 4-week-old WT plants, *psad1-1* mutants and T2 generation of WT control and *psad1-1* mutant plants transformed with *PsaD1*-cDNA fused to the 35S promoter. **(b)** Presence and overexpression of the transgene in the complemented mutant and WT control plants was confirmed by PCR and RT-PCR (see Figure 3.6b for details).

Increased dosage of either *PsaD1* or *PsaD2* in *psad1-1* could, in fact, restore the WT phenotype. In particular, the effect of the *psad1-1* mutation on effective quantum yield of PSII (WT,  $0.76 \pm 0.01$ ; *psad1-1*,  $0.52 \pm 0.03$ ; 35S::*PsaD1 psad1-1*,  $0.76 \pm 0.03$ ; 35S::*PsaD2 psad1-1*,  $0.77 \pm 0.02$ ), growth and leaf coloration could be fully reversed, demonstrating that *PsaD1* and *PsaD2* encode proteins with redundant functions. Successful complementation and expression of the transgene in the transformed plants were confirmed by RT-PCR analysis (Figures 3.6b, 3.7b).

### 3.4 PSI composition, accumulation of other thylakoid proteins and leaf pigments

Western analyses of thylakoids demonstrated that the *psad1-1* mutant had 40% of WT PSI-D levels, while in *psad2-1* plants PSI-D was reduced by only 10% (Figure 3.8a; Table 3.1). In the double mutant *psad1-1 psad2-1*, no PSI-D was detected (Figure 3.8b; Table 3.1). Due to the prediction, PSI-D1 and PSI-D2 proteins differ slightly in the lengths of the mature proteins (PSI-D1, 164 amino acids; PSI-D2, 161 amino acids). Closer inspection of the D-specific immunoblot signals revealed that the gene products of *PsaD1* and *PsaD2* indeed differed slightly in molecular mass in the two single-gene mutants. In agreement with the transcription data, in *psad1-1*, only PSI-D2, and in *psad2-1*, only PSI-D1 was detectable.

When a mix of *psad1-1* and *psad2-1*, or of *psad1-1* and WT, or of *psad2-1* and WT thylakoid proteins was analyzed, WT-like bands were detected (data not shown). This indicates that the two PSI-D forms can be discriminated only in the corresponding mutant backgrounds. Because residual PSI-D level in the two single mutants added up to more than WT levels, it was concluded that- at least in *psad2-1*- the effects of the single-gene mutations were partially compensated by increased accumulation of the alternative PSI-D form. But still this compensation was not enough to restore WT phenotype in *psad1-1* mutant plants. The decrease in the amount of PSI-D in the *psad1-1* mutant was paralleled accompanied by the decrease in the levels of several PSI polypeptides, particularly of PSI-F, -H and -L, as well as of the four LHCI proteins (Figure 3.8a; Table 3.1). In the case of the *psad1-1* mutant, because of its reduced chlorophyll content, relatively more proteins were loaded. Relative values for the mutant genotypes, reflecting the ratio of expression between the mutant and WT (see Table 3.1), were normalized on the basis of their chlorophyll content (see Table 3.2).

In the double mutant *psad1-1 psad2-1* no accumulation of PSI core proteins, with the exception of traces of PSI-F, were detectable. LHCI proteins were present but to a much lesser extent than in the WT (Figure 3.8b; Table 3.1), which is consistent with previous studies of barley (*Hordeum vulgare*) mutants that only can accumulate LHCI but no PSI core proteins (Hoyer-Hansen *et al.*, 1988; Nielsen *et al.*, 1996).

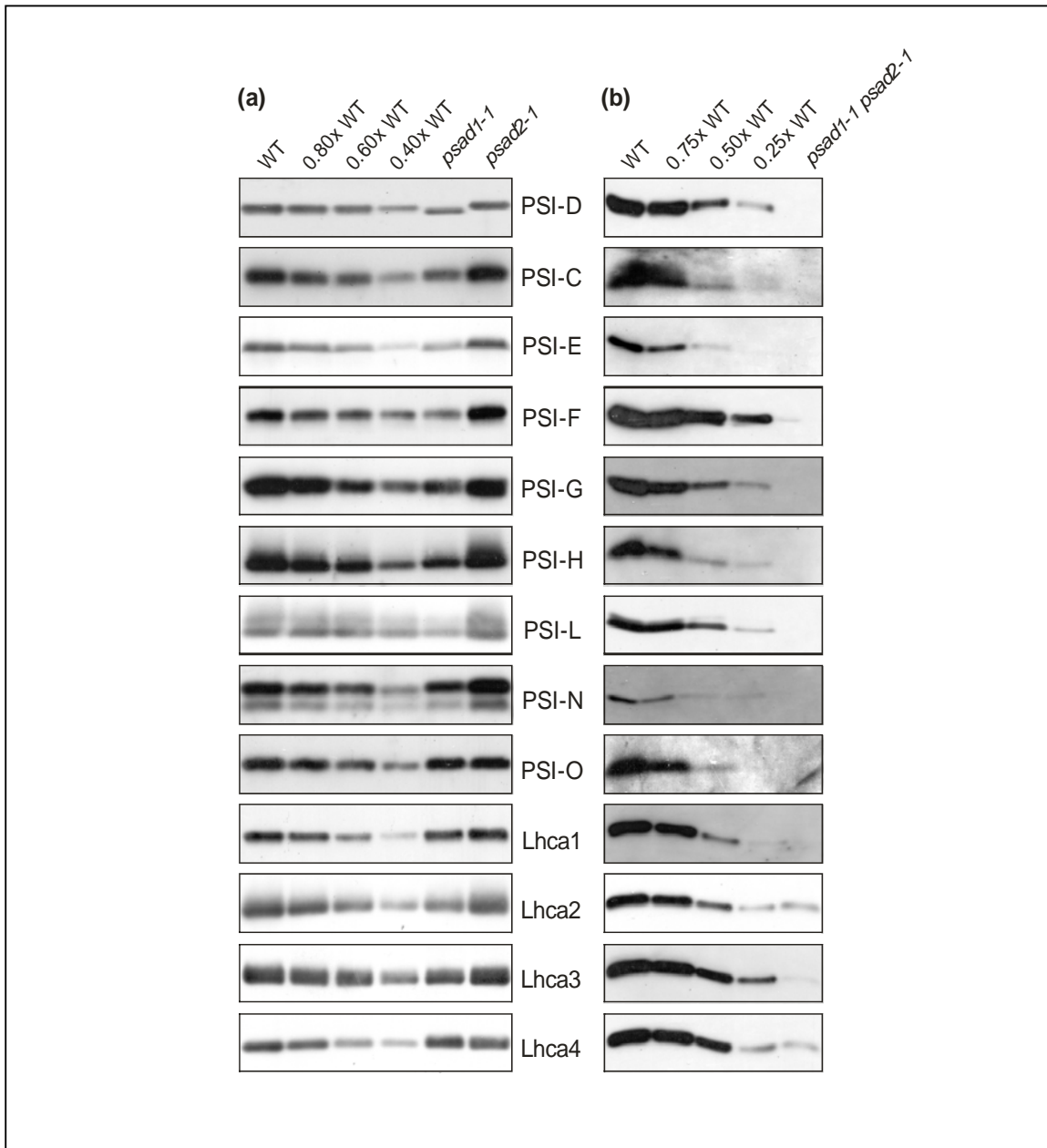


**Figure 3.8**

Levels of PSI polypeptides in mutant and WT plants. Aliquots of thylakoid proteins corresponding to 5  $\mu\text{g}$  of chlorophyll (*psad1-1*, *psad2-1* and WT plants; panel (a)), or 40  $\mu\text{g}$  of total protein (*psad1-1* *psad2-1* and WT plants; panel (b)) were loaded in each lane, and decreasing amounts of WT proteins were added to lanes 0.8x, 0.6x and 0.4x WT in panel (a), or to lanes 0.75x, 0.5x and 0.25x WT in panel (b). Replicate filters were immunolabelled with antibodies raised against individual PSI or LHCI polypeptides. Three independent experiments were performed, and representative results are shown. Signals obtained in three independent experiments were quantified using lumi analyst 3.0 (Boehringer Mannheim/Roche).

To test whether mutations in *PsaD* genes influence also the accumulation of other thylakoid proteins, 2-D PAGE analyses were performed (Figure 3.9) and the intensity of signals was quantified (Table 3.1). Thylakoid proteins were first separated by LDS-PAGE (see Figure 3.9a, c) and then fractionated on a denaturing SDS-PAGE gel. Positions of WT thylakoid proteins have been previously identified by Western analyses with appropriate antibodies (Figure 3.9b, d). Considering the different leaf chlorophyll contents of the two genotypes, quantification was performed as described in the legend of Figure 3.8 and listed in Table 3.1.

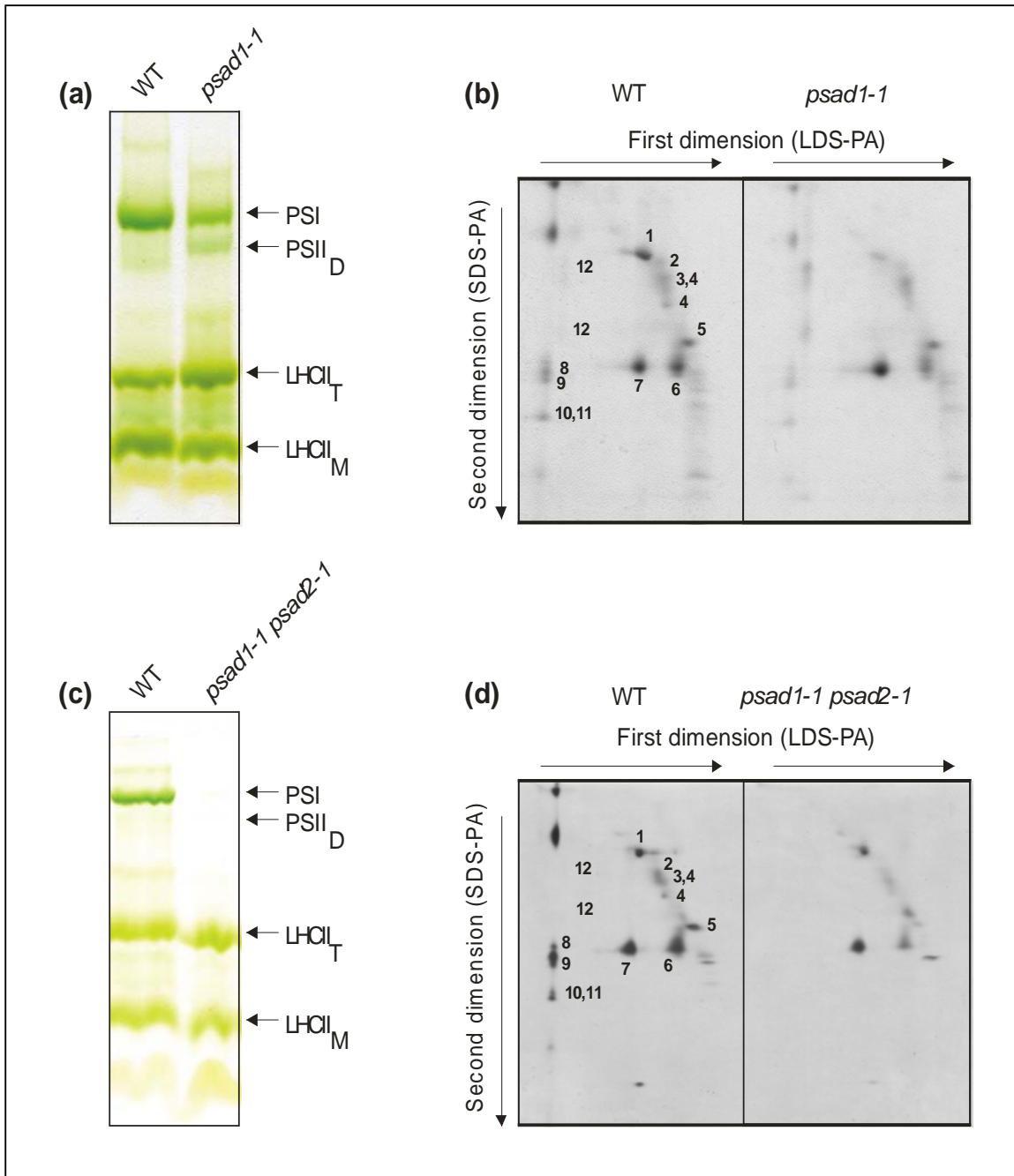
In *psad1-1*, the level of PSI proteins was decreased, whereas PSII dimers accumulated to higher levels than in the WT (PSII<sub>D</sub> band in Figure 3.9a; spot 12 in Figure 3.9b). This accumulation was at the cost of monomeric forms (spots 2-4 in Figure 3.9b), suggesting that such dimeric forms are more stable in the mutant, possibly because of an altered pigment composition (see Table 3.2).

In *psad1-1 psad2-1* double mutant plants, no bands indicative for PSI complexes or for PSII dimers could be observed (Figure 3.9c, d), suggesting a drastic reduction of PSII and pointing again to the absence of PSI complexes in this genotype. Relative accumulation of proteins in the double mutant was not quantified because of non-linearity of silver staining.

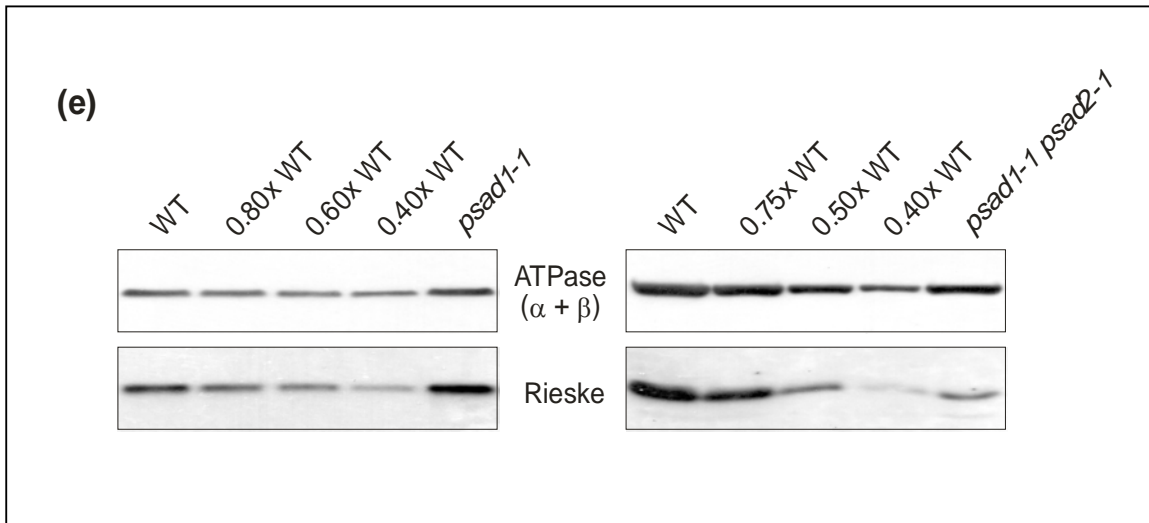
Immunoblot analyses of proteins separated by denaturing 1-D PAGE (Figure 3.9e) revealed that in *psad1-1* thylakoids the accumulation of the Rieske protein, a subunit of the *cyt b<sub>6</sub>f* complex, was increased. The concentration of the  $\alpha$ - and  $\beta$ -subunits of the ATPase complex appeared unchanged in *psad1-1* plants. This finding was in contrast to the results of 2-D PAGE analysis (Figure 3.9b), where a marked reduction of the  $\alpha$ - and  $\beta$ -subunits of the chloroplast ATPase was detected. This discrepancy between the results of immunoblot analysis and 2-D gel analysis was reported before for another photosynthetic mutant (Varotto *et al.*, 2002b), and was interpreted as the result of a decreased stability of mutant ATPase during 2-D PAGE.

In contrast to the *psad1-1* mutant, the accumulation of the Rieske protein and of the ATPase ( $\alpha$ - and  $\beta$ -subunits) was decreased in the *psad1-1 psad2-1* double mutant (Figure 3.9e).



**Figure 3.9**

Protein composition of thylakoid membranes in mutant and WT plants. **(a, c)** Thylakoid membranes corresponding to 30  $\mu\text{g}$  of chlorophyll from WT and *psad1-1* (grown in the greenhouse) (a), or corresponding to 20  $\mu\text{g}$  of chlorophyll from WT and *psad1-1 psad2-1* (grown in sterile culture) (c), were fractionated by electrophoresis on a LDS-PA gel. The bands were assigned to PSI, photosystem II dimers (PSII<sub>D</sub>), LHCII trimers (LHCII<sub>T</sub>) and monomers (LHCII<sub>M</sub>). **(b, d)** Positions of WT thylakoid proteins are indicated by numbers to the right of the corresponding spots: 1,  $\alpha$ - and  $\beta$ -subunits of the ATPase complex; 2, D1–D2; 3, CP47; 4, CP43; 5, oxygen-evolving complex (OEC); 6, LHCII monomer; 7, LHCII trimer; 8, PSI-D; 9, PSI-F; 10, PSI-C; 11, PSI-H; 12, PSII dimers.



**(e)** Aliquots of thylakoid proteins corresponding to 5  $\mu\text{g}$  of chlorophyll (*psad1-1* and WT plants; left panel), or 40  $\mu\text{g}$  total protein (*psad1-1 psad2-1* and WT plants; right panel) were analysed as in Figure 5. Immunolabelling was performed with antibodies raised against the Rieske protein and the chloroplast ATPase ( $\alpha$ - and  $\beta$ -subunits). Note that in the electrophoresis conditions used the  $\alpha$ - and  $\beta$ -subunits of the chloroplast ATPase could not be discriminated.

In order to understand additional consequences of *PsaD* mutations, leaf pigment composition of single and double mutants were studied by HPLC (Table 3.2). In the *psad1-1* single mutant plants a disproportionate increase in the abundance of xanthophylls violaxanthin, antheraxanthin and zeaxanthin (VAZ) with respect to neoxanthin and lutein was observed. Chlorophyll content (Chl *a* + *b*) decreased by about 25% in *psad1-1*, which is consistent with the reduced amount of PSI and- to a less extent- of PSII complexes. In contrast, WT levels of leaf pigments were detected in *psad2-1* single mutant plants.

The *psad1-1 psad2-1* double mutant resulted in a drastic decrease of chlorophyll (Chl *a* + *b*) and  $\beta$ -carotene content. Together with the lower chlorophyll *a/b* ratio, the data highlights a significant reduction of PSII and, in particular, of PSI complexes. The relative increase of the VAZ pool size supports the extreme photosensitivity of the double mutant.

**Table 3.1** Levels of thylakoid polypeptides in *psad1-1*, *psad2-1* and *psad1-1 psad2-1* relative to WT in [%]

	<i>psad1-1</i>	<i>psad2-1</i>	<i>psad1-1 psad2-1</i> *
<b>C</b>	50	100	nd
<b>D</b>	40	90	nd
<b>E</b>	40	100	0
<b>F</b>	20	100	2
<b>G</b>	40	90	0
<b>H</b>	50	100	0
<b>L</b>	20	100	0
<b>N</b>	50	100	0
<b>O</b>	70	100	0
<b>Lhca1</b>	70	100	1
<b>Lhca2</b>	50	100	30
<b>Lhca3</b>	50	100	5
<b>Lhca4</b>	70	100	20
<b>Rieske</b>	120	110	50
<b>ATPase (<math>\alpha+\beta</math>)</b>	100	100	70
<b>ATPase (<math>\alpha+\beta</math>)*</b>	20	nd	nd
<b>PSII core*</b>	70	nd	nd
<b>OEC*</b>	70	nd	nd
<b>LHCII*</b>	70	nd	nd
<b>PSI*</b>	40	nd	nd

Signals from three independent experiments were quantified using lumi analyst 3 (Boehringer Mannheim/Roche). Quantifications of proteins based on 2-D gel analysis are indicated by an asterisk (\*). Relative values for the single mutant genotypes, reflecting the ratio of expression between the mutant and WT, were normalized on the basis of total chlorophyll content (see Table 3.2). Standard deviations were all within  $\pm 10\%$ . Relative accumulation of proteins in the double mutant were not quantified after 2-D gel analysis (Figure 3.9d), because of non-linearity of silver staining. nd = data not determined.

**Table 3.2** Pigment composition of leaves from *psad* single mutants compared to WT

Leaf pigments	<i>psad1-1</i>	<i>psad2-1</i>	WT
<b>Nx</b>	36 ± 1	33 ± 1	33 ± 1
<b>VAZ</b>	80 ± 2	39 ± 0	36 ± 3
<b>Lu</b>	121 ± 2	116 ± 1	111 ± 2
<b>β-Car</b>	67 ± 1	76 ± 2	79 ± 3
<b>Chl <i>a/b</i></b>	3.41 ± 0.03	3.46 ± 0.06	3.50 ± 0.06
<b>Chl <i>a + b</i></b>	681 ± 121	883 ± 24	907 ± 115

Leaf pigments	<i>psad1-1 psad2-1</i> *	WT*
<b>Nx</b>	58 ± 1	40 ± 1
<b>VAZ</b>	57 ± 3	24 ± 1
<b>Lu</b>	239 ± 43	130 ± 1
<b>β-Car</b>	25 ± 3	86 ± 1
<b>Chl <i>a/b</i></b>	2.38 ± 0.03	3.05 ± 0.02
<b>Chl <i>a + b</i></b>	223 ± 71	1797 ± 275

Pigment content was determined by HPLC of three plants for each genotype. The carotenoid content is given in mmol per mol Chl (*a + b*), and the Chl content is expressed as nmol Chl (*a + b*) per g FW. Mean values ± SD are shown. Nx, neoxanthin; VAZ, xanthophyll cycle pigments (violaxanthin + antheraxanthin + zeaxanthin); Lu, lutein; β-Car, β-carotene. The asterisk indicates genotypes grown on MS medium supplemented with sucrose.

### 3.5 Photosynthetic electron flow

Photosynthetic electron flow was characterized by measuring parameters of chlorophyll fluorescence and of P700<sup>+</sup> absorbance (Table 3.3). In *psad1-1* plants, the maximum quantum yield of PSII ( $F_v/F_m$ ) was reduced when compared to *psad2-1* and WT plants. Moreover, the effective quantum yield of PSII ( $\Phi_{II}$ ) was substantially decreased in *psad1-1*, but not in *psad2-1* plants. Similarly, *psad2-1* showed normal photochemical (qP) and non-photochemical (qN) quenching. In contrast, in *psad1-1* the fraction of Q<sub>A</sub>- the primary electron acceptor of PSII- present in the reduced state (1-qP), was increased by about sixfold, indicating a partial block in the electron transfer steps downstream of Q<sub>A</sub>.

Also, qN slightly increased, supporting the conclusion that, as a consequence of the perturbation in photosynthetic electron flow, the thermal dissipation of excitation energy in the antenna of PSII was higher in *psad1-1* than in WT. Only negligible alterations in the reduction rate of P700 were found in the two single-gene mutants:  $t_{1/2ox}$  was not altered in *psad2-1*, but a pronounced delay in P700 oxidation was noted for *psad1-1*, suggesting an impairment of electron transfer from PSI to ferredoxin.

State transition quenching were followed by measuring maximum PSII fluorescence signals in states 1 ( $F_m^1$ ) and 2 ( $F_m^2$ ), after irradiating plants at wavelengths that target PSII and PSI, respectively, and normalizing the values to the maximum PSII fluorescence of dark-adapted leaves ( $F_m$ ). In the WT,  $F_m^1/F_m$  and  $F_m^2/F_m$  differed significantly ( $0.84 \pm 0.02$  versus  $0.75 \pm 0.02$ ), while in the *psad1-1* mutant, the two values were essentially the same ( $0.76 \pm 0.02$  versus  $0.74 \pm 0.02$ ). This corresponds to a reduction of 70% in state transition quenching (qT) in the *psad1-1* mutant (Table 3.3), indicating a severe impairment in the redistribution of excitation energy between the photosystems. In *psad2-1*, state transition quenching was similar to that in the WT ( $F_m^1/F_m$  versus  $F_m^2/F_m$ :  $0.82 \pm 0.02$  versus  $0.75 \pm 0.01$ ).

In *psad1-1 psad2-1* double mutants, photosynthetic electron flow was severely perturbed (Table 3.4).  $F_v/F_m$  was substantially decreased as expected from a drastic reduction in the amount of active PSII centers. Moreover, the strong reduction in  $\Phi_{II}$  was consistent with the high photosensitivity of the double mutant. The drastic increase of reduced  $Q_A$  ( $1 - qP$ ) suggested that electron flow through PSII still occurred, while it was blocked at a later electron transfer step.

In summary, concerning single mutants of *psad* only a mutation in *psad1-1* alters photosynthetic electron flow, while it remains unchanged in *psad2-1* mutants. Complete lack of PSI-D in *psad1-1 psad2-1* double mutants abolished photosynthetic electron flow and resulted in a dramatically increased photosensitivity.

**Table 3.3** Spectroscopic data for *psad* single mutant and WT leaves

Parameter	<i>psad1-1</i>	<i>psad2-1</i>	WT
$F_v/F_m$	$0.77 \pm 0.02$	$0.82 \pm 0.01$	$0.83 \pm 0.01$
$\Phi_{II}$	$0.52 \pm 0.03$	$0.75 \pm 0.02$	$0.76 \pm 0.01$
<b>1 - qP</b>	$0.30 \pm 0.05$	$0.06 \pm 0.02$	$0.05 \pm 0.01$
<b>qN</b>	$0.23 \pm 0.03$	$0.14 \pm 0.01$	$0.17 \pm 0.01$
<b>qT</b>	$0.03 \pm 0.02$	$0.09 \pm 0.03$	$0.12 \pm 0.01$
$t_{1/2\text{red}}$ (msec)	$63 \pm 4$	$59 \pm 2$	$57 \pm 2$
$t_{1/2\text{ox}}$ (sec)	$1.43 \pm 0.16$	$0.54 \pm 0.06$	$0.47 \pm 0.06$

Mean values for five plants ( $\pm$ SD) are shown.  $t_{1/2\text{red}}$  and  $t_{1/2\text{ox}}$  were calculated from the recorded kinetics of P700 reduction and re-oxidation. For greenhouse-grown plants, an actinic light intensity of  $65 \mu\text{mol photons m}^{-2} \text{sec}^{-1}$  was used to drive electron transport before measuring. nd: not determined.

**Table 3.4** Spectroscopic data for *psad1-1 psad2-1* double mutant and WT leaves

Parameter	<i>psad1-1 psad2-1</i> *	WT*
$F_v/F_m$	0.40 ± 0.07	0.80 ± 0.01
$\Phi_{II}$	0.07 ± 0.01	0.76 ± 0.01
<b>1 qP</b>	0.78 ± 0.03	0.03 ± 0.01
<b>qN</b>	0.22 ± 0.08	0.05 ± 0.02
<b>qT</b>	nd	nd
<b><math>t_{1/2red}</math> (msec)</b>	nd	nd
<b><math>t_{1/2ox}</math> (sec)</b>	nd	nd

Mean values for five plants ( $\pm$ SD) are shown.  $t_{1/2red}$  and  $t_{1/2ox}$  were calculated from the recorded kinetics of P700 reduction and re-oxidation. Because of its high photosensitivity, the double mutant and WT control plants were grown under low-light conditions (15  $\mu$ mol photons  $m^{-2} sec^{-1}$ ) on MS + sucrose (indicated by an asterisk (\*)), and an actinic light intensity of 15  $\mu$ mol photons  $m^{-2} sec^{-1}$  was applied to drive electron transport before measuring. nd: not determined.

### 3.6 Expression of nuclear genes encoding chloroplast proteins in *psad1-1* mutants

To test further effects of the absence of PSI-D on photosynthesis and other chloroplast functions, the expression of nuclear genes contributing to the chloroplast proteome was determined at mRNA level by using the technique of DNA array analysis. This method was carried out on the *psad1-1* mutant, using a set of 3292 nuclear genes spotted on nylon membranes, of which 81% were coding for chloroplast-targeted proteins. The observed mRNA expression patterns were compared to those of WT as described by Kurth *et al.* (2002), Pesaresi *et al.* (2003a) and Richly *et al.* (2003). Differential gene expression values (*psad1-1* versus WT) were determined by comparing hybridization signals. Of the 1101 genes resulting in differential expression, 574 were up- and 527 downregulated. The differentially expressed genes were grouped in 13 major functional categories, including photosynthesis (dark or light reaction), metabolism, secondary metabolism, transcription, protein synthesis, protein phosphorylation, protein modification and fate, sensing, signalling and communication, stress

response and transport (Figure 3.10). In general, genes for secondary metabolism, protein modification and fate, as well as for stress response, were upregulated more than others, supporting the conclusion that the impaired function of the thylakoid electron transport chain has profound effects on plant functions not directly related to photosynthesis. Preferentially, genes involved in the light reaction of photosynthesis and transcription were downregulated, implying that a response of the plant exists, which is aiming to limit and/or compensate the perturbation in the photosynthetic electron flow by downregulating both chloroplast- and nucleus-encoded photosynthetic genes.

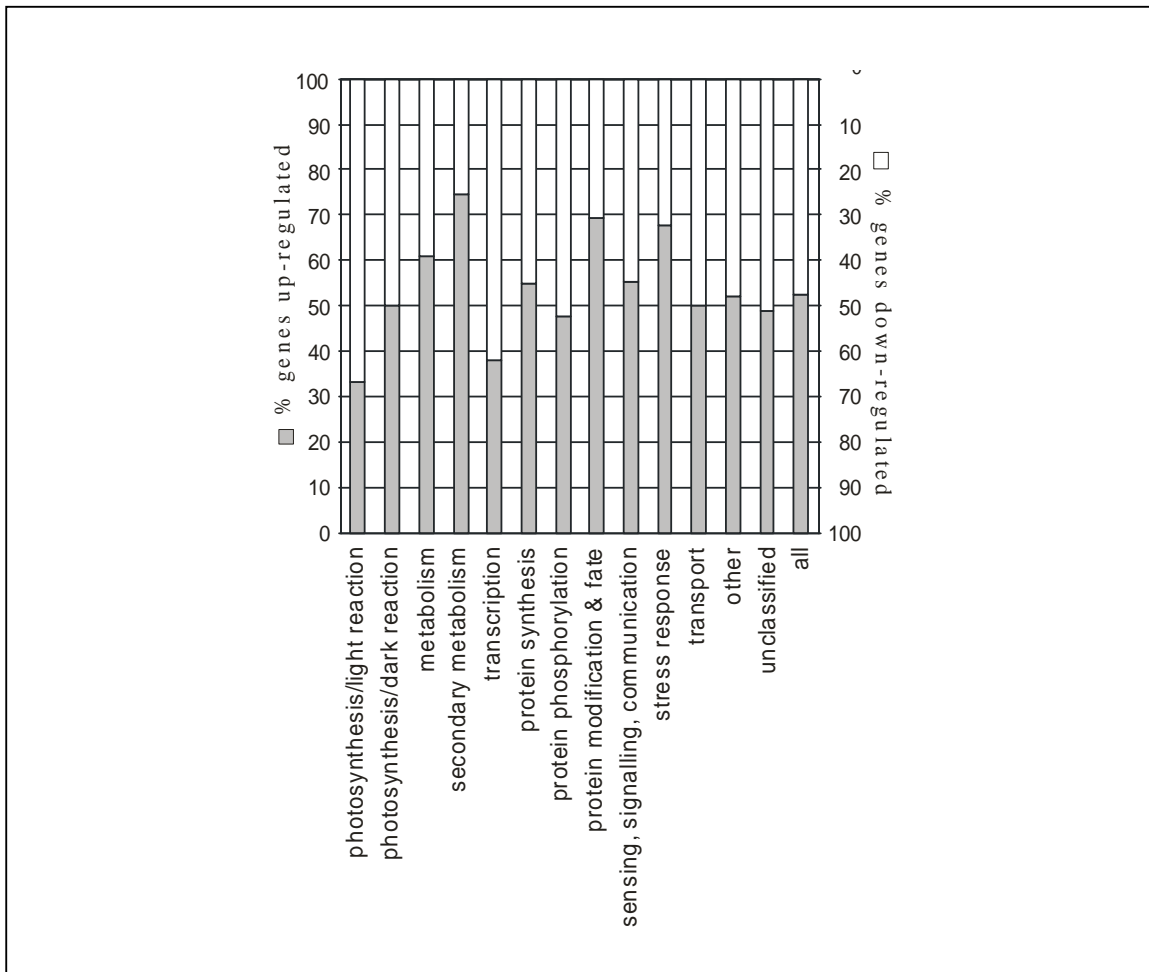


**Figure 3.10**

Effects of the *psad1-1* mutation on the accumulation of nuclear transcripts encoding chloroplasts proteins. The fraction of up- and downregulated genes in 13 major functional categories is shown. A complete list of significantly differentially expressed genes is available at GEO (<http://www.ncbi.nlm.nih.gov/geo/>), Accession number GSM11018.



## DISCUSSION

Photosystem I subunit D is a hydrophilic subunit of PSI exposed to the stromal side and known to interact with ferredoxin in both eukaryotes and cyanobacteria (Andersen *et al.*, 1992; Merati and Zanetti, 1987; Zilber and Malkin, 1988). Together with PSI-C and -E, PSI-D forms a compact interconnected structure, the so-called stromal ridge (Jordan *et al.*, 2001; Klukas *et al.*, 1999; Kruip *et al.*, 1997).

Among single-gene mutations only a lack of PSI-D1 leads to general alteration in the polypeptide composition. The characterization of *psad1-1* and *psad1-1 psad2-1* indicates that PSI-D is necessary for the stability of PSI in *Arabidopsis*, although it was shown in *Synechocystis* that PSI without PSI-D can still reduce flavodoxin (Xu *et al.*, 1994). But in *Arabidopsis*, complete lack of the D subunit leads to seedling lethality under photoautotrophic conditions. The instability of *Arabidopsis* PSI without PSI-D can be explained either by an increase in degradation of the incomplete PSI complex or by downregulation of the synthesis of PSI subunits.

The N-terminal extension of PSI-D stabilizes the interaction of PSI-C with the rest of PSI core (Naver *et al.*, 1995). Cross-linking experiments carried out in barley have suggested that PSI-D exerts its stabilizing effect via an interaction with PSI-H, an integral membrane protein located near PSI-I and PSI-L (Naver *et al.*, 1995). This is also supported by the analysis of transgenic *Arabidopsis* lines showing co-suppression of the gene encoding the PSI-H subunit, in which PSI-C is not as tightly bound to the PSI core as in the WT (Naver *et al.*, 1999). Our data are compatible with the hypothesis that PSI-D is in physical contact with PSI-H: in the *psad1-1* and *psad1-1 psad2-1* mutants, the decrease of PSI-D is, in fact, associated with a parallel reduction in the level of PSI-H. Similar decrease in the level of PSI-H was observed in *psae1-1* mutant plants, affected in another stromal subunit of PSI, PSI-E.

But unlike the *psae1-1* mutant (Varotto *et al.*, 2000a), *psad1-1* plants show also a reduction in the level of PSI-F and -N proteins (Table 3.1); a similar behaviour has been reported for antisense *F* lines (Haldrup *et al.*, 2000), supporting the observation that PSI-N co-varies with PSI-F (Pesaresi *et al.*, 2003b).

In summary, the changes of PSI polypeptide levels in *psad1-1* are comparable to those observed in the *psae1-1* mutant (Pesaresi *et al.*, 2002; Varotto *et al.*, 2000a) and in *PsaF* antisense plants (Δ*F*; Haldrup *et al.*, 2000).

Available results indicate that an alteration in the expression of any of the peripheral stromal subunits de-stabilizes the entire stromal domain of PSI. In this context, it is not surprising that as shown by Maiwald *et al.* (2003) in the *psad1-1* mutant background the mRNA expression pattern of 3292 nuclear genes, most of them coding for chloroplast proteins, is very similar to that of *psae1-1* mutants. This supports the conclusion that a decreased accumulation of either PSI-E or -D induces similar changes in the physiological state of the chloroplast.

Interestingly, the chlorophyll fluorescence parameters of *psad1-1* were also similar to those observed for *psae1-1* (Pesaresi *et al.*, 2002; Varotto *et al.*, 2000a), supporting the fact that a reduction in the level of either of these stromal proteins –which interact directly (Klukas *et al.*, 1999) –has similar effects on PSI function.

The suppression of state transitions in *psad1-1* is probably associated with a decrease in the abundance of PSI-H, the presumed docking site of LHCII (Lunde *et al.*, 2000). In *psae1-1*, a stable LHCII-PSI aggregate seems to be responsible for the suppression of state transitions (Pesaresi *et al.*, 2002).

Recently, the analysis of antisense lines with 5-60% of PSI-D showed that downregulation of PSI-D de-stabilizes PSI, results in increased photosensitivity and further in an altered thiol disulphide redox state of the stroma (Haldrup *et al.*, 2003), which is in accordance with our data.

The complementation of the *psad1-1* mutant by increasing the dosage of the *PsaD2* gene indicates that the two corresponding proteins are functionally redundant. The *psad1-1* phenotype is the result of a dosage effect of the two genes encoding the D subunit, where *PsaD2* seems to be expressed at lower level. The presence of two functional *Arabidopsis PsaD* genes raises the question of why these and other PSI genes have duplicated in the nuclear genome of *A. thaliana*. All these gene pairs for PSI-E, -H and -D appear to have originated from relatively recent segmental duplications (between 24 and 40 million years ago; Blanc

*et al.*, 2003). The persistence of two functional genes for the same protein might have been under positive selection because it might have enabled responses of the same subunit to different signal transduction pathways. This opportunity of differential regulation would allow the plant cell to react more flexibly to varying environmental stimuli. An example has been shown for the *PsaD* gene family in *Nicotiana sylvestris*, where the *PsaD1* and *PsaD2* genes are differentially expressed during leaf development (Yamamoto *et al.*, 1993).

## **4. FUNCTIONAL ANALYSIS OF PSI-D1 PHOSPHORYLATION**

Recently, protein phosphorylation was found in photosystem I. Hannsson and co-workers identified phosphorylation site at the first threonine in the N-terminus of PSI-D1, which is the first thylakoid protein shown to be phosphorylated not belonging to PSII and LHCII. This finding opens a new direction of studies in terms of possible PSI regulation by redox-controlled protein phosphorylation. In this chapter impact of PSI-D1 phosphorylation was investigated by complementing *psad1-1* mutants with the *PsaD1* gene mutated at the phosphorylation site.

## **RESULTS**

### **4.1 Detection of PSI-D1 phosphorylation by mass spectrometry**

To confirm the presence of a phosphorylation site at the N-terminus of the PSI-D1 protein, mass spectrometric analyses of isolated PSI fractions were performed.

Thylakoids were isolated from greenhouse-grown wild-type plants and loaded on a 0.4 M sucrose gradient. After overnight centrifugation thylakoids were separated in three fractions: upper LHC with free pigments, medium PSII and lower PSI. As shown in Figure 4.1a, 0.4 M sucrose gives a clear separation of the PSI and PSII band. In order to test the purity of the fractions obtained by sucrose gradient centrifugation, each of them were separated by SDS-PAGE, which were later stained with Coomassie (Figure 4.1b).

After separation of the fractions dialysis of the PSI phases were performed and samples were concentrated. It has been demonstrated before that all protein phosphorylation sites in thylakoid membranes are restricted to surface-exposed regions of membrane proteins. This was experimentally shown by the removal of all phosphopeptides from the membrane when treated with trypsin (Vener *et al.*, 2001; Bennett, 1980). Therefore, the isolated and concentrated PSI phases were digested with trypsin in order to release the surface-exposed peptides and remove the hydrophobic segments of the proteins.

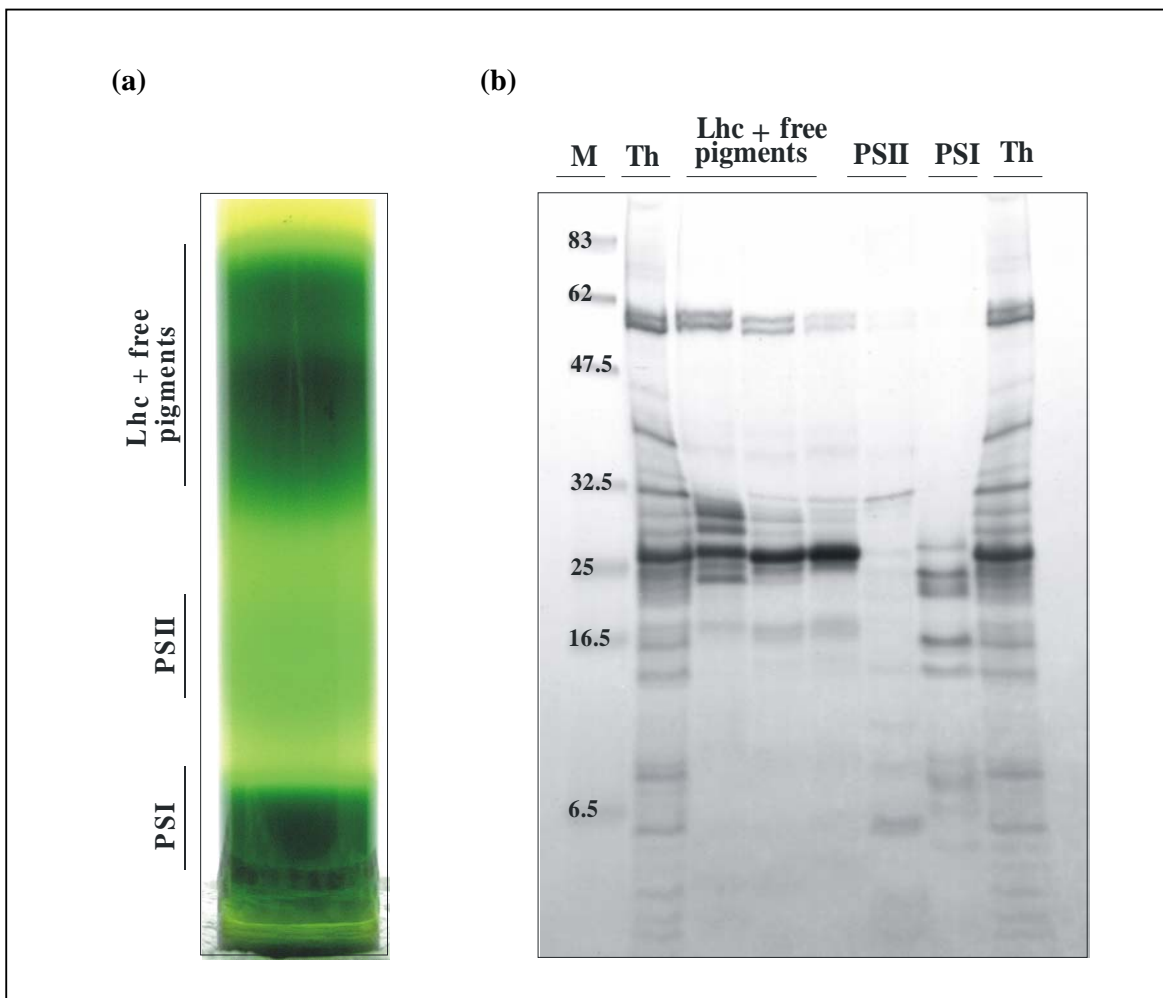


**Figure 4.1**

PSI, PSII and LHC fractions obtained after separation of thylakoid membranes on the sucrose gradient (a) were separated by SDS-PAGE and stained with Coomassie (b) in order to test purity of the isolation.

The mixtures of released hydrophilic peptides from the PSI phases were then analyzed by mass spectrometry using multidimensional protein identification technology (MudPIT) (Link *et al.*, 1999; Wu *et al.*, 2003). The ESI-ion trap instrument was employed and the SEQUEST algorithm was used to interpret the MS/MS spectra, which were subsequently Blasted against the *Arabidopsis thaliana* protein database. The presence of a PSI-D1 phosphorylation that had before been identified by Hannsson *et al.* (2003) was confirmed. The phosphorylation site was present in the detected B fragment ions (N-terminal) (Figure 4.2a). The fragmentation spectrum of detected PSI-D1 peptide ions is shown in Figure 4.2b. Additionally to previous results, two

other phosphorylation sites at serine residues belonging to the following N-terminal peptide of the PSI-D1 protein- T#DS#S#AAAAAATK- were detected (Figure 4.2a).

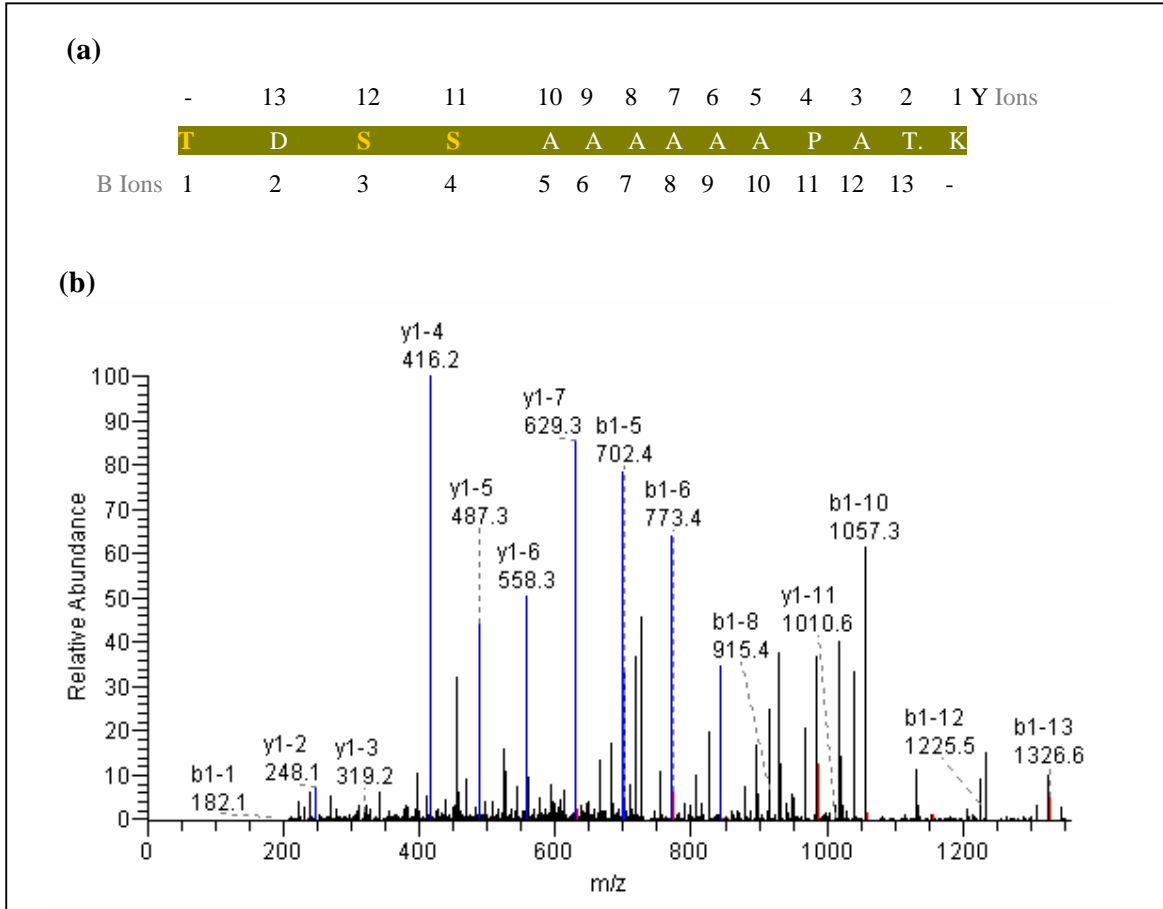


**Figure 4.2**

Identification of the phosphorylation sites (T and S) present in the N-terminal domain of the PSI-D1 protein. The product ion spectrum obtained by MudPIT is shown. **(a)** The detected B (N-terminal) and Y (C-terminal) fragment ions. **(b)** The fragmentation spectrum of detected PSI-D1 peptide ion.

#### 4.2 Complementation of *psad1-1* mutants with the *PsaD1* gene mutated at the phosphorylation site

In order to understand possible functions of the phosphorylation site present in the PSI-D1 protein, complementation of the *psad1-1* mutants with a *PsaD1* gene mutated at the phosphorylation site was attempted. This construct was under transcriptional control of the 35S promoter.

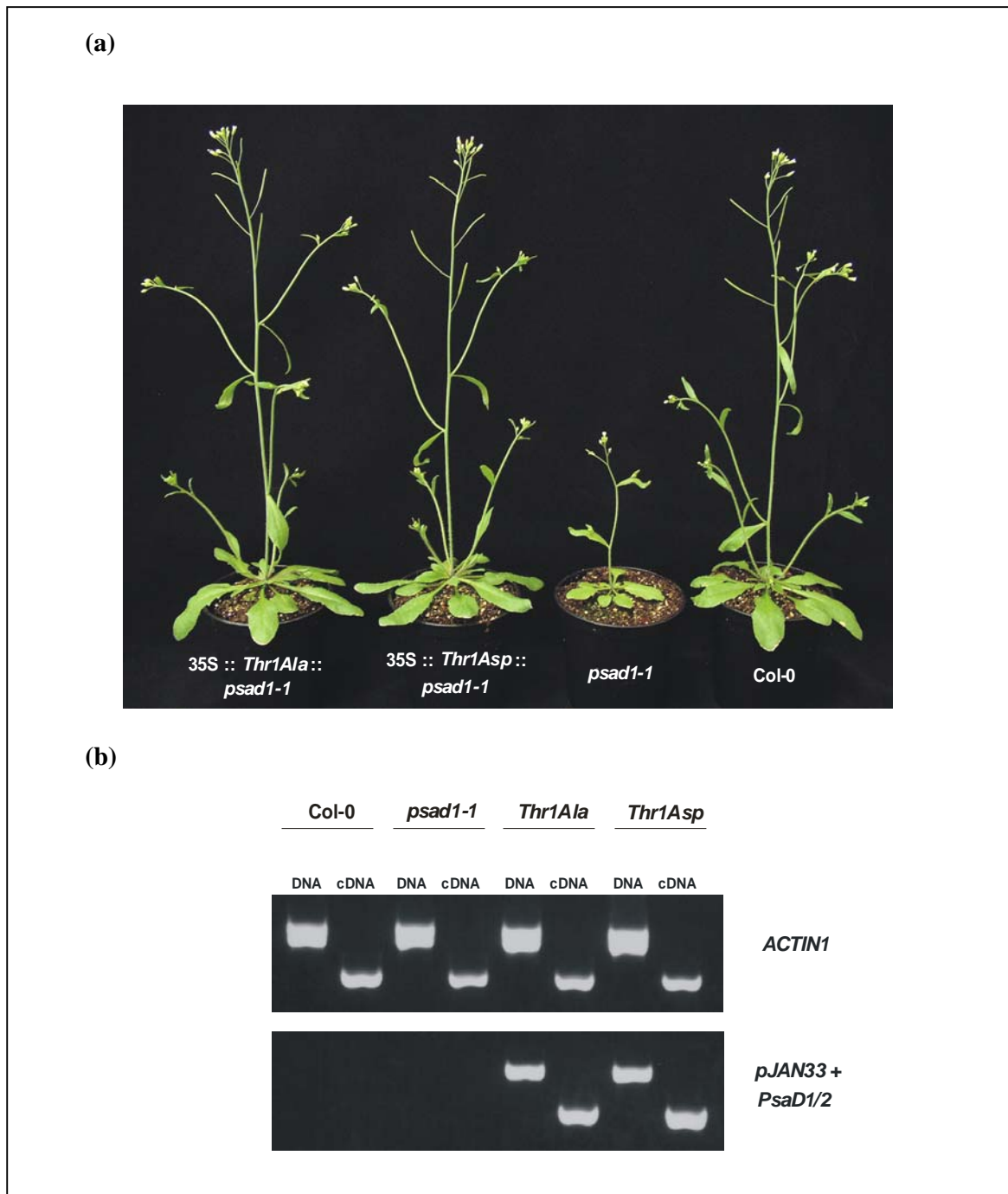


**Figure 4.3**

Complementation test of *psad1-1* mutants with the *PsaD1* gene mutated at the phosphorylation site. (a) 4 week-old WT plants, *psad1-1* mutants and T2 generation of *psad1-1* mutant plants transformed with the mutated *PsaD1*-cDNA fused to the 35S promoter. (b) Presence and overexpression of the transgene in the complemented mutant plants was confirmed by PCR and RT-PCR. Products obtained after PCR for 35 cycles with primers specific for the transgene (*PsaD1/2-441as* and *pJAN33*) were analysed on a 2.0% agarose gel. The differences in size between cDNA and DNA are due to the presence of an intron in the vector used for the complementation test. As a control, PCR with control primers for the *ACTIN1* gene was performed.

In the mutated PSI-D1 protein the residue Thr-1 had been replaced by either alanine or aspartic acid. Alanine is a neutral amino acid lacking the hydroxyl group required for the attachment of a phosphate group. Aspartic acid is an acidic residue, which has been shown to mimic phosphorylated serine in some systems (Wang, 1992).

Under greenhouse conditions both transformed *psad1-1* mutants, *35S::Thr1Ala::psad1-1* and *35S::Thr1Asp::psad1-1*, behaved like WT; they showed normal growth and leaf coloration (Figure 4.3a). Successful complementation and overexpression of the transgene were confirmed by RT-PCR analysis (Figures 4.3b).

Substitutions of the threonine by either alanine or aspartic acid were confirmed by sequencing DNA fragments isolated from *psad1-1* transformed plants, which covered the point mutations (Figure 4.4).

<b>WT</b>	5'GCC	GAG	AAA	<u>ACA</u>	GAT	TCC	TCC	GCC	GCC <sup>3'</sup>
	Ala	Glu	Lys	<b>Thr</b>	Asp	Ser	Ser	Ala	Ala
<b>Thr1Ala</b>	5'GCC	GAG	AAA	<u>GCT</u>	GAT	TCC	TCC	GCC	GCC <sup>3'</sup>
	Ala	Glu	Lys	<b>Ala</b>	Asp	Ser	Ser	Ala	Ala
<b>Thr1Asp</b>	5'GCC	GAG	AAA	<u>GAT</u>	GAT	TCC	TCC	GCC	GCC <sup>3'</sup>
	Ala	Glu	Lys	<b>Asp</b>	Asp	Ser	Ser	Ala	Ala

**Figure 4.4**

Sequences of the *PsaD1* codon mutations (underlined) and the corresponding N-terminal region of the PsaD1 protein. Mutated nucleotides and amino acids are indicated in boldface.

In plants, protein phosphorylation plays a role in response to environmental signals such as wounding (Usami *et al.*, 1995), light (Allen, 1992) or cold stress (Bergantino *et al.*, 1995). It is also involved in protein degradation and many other processes.



To test if phosphorylation of the PSI-D1 protein is involved in response to one of those cues, the influence of high light on transformed plants was investigated. Therefore, *psad1-1* plants transformed with mutated *PsaD1*, *psad1-1* mutants and Col-0 plants were grown for 5 weeks under high light stress. As shown in Figure 4.5 there were no visible differences between WT plants and *psad1-1* mutants transformed with the mutated *PsaD1* gene.

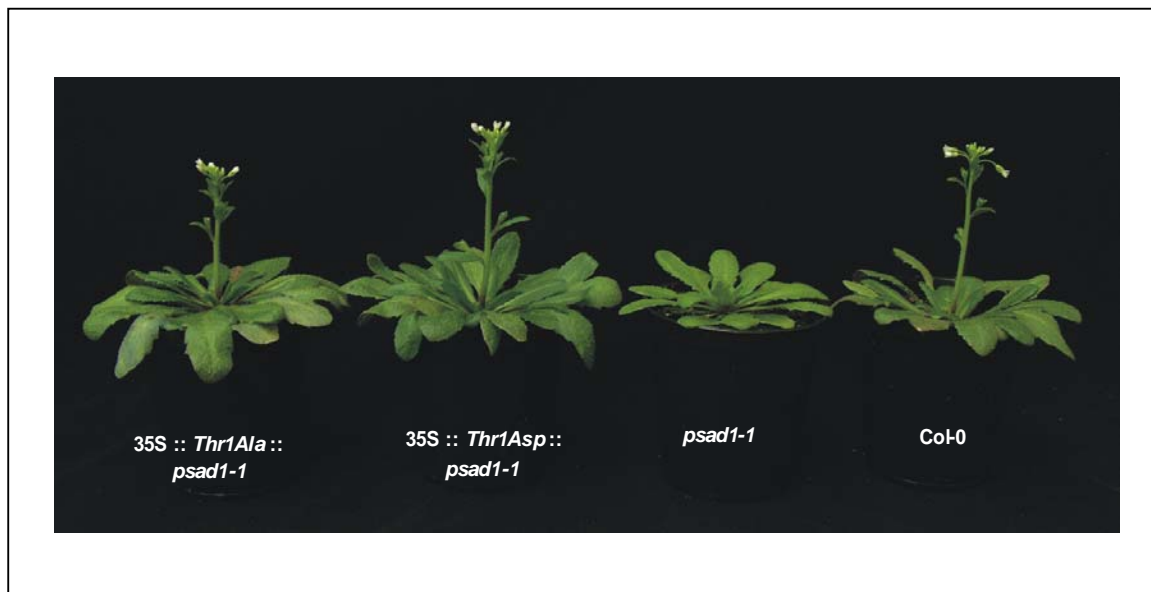


**Figure 4.5**

Phenotypes of 35S::*Thr1Ala*::*psad1-1* and 35S::*Thr1Asp*::*psad1-1* transformed plants. WT, *psad1-1* and T2 generation of *psad1-1* mutant plants transformed with the mutated *PsaD1* gene (6 weeks old) were grown in the growth chamber under high-light conditions.

For determination of thylakoid protein phosphorylation *in vivo*, photosynthetic membranes were isolated from WT as well as from *psad1-1* mutant leaves. These were first labeled with [ $P^{33}$ ] orthophosphoric acid and then exposed to different light conditions ( $80 \mu\text{mol photons m}^{-2} \text{s}^{-1}$ , 2 h for low light adaptation,  $800 \mu\text{mol photons m}^{-2} \text{s}^{-1}$ , 2 h for high-light stress and dark adaptation). Thylakoid proteins were then separated by SDS-PAGE and incorporation of radioactivity was detected by phosphoimager (Figure 4.6) (data shown only for low-light adaptation). According to the high sensitivity of this method and the lack of clear detection of the PSI-D1 phosphopeptide, it can be assumed that the level of PSI-D1 phosphorylation is relatively low.

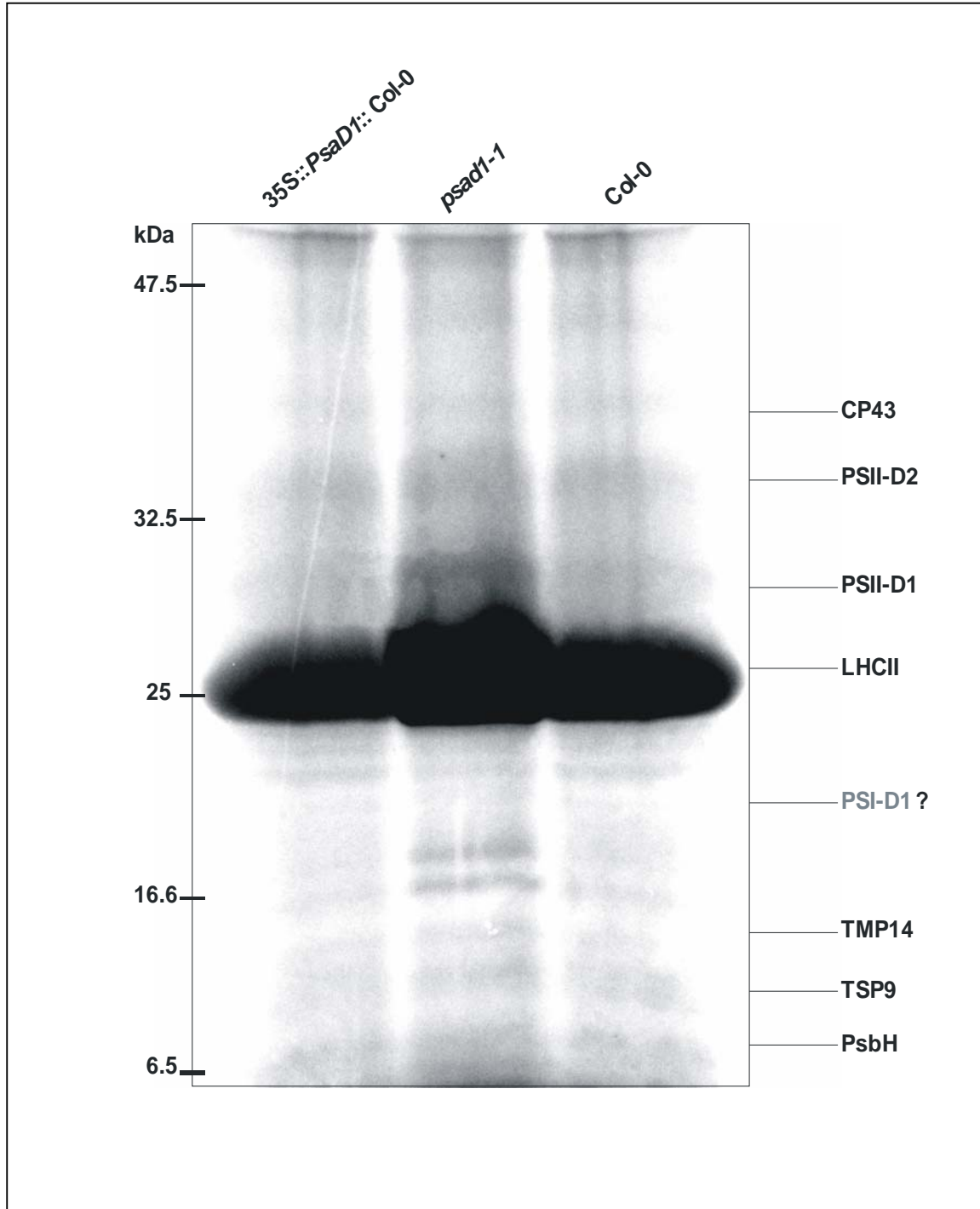


**Figure 4.5**

*In vivo* phosphorylation of thylakoid proteins from WT plants, *psad1-1* mutants transformed with *PsaD1*-cDNA fused to the 35S promoter (35S::*PsaD1*::*psad1-1*) and *psad1-1* mutants grown under low light. Thylakoids were separated by SDS-PAGE. Incorporation of radioactivity was detected by phosphoimager (Storm 860, Molecular Dynamics).

## DISCUSSION

PSI-D is a key subunit in the assembly and functionality of PSI. It was shown that the Ycf3 protein, which is essential for the accumulation of the PSI complex, interacts directly with the PSI-D subunit (Naver, 2001). It has been also demonstrated that PSI-D is the first nuclear-encoded subunit, accumulating in the thylakoid membranes during the greening of etiolated seedlings (Lotan, 1993). Together with the two other subunits exposed to the stromal side of PSI, which are PSI-E and PSI-C, it is directly involved in the binding of ferredoxin. As it was shown in this thesis, the complete lack of the D subunit in *Arabidopsis thaliana* leads to seedling lethality under photoautotrophic conditions (see Chapter 3).

As compared to its cyanobacterial orthologue, the mature PSI-D subunit from eukaryotic species contains an N-terminal extension of 20-30 amino acid residues. It was shown before by Hannsson and Vener (2003) and confirmed in this work that the N-terminus of the PSI-D1 protein contains phosphorylated serine/threonine residues. In order to verify presence of phosphorylation sites in PSI-D1 protein the ESI-ion trap instrument was employed and the SEQUEST algorithm was used to interpret the MS/MS spectra. Series of detected B fragment (N-terminal) and Y fragment (C-terminal) ions indicated that the N-terminus of PSI-D1 protein is very likely to be phosphorylated. Additionally to previous results, two other phosphorylation sites at serine residues belonging to the following N-terminal peptide of the PSI-D1-T#DS#S#AAAAAAPATK- were detected.

Protein phosphorylation, which is one of the most widespread and not arguably best understood posttranslational modifications, is involved in regulation of many cellular processes in plants. The identification of phosphorylation sites is necessary for functional analysis of particular phosphoproteins. Following reasons contribute to the relevance of the discovery of PSI-D1 phosphorylation. Firstly, it is the first phosphopeptide found in photosystem I. All phosphopeptides identified so far belong to photosystem II and its antenna complex. These phosphopeptides were shown to be involved either in the regulation of the light energy distribution between the two photosystems or in the light-induced turnover of PSII reaction center subunits.

Secondly, phosphorylation sites that have been identified in PSI-D1 protein are located in the N-terminal domain that is specific for eukaryotes and not present in its cyanobacterial counterpart. This N-terminus of PSI-D is exposed to the stromal side of PSI as has recently been demonstrated by Ben-Shem *et al.* (2003). In agreement with this finding is that all of the phosphorylation sites, which have been detected so far, are restricted to stromal-exposed regions of membrane proteins. This stromal exposure of the N-terminus allows attachment of phosphate groups by kinase signaling pathways from the stroma.

In order to understand possible functions of the PSI-D1 phosphorylation, complementation analysis were performed. No differences were observed when phosphorylated threonine (Thr-1) was replaced by alanine, which lacks the hydroxyl group required for attachment of a phosphate group. The *psad1-1* phenotype was also complemented when *PsaD1* instead of Thr-1 contained aspartic acid; residue that was shown previously to mimic phosphorylated serine in some systems (Wang, 1992). Under greenhouse conditions both *35S::Thr1Ala::psad1-1* and *35S::Thr1Asp::psad1-1* expressed in *psad1-1* background, showed normal growth and leaf coloration. Also when grown under high light conditions no differences have been observed between *psad1-1* containing above described transgenes, *psad1-1* mutants and WT plants. Even though phosphorylation of PSI-D1 protein does not seem to be involved in adaptation to high light stress, it can not be excluded that it plays a role in adaptation to other environmental conditions not tested in these analyses. In general, it can be assumed that the level of PSI-D1 phosphorylation is relatively low, as PSI-D1 phosphopeptide can not even be detected by such highly sensitive method as *in vivo* labeling with [ $P^{33}$ ] orthophosphoric acid.

Another interesting aspect is that the biogenesis and assembly of PSI-D with PSI was found to proceed in a rather unusual way (Cohen *et al.*, 1992; Minai *et al.*, 1996 and 2001). One open question is if phosphorylation is involved in this process. The precursor PSI-D (pre-PSI-D) is first assembled with PSI and then the precursor protein is processed, yielding mature PSI-D associated with PSI. This processing, which form the mature PSI-D is most probably accompanied by a conformational change that allows the formation of electrostatic interactions between PSI-D and PSI. Protein phosphorylation has been proposed to be involved in conformational changes of proteins located in thylakoid membranes (Croce, 1996).

Most probably these electrostatic interactions between PSI-D and PSI also play a role in PSI-D protection from proteolytic digestion, while mature PSI-D is resistant to proteolysis only when located in the thylakoid membranes (Minai *et al.*, 1996).

The PsaD protein has only a few elements of secondary structure and no stable three-dimensional structure in solution, whereas it forms a well defined three-dimensional structure after assembling with PSI- with an antiparallel four-stranded  $\beta$ -sheet followed by a second two-stranded  $\beta$ -sheet and a short loop connecting the fourth  $\beta$ -strand to the only  $\alpha$ -helix (Antonkine, 2003; Fromme, 2001). It has already been suggested by Hansson *et al.* (2003) that “significant structural changes and flexibility of PSI-D together with its control position at the electron acceptor site of PSI may be employed by regulatory mechanisms operating via protein phosphorylation”.

Overall, due to our complementation analysis of *psad1-1* mutant plants with the mutated *PsaD1*, it can be assumed that phosphorylation of PSI-D1 protein does not play a key function in the PSI regulation. Anyhow, it can not be excluded that PSI-D1 phosphorylation might play a role, if plants are grown under particular environmental conditions, not tested in these analyses.

The distinct function of the additional N-terminus sequence of the eukaryotic PSI-D1 protein, in which phosphorylation sites have been detected, is unknown. Some authors have suggested that the N-terminal extension of PSI-D is required for an efficient cleavage of the transit peptide (Cohen *et al.*, 1992). In other studies this N-terminal domain was shown to stabilize the interaction of PSI-C with the rest of the PSI core (Naver *et al.*, 1995). PSI-D is not the only PSI subunit containing the N-terminal extension that is specific for eukaryotes. Also PSI-E, which is another stromal subunit of PSI contain such extension. In order to understand the functions of these N-terminal extensions, as well as clarify the role of PSI-D1 phosphorylation, further molecular, biochemical and physiological studies are in progress. The biological consequences of a lack of these N-terminal domains and their importance for photosynthesis in plants are being analysed.

## **5. EFFECTS OF *psad1-1* AND *psae1-3* MUTATIONS ON THE LEVEL OF THYLAKOID PROTEIN PHOSPHORYLATION**

The changes of PSI polypeptide levels in *psad1-1* are similar to those observed in the *psae1-1* mutant (Pesaresi *et al.*, 2002; Varotto *et al.*, 2000a). Moreover, available results indicate that alterations in the expression of any of the peripheral stromal subunits de-stabilize the entire stromal domain of PSI. The mRNA expression pattern of 3292 nuclear genes, most of them coding for chloroplast proteins, is very similar for the *psad1-1* and *psae1-1* mutants (Maiwald *et al.*, 2003). Additional similarities between these two mutations concern alterations in the photosynthetic electron flow, state transition and general polypeptide composition of thylakoid membranes. Further interesting effects of *psad1-1* and *psae1-3* mutations concerning changes in phosphorylation level of thylakoid proteins are described in this chapter.

### **RESULTS**

#### **5.1 The level of thylakoid protein phosphorylation is significantly higher in *psad1-1* and *psae1-3* mutants**

For the determination of thylakoid protein phosphorylation in *psad1-1* mutants, *in vivo* labelling with  $^{33}\text{P}$ -orthophosphate has been performed (see Chapter 4). Interestingly, in *psad1-1* mutants significantly higher levels of thylakoid protein phosphorylation as compared to WT plants were observed. As several similarities in physiological/biochemical properties exist between *psad1-1* and *psae1-3* mutants, and as both subunits PSI-D and PSI-E are located on the stromal side of PSI, experiments were carried out to investigate if these mutations also have a comparable effect on the level of thylakoid protein phosphorylation. In order to examine level of thylakoid protein phosphorylation, thylakoid membranes from WT, *psad1-1* and *psae1-3* mutant leaves were isolated in the presence of an inhibitor of dephosphorylation and then separated by gradient SDS-PAGE (Figure 5.1). When filters were hybridized with phosphothreonine antibodies, significantly higher levels of protein phosphorylation were

detected in *psad1-1* and *psae1-3* mutants. Furthermore, some additional phosphopeptides were detected in both mutants, which could not be observed in WT (Figure 5.1b).

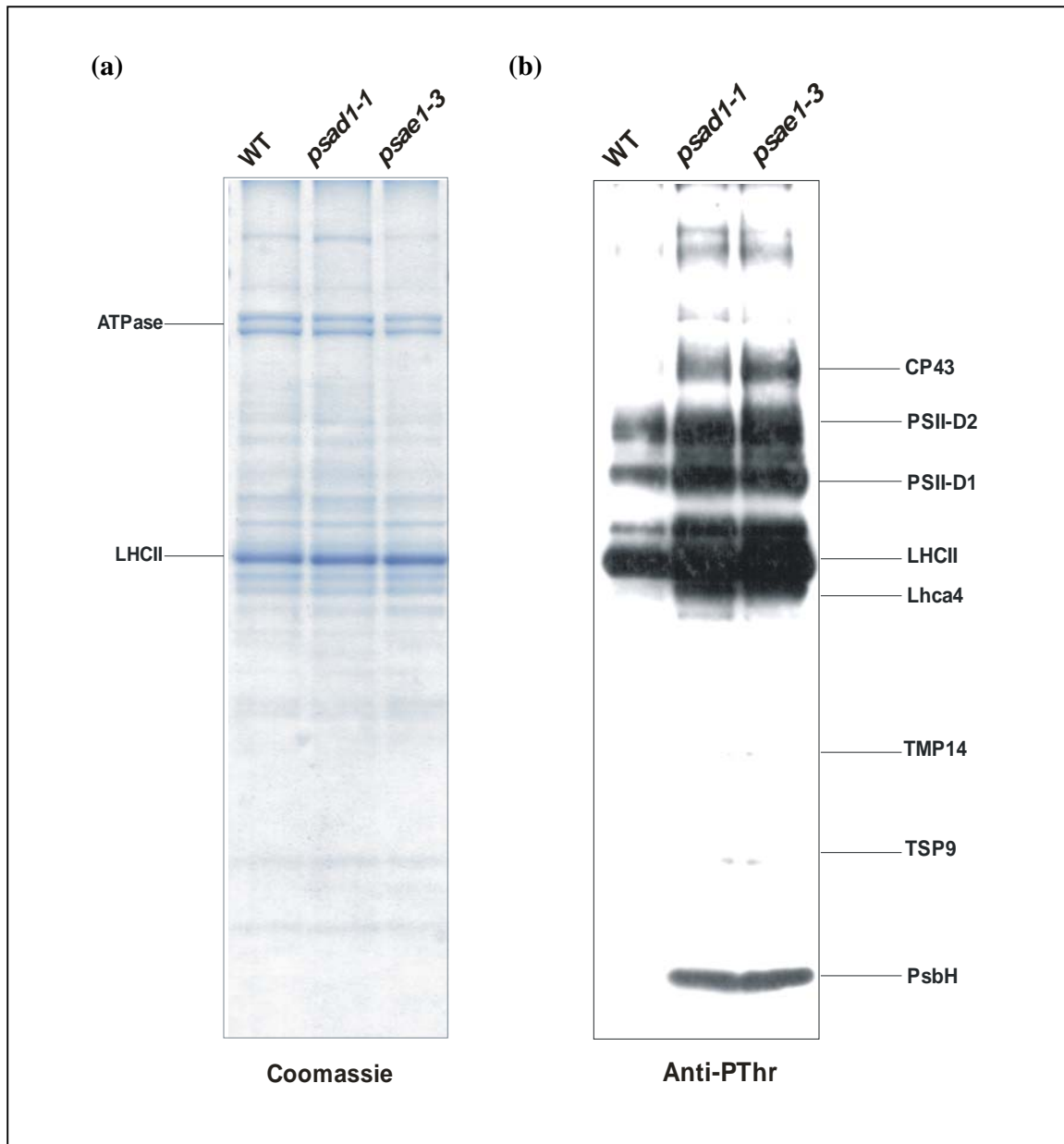


**Figure 5.1**

Level of protein thylakoid phosphorylation in WT, *psad1-1* and *psae1-3* mutant plants. Thylakoid proteins corresponding to 5  $\mu$ g of chlorophyll from WT, *psad1-1* and *psae1-3* mutants were separated by SDS-PAGE. Corresponding amounts of loaded thylakoid proteins were checked by Coomassie-blue staining (a). Immunolabelling was performed with antibodies against phosphothreonine (b). Three independent experiments were performed and representative results are shown.

## 5.2 Identification of Lhca4 phosphorylation

With respect to the above mentioned increase in overall thylakoid protein phosphorylation in *psad1-1* and *psae1-3* mutants the question arised, if these mutations also show an effect on the phosphorylation state of PSI proteins.

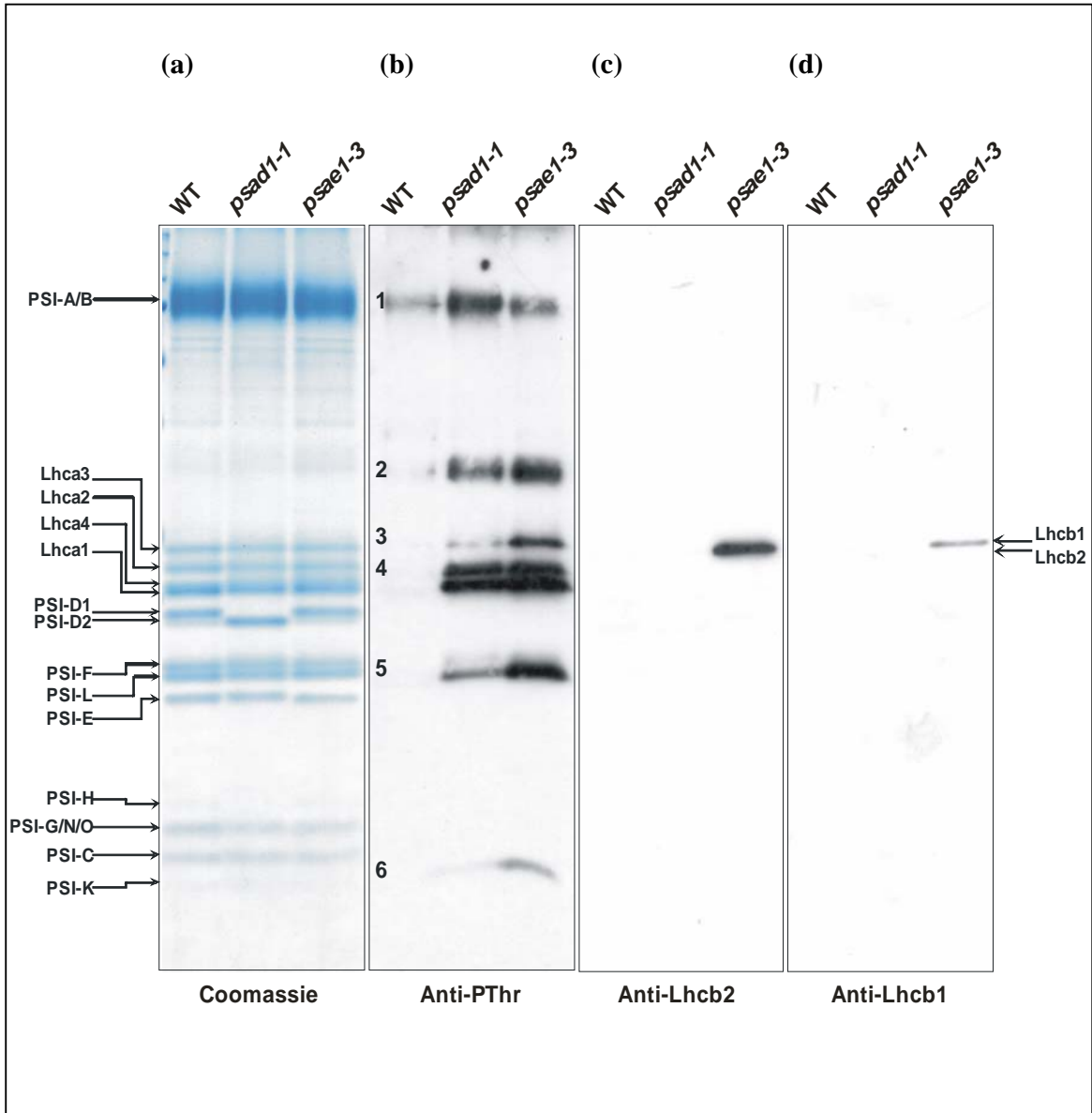


**Figure 5.2**

PSI complexes from WT, *psad1-1* and *psae1-3* mutant plants, corresponding to 5  $\mu$ g of chlorophyll, were separated by SDS-PAGE. Corresponding amounts of loaded PSI proteins were checked by Coomassie-blue staining (a). Immunolabelling was performed with antibodies raised against the phosphothreonine (b), Lhcb2 (c) and Lhcb1 (d). Three independent experiments were performed, and representative results are shown.



To answer this, thylakoid membranes were isolated from WT, *psad1-1* and *psae1-3* mutants and subsequently PSI complexes were separated on a 0.4 M sucrose gradient (see Chapter 4). Immunological analyses with antibodies raised against phosphothreonine were performed. Interestingly and surprisingly some new, unknown phosphopeptides could be detected in PSI complexes isolated from *psad1-1* and *psae1-3* mutants (Figure 5.2 b). So far, the only protein in PSI that has been reported to be phosphorylated was PSI-D1 (see Chapter 4).

It was shown before by Pesaresi *et al.* (2002) that a stable LHCII-PSI aggregate exists in *psae1-1* mutants, which causes suppression of state transitions observed in that mutation. When thylakoid membranes from *psad1-1* mutants were separated by LDS-PAGE, only a slight band was observed indicating that small amount of such aggregate might also exist in this mutant (band indicated by an asterisk (\*) in Figure 5.3).

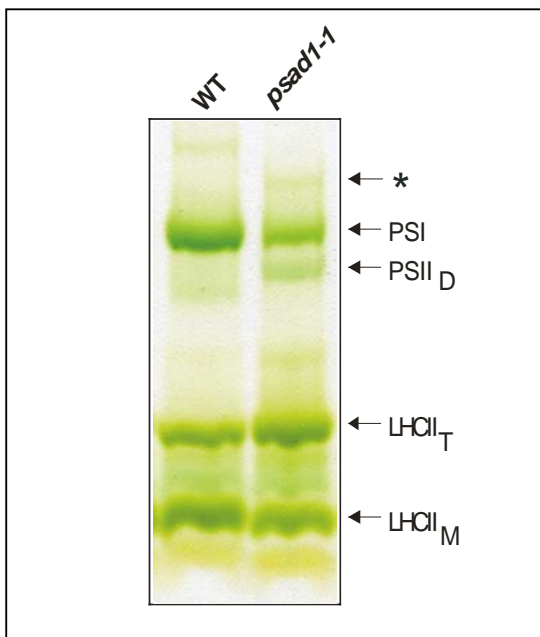
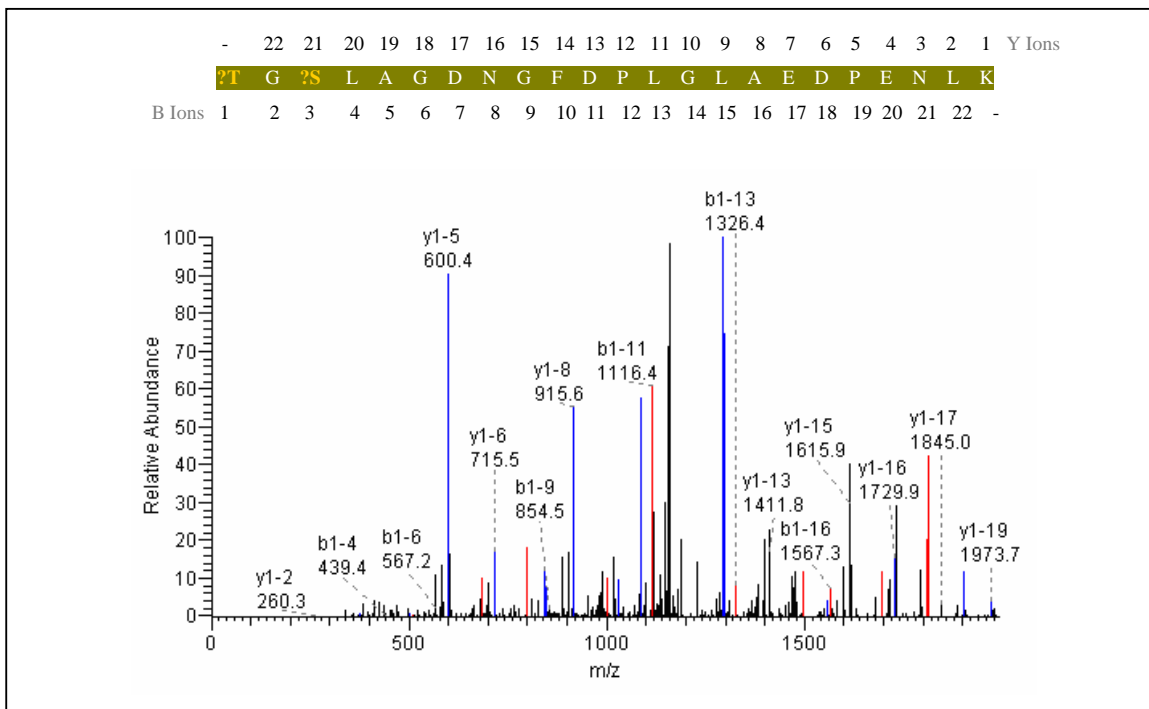


**Figure 5.3**

Native gel analysis. Thylakoid membranes corresponding to 30  $\mu$ g of chlorophyll from WT and *psad1-1* were fractionated by electrophoresis on a LDS-PA gel. The bands were assigned to PSI, photosystem II dimers (PSII<sub>D</sub>), LHCII trimers (LHCII<sub>T</sub>) and monomers (LHCII<sub>M</sub>). Asterisk (\*) indicate the position of the mutant-specific band that have previously been detected in *psae1-1* mutant by Pesaresi *et al.* (2002).

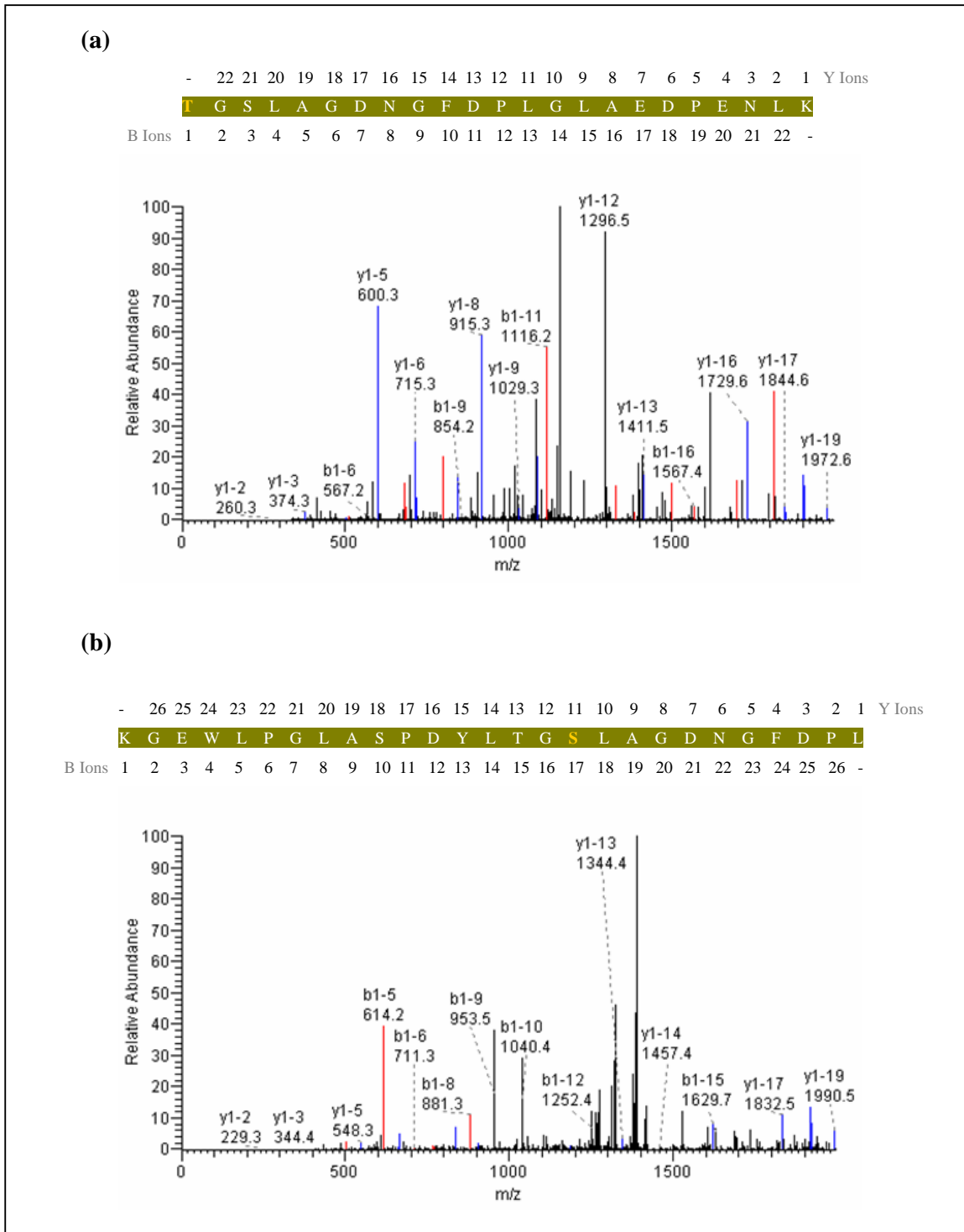
Accordingly, it is possible that some of phosphopeptides, detected with phosphothreonine antibodies in *psad1-1* and *psae1-3* mutants, belong to LHCII. Previously it has been demonstrated that when the mobile pool of LHCII becomes phosphorylated, it migrates from PSII-containing grana to the PSI-rich stromal lamellae and attaches to PSI (Lunde *et al.*, 2000). In this project Western analyses were performed using antibodies against Lhcb1 and Lhcb2, two major subunits of the mobile pool of LHCII. In accordance to previous data (Pesaresi *et al.*, 2002) significant amounts of Lhcb2 and also of some Lhcb1, were present in the PSI isolated

from *psae1-3* mutants (Figure 5.2c, d). Even after saturation of the signals (data not shown) only weak bands of Lhcb1 and Lhcb2 were observed in *psad1-1* mutants. Regarding the above mentioned immunoblot analysis with Lhcb1 and Lhcb2 antibodies, it seems very likely that some of the phosphopeptides (band 3 in Figure 5.2) detected in *psae1-3* mutants belong to LHCII. Might be that small amount of phosphorylated mobile pool of LHCII is attached to PSI also in *psad1-1* mutants (band 3 in Figure 5.2 and band indicated by an asterisk in Figure 5.3). The phosphopeptides detected by immunoblot analyses were further analysed by mass spectrometry using multidimensional protein identification technology (MudPIT). PSI fractions isolated from *psad1-1* and *psae1-3* mutants were digested with trypsin to release the surface-exposed peptides and remove the hydrophobic segments of the proteins. After digestion, samples were analysed by LC-ESI MS/MS- method in which peptide ions are introduced to the mass spectrometer in the gas phase. The SEQUEST algorithm was used to interpret the MS/MS spectra. In PSI fractions isolated from both *psad1-1* and *psae1-3* mutants, phosphorylation sites have been identified in peptides belonging to a 22-kDa protein - Lhca4. The fragmentation spectra of chosen Lhca4 phosphopeptides are shown in Figure 5.4 and 5.5.



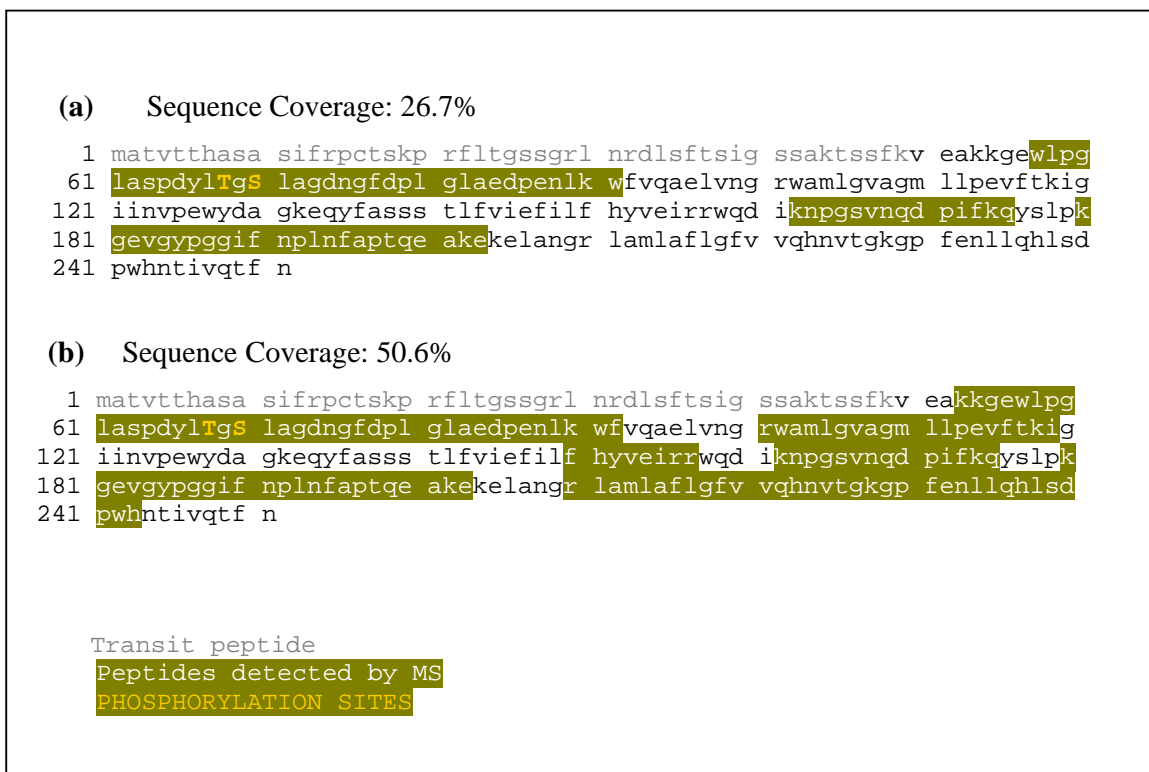
**Figure 5.4**

Identification of phosphopeptide belonging to the N-terminus of Lhca4 protein. Phosphopeptide was detected in PSI phase isolated from *psad1-1* mutants. Shown is the product ion spectrum obtained by MudPIT and detected B (N-terminal) and Y (C-terminal) fragment ions. The exact phosphorylation site (T or S) is unclear.

**Figure 5.5**

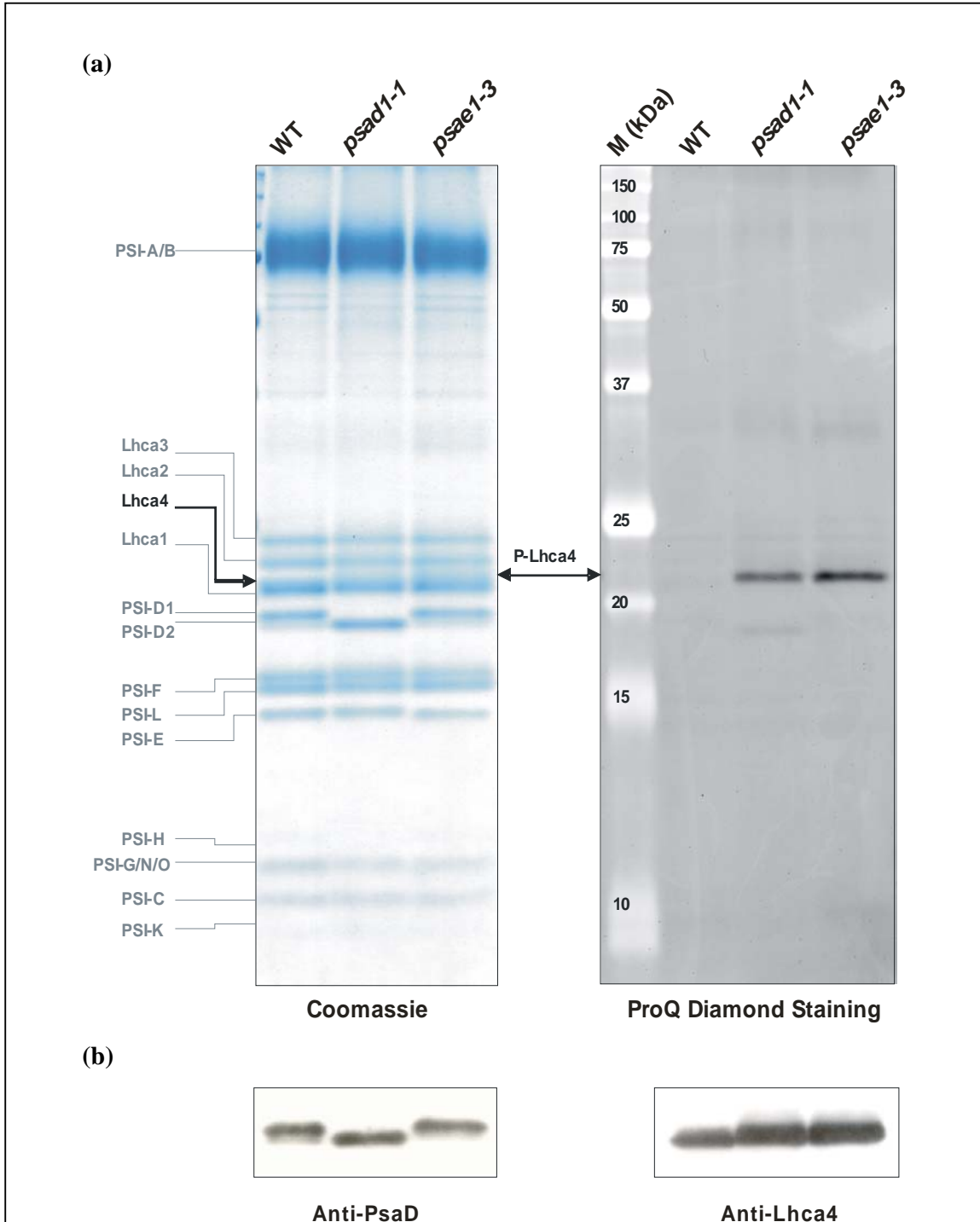
Identification of threonine (T) **(a)** and serine (S) **(b)** phosphorylation present in N-terminus of Lhca4 protein. Phosphopeptides were detected in PSI phase isolated from *psae1-3* mutants. Shown are the product ion spectra obtained by MudPIT and detected B (N-terminal) and Y (C-terminal) fragments ions.

The series of B (N-terminal) and Y (C-terminal) fragment ions revealed the peptides sequences belonging to Lhca4 protein. The spectrum shown in Figure 5.4 indicates that peptide, which has been detected in *psad1-1* mutant, is very likely to be phosphorylated, but also that the exact phosphorylation site remains unclear. In the PSI fraction isolated from *psae1-3* mutants also some phosphopeptides were detected, all belonging to Lhca4 protein. Both serine and threonine residues were shown to be likely phosphorylated (Figure 5.5). In both mutants these novel phosphorylation sites were detected in the N-terminal part of Lhca4 protein. Peptides detected in PSI fraction isolated from *psad1-1* mutants cover 26.7% of the amino acid sequence of the Lhca4 protein (Figure 5.6a); in *psae1-3* mutants sequence coverage is even higher - 50.6% (Figure 5.6b).



**Figure 5.6**

The amino acid sequences of the *Arabidopsis* Lhca4 protein (Accession numbers: At3g47470). Peptides which were detected in PSI fraction from *psad1-1* mutants cover 26.7% of the sequence of Lhca4 protein **(a)**, in *psae1-3* mutants sequence coverage is 50.6% **(b)**.

**Figure 5.7**

PSI complexes isolated from WT, *psad1-1* and *psae1-3* mutant plants, corresponding to 5  $\mu$ g of chlorophyll, were separated by SDS-PAGE. Corresponding amounts of loaded PSI proteins were checked by Coomassie-blue staining and stained with Pro-Q® Diamond phosphoprotein gel stain (a). Immunolabelling was performed with antibodies raised against PsaD and Lhca4 (b). In *psad1-1* and *psae1-3* mutants, additional SDS-PAGE bands appeared when filters were hybridized with antibodies against Lhca4 protein.

Furthermore, mass spectrometry results are in agreement with the Western analysis. Filters hybridized with antiphosphothreonine antibodies showed bands slightly bigger than 22 kDa in both *psad1-1* and *psae1-3* mutants that were not present in WT (Figure 5.2b).

Moreover, double bands were detected in *psad1-1* and *psae1-3* mutants by immunoblotting with the Lhca4 antibody (Figure 5.7b). This could be explained by a slower-migrating, phosphorylated form of the Lhca4 protein, additional to a faster-migrating non-phosphorylated one. These results were confirmed by the Pro-Q® Diamond phosphoprotein gel stain – technology, which uses a novel fluorophore that recognizes phosphate groups on proteins and peptides directly on the gels. When PSI complexes isolated from *psad1-1* and *psae1-3* mutants were separated by gradient SDS-PAGE and stained with Pro-Q® Diamond, again bands of about 22-kDa were visible on the gel (Figure 5.7a).

## DISCUSSION

Although light-induced phosphorylation of thylakoid proteins has already been intensively studied, there are many open questions still to be answered. The most abundant phosphoproteins in thylakoids belong to PSII and its light-harvesting complex. Among them are the D1 and D2 reaction center proteins, the 43-kDa chlorophyll *a*-binding protein, PsbH, as well as Lhcb1, Lhcb2 and Lhcb4, of which the latter ones are part of LHCII. Recently, protein phosphorylation was found in thylakoid membranes outside of PSII and LHCII (see Introduction, Chapter 4).

During this work an immunological approach using a polyclonal phosphothreonine antibody was applied for the analysis of thylakoid protein phosphorylation *in vivo*. Using this approach the same PSII core and LHCII phosphoproteins earlier identified by radiolabeling experiments were recognized, which is in accordance to other studies (Rintamäki *et al.*, 1997, see also Chapter 4). But interestingly, the levels of thylakoid protein phosphorylation were significantly higher in *psad1-1* and *psae1-3* mutants as compared to WT plants. Not only phosphorylation of already known proteins was increased, but also new phosphoproteins were shown to exist in *psad1-1* and *psae1-3* mutants. Even the level of PSI phosphorylation was affected by these mutations, which is striking as the only PSI phosphopeptide detected so far was the PSI-D1 protein (see Chapter 4). In this work presence of other unknown phosphopeptides belonging to the PSI complex have been shown.

A possible explanation for the high levels of protein phosphorylation in both mutants could be an over-reduction of the plastoquinone pool. The reduction of the plastoquinone pool together with its binding to the quinol-oxidation site of a cytochrome *b6/f* complex was shown to play a key role in the regulation of protein phosphorylation in thylakoid membranes (see Introduction). It is also well known that oxidation of the plastoquinone pool is caused by excess stimulation of PSI. Biochemical data of *psad1-1* and *psae1-3* mutants indicate that several alterations exist in the polypeptide composition of PSI complexes. Moreover, it was shown that mutations in both *psad1-1* and *psae1-3* cause similar alterations in photosynthetic electron flow. Spectroscopic data indicate an impairment of electron transfer from PSI to ferredoxin (see Chapter 3), supporting the view that a reduction in amount of either of these stromal-exposed

proteins has a similar effects on PSI functions. Taken together these data, it can be assumed that in *psad1-1* and *psae1-3* plants, PSII reduces more plastoquinone than can be reoxidized by PSI. As a result, the plastoquinone pool is over-reduced and a significantly higher level of thylakoid protein phosphorylation is observed. It was already suggested by Haldrup *et al.* (2003) that a lower content of PSI in the antisense D plants leads to over-reduction of the plastoquinone pool and therefore to PSII photoinhibition in plants.

A striking feature of *psae1* mutants is the presence of a stable LHCII-PSI complex, which is associated with an almost complete suppression of state transition, a drastic increase in the levels of phosphorylated LHCII and a permanent reduction in PSII antenna size (Pesaresi *et al.*, 2002). The presence of Lhcb1 and Lhcb2 proteins associated with the PSI complex were confirmed in these studies by Western analysis of PSI isolated from *psae1-3* mutants. Regarding the native gel and immunoblot analyses, it seems very likely that at least two phosphopeptides detected in *psae1-3* mutants belong to the major subunits of the mobile LHCII pool and that most probably small amounts of Lhcb1 and Lhcb2 are also attached to PSI in *psad1-1* mutants.

The recent progress in mass spectrometry (MS) techniques and methods of proteomics allowed the successful identification and analysis of one previously unknown phosphoprotein Lhca4 detected in *psad1-1* and *psae1-3* mutants. This is the first phosphorylated light-harvesting protein outside of LHCII. Some peptides belonging to Lhca4, which were detected by MS in *psad1-1* and *psae1-3* mutants, are very likely to be phosphorylated. The novel phosphorylation sites were detected in the N-terminal part of the protein. This N-terminus contains two residues in near vicinity, serine (Ser-2) and threonine (Thr-1), which are possible targets of phosphorylation. In the case of phosphopeptides detected in *psae1-3* PSI, it seems likely that both serine (Ser-2) and threonine (Thr-1) residues are phosphorylated. Since the threonine (Thr-1) was the first residue of the detected phosphopeptide in *psad1-1* PSI, MS was unable to detect this signal. Therefore, the exact phosphorylation site in the phosphopeptide identified in *psad1-1* mutant has not been determined. There is a hint that the serine residue might be the phosphorylated one.



The localization of serine/threonine phosphorylation sites at the N-terminal of the Lhca4 protein is in agreement with previous studies. All PSII and LHCII phosphopeptides identified so far belong to the N-terminus of the protein located at the stromal surface of the thylakoid membranes (Michael and Bennett, 1987 and 1989), mostly at threonine residues. Phosphorylation of other residues, like serine and tyrosine, were also reported (Garcia and Lucero, 1990; Tullberg *et al.*, 1998) but those phosphoproteins were not well characterized. Peptides detected in the PSI fraction isolated from *psad1-1* mutants cover 26.7% of the amino acid sequence of the Lhca4 protein while even 50.6% of sequence was covered in *psae1-3* PSI.

The Western analysis conducted in this thesis supports the above mass spectrometry data. Using antibody against Lhca4, two bands could be detected in *psad1-1* and *psae1-3* mutants. This could be explained by a slower-migrating, phosphorylated form of the Lhca4 protein, additional to a faster-migrating non-phosphorylated one. Moreover, by immunoblotting with antiphosphothreonine antibodies bands slightly bigger than 22 kDa were detected in both *psad1-1* and *psae1-3* mutants. Furthermore, these results are in agreement with Pro-Q® Diamond phosphoprotein gel stain. Using this approach phosphorylated proteins of about 22 kDa were detected in PSI isolated from *psad1-1* and *psae1-3* mutants.

Lhca4 was the first LHCI protein that was functionally investigated, employing antisense plants, in *Arabidopsis thaliana* (Zhang *et al.*, 1997). Because transgenic plants of undetectable Lhca4 level did not show any phenotype it was suggested that Lhca4 is not essential for photosynthesis in plants. The unique feature of all LHCI compared to those of other chlorophyll-*a/b* binding proteins is their red-shifted absorbance and their formation of dimers. Stoichiometric determination performed by Ballottari *et al.* (2004) suggested that in higher plants one Lhca polypeptide is present per one PSI core. These results are in agreement with the recently resolved PSI crystal structure (Ben Shem, 2003). LHCI was shown to be composed of hetero dimers of Lhca1 and Lhca4 that in this form show a fluorescence emission maximum at 730 nm (LHCI-730), and hetero or homo dimers of Lhca2 and Lhca3 with a maximum at 680 nm (LHCI-680) (Haworth *et al.*, 1983; Jansson *et al.*, 1996; Schmid *et al.*, 1997). In general, the demand for four different LHCI genes is not obvious as all LHCI proteins share high sequence homology and spectral properties. But the discovery of Lhca4 phosphorylation adds a new aspect to the analyses of its specific functions.

Plants are exposed to constant fluctuations in their growth environment, in terms of light quantity and quality. Such environmental changes occur on varying timescales, ranging from seconds to days or even weeks. To improve photosynthetic parameters and protect themselves against damages caused by excess light, a number of mechanisms to accommodate these differing levels of irradiance have evolved in plants. Photosynthetic acclimation of *Arabidopsis thaliana* in response to varying light levels during growth has been investigated by Bailey and coworkers (2001). Some distinct strategies for acclimation to low and high irradiance were revealed. One observation was that when *Arabidopsis* plants were grown under extreme low light conditions, PSI content increased dramatically. Interestingly, this was not accompanied by an increase in any of the LHCI light-harvesting polypeptides, but drastic increases in the levels of major and minor LHCII were observed. When exposed to high light conditions, changes in the composition of all PSI light-harvesting antenna could be observed in the plant. The most spectacular change in the protein levels was a striking decline of Lhca4 during growth at  $600 \mu\text{mol m}^{-2} \text{s}^{-1}$ .

As it was shown in several studies, posttranslational modification like phosphorylation can regulate the activity of the protein or the ability of its interaction to other proteins. Distinct strategies for acclimation to extreme high or low light conditions may involve major structural and functional changes of one or both photosystems (Bailey *et al.*, 2001), in which protein phosphorylation might be employed as one regulatory mechanism. The observed phosphorylation of Lhca4 could be involved in a photo-protection of PSI under particular stress conditions as found in the *psae1-3* and *psad1-1* mutants. The additional phosphate group might cause conformational changes of the Lhca4 protein leading to a modification of its chlorophyll organization and thus changes in its spectroscopic properties. This could lead to a decrease of reduced plastoquinone pool and thus release partly the photoinhibition. It has already been demonstrated that CP29, which is the minor light-harvesting protein of PSII, is phosphorylated under heavy stress conditions. Consequently a conformational change occurs that through modifying chlorophyll organization leads to an increase in non-radiative energy dissipation (Croce, 1996). Similarly, it was proposed by Bergantino *et al.* (1998) that phosphorylation of CP29 could be involved in decreasing over-reduction of the plastoquinone pool and thus photoinhibition.

Another interesting experiment was performed by Andersson and coworkers (2003). They showed that antisense plants lacking Lhcb1 and Lhcb2 were markedly reduced in fitness under field conditions, although they were largely unaffected in some aspects of photosynthesis. Even though, these antisense plants were lacking the two major LHCII protein subunits, only small parallel reductions in the relative levels of Lhcb3 and PsbS were observed. Interestingly, plants lacking Lhcb1 and Lhcb2 showed increased amounts of two other antenna proteins – CP26 and Lhca4. Nevertheless, the increase in CP26 and Lhca4 does not complement for the loss of these proteins in antisense plants (Andersson *et al.*, 2003). The elevated level of Lhca4 detected in asLhcb2 plants indicates that LHCII indeed is important for PSI. It was suggested that increased amount of an LHCI protein observed in asLhcb2 plants grown in constant moderate light intensity, could mean that PSI senses a decrease in antenna size which initiates an increase in Lhca4 (Andersson *et al.*, 2003).

In summary, above data indicate that the photosynthetic acclimation to growth under different light levels is more complex than it was previously reported. Further analysis of *psad1-1* and *psae1-3* mutants might prove helpful in answering some of the remaining questions. Anyhow, a distinct role for Lhca4 phosphorylation present in *psad1-1* and *psae1-3* mutants has not been clarified yet. Further studies are needed in order to elucidate the reason for Lhca4 phosphorylation and to get further insight into the consequences of high level of thylakoid protein phosphorylation observed in *psad1-1* and *psae1-3* mutants.

## **6. FUNCTIONAL ANALYSIS OF PSI-E**

PSI-E is a hydrophilic subunit located on the stromal side of PSI that plays a significant role in photosynthesis. The PSI-E subunit shows a high degree of conservation from cyanobacteria to higher plants. In *Arabidopsis thaliana*, there are two copies of the *PsaE* gene that are highly homologues.

As it was shown by Varotto *et al.* (2000), *Arabidopsis* plants in which one of the two *PsaE* genes is inactivated have reduced amounts of PSI-E and show a more general decrease in the polypeptide level of the whole stromal ridge of PSI. Plants with less PSI-E also show a marked increase in light sensitivity, photoinhibition and have an almost 50% decrease in growth rate. An interesting feature of *psae1* mutant is the formation of a stable LHCII-PSI aggregate the existence of which is associated with an almost complete suppression of state transitions, a drastic increase in the levels of phosphorylated LHCII and a permanent reduction in PSII antenna size. In order to understand the biological significance of a complete lack of PSI-E subunits, a double mutant was generated and characterized.

## **RESULTS**

### **6.1 Generation of *psae1-3 psae2-1* double mutant**

The *psae1-1* mutant used in previous studies (Varotto *et al.*, 2000; Pesaresi *et al.*, 2002) was identified on the basis of a decrease in the effective quantum yield of photosystem II, in a collection of plants subjected to transposon tagging with the *Enhancer* element. Because of the high activity of the transposon in this *psae1-1* mutant line, some *PsaE1* transcript was still present in small groups of wild-type cells resulting from somatic reversions. As a consequence, slight amounts of PsaE1 protein were still present in the mutant.

To obtain plants with a complete lack of PSI-E subunits, additional stable mutant alleles of the *PsaE1* gene had to be identified, as well as mutant lines for the second *PsaE2* gene. Populations of T-DNA insertion lines were screened by conducting PCR with gene specific primers in combination with different T-DNA specific primers. For the *PsaE1* allele, a mutant

line was found in the INRA-Versailles collection of *Arabidopsis* T-DNA insertion lines (<http://weedsworld.arabidopsis.org.uk/Vol2ii/pelletier.html>). This mutant line that carries a copy of the pGKB5 T-DNA inserted in the first exon of the *PsaE1* gene, 122 bp downstream of the ATG codon, was designated *psae1-3*.

A mutated line for the second allele was identified by screening the AFGC population (*Arabidopsis* Functional Genomics Consortium; <http://afgc.stanford.edu>). This line that carries a copy of the pD991-AP3 T-DNA inserted in the first exon of the *PsaE2* gene, 44 bp downstream of ATG, was designated *psae2-1*.

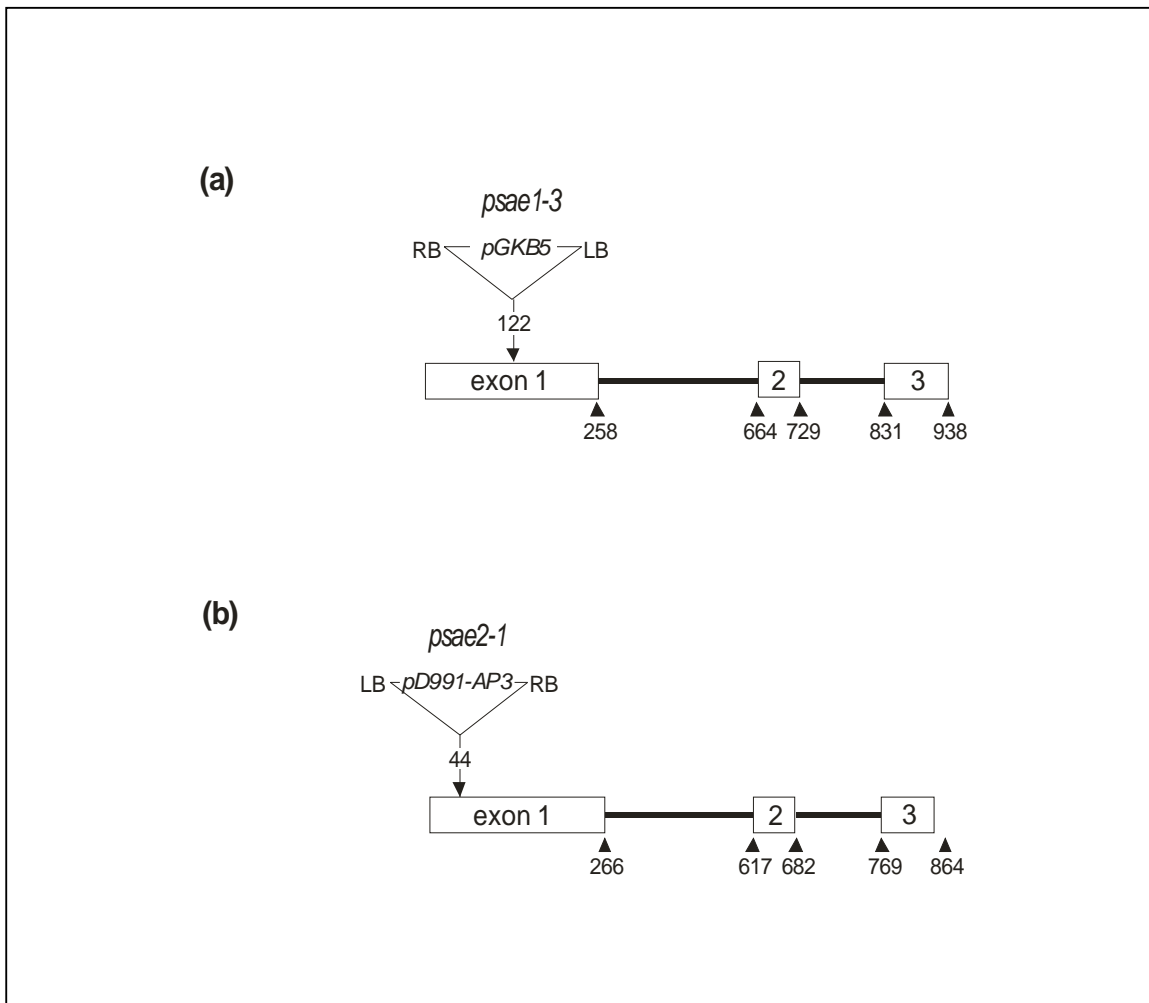


**Figure 6.1**

Tagging of the *PsaE1* and *PsaE2* genes. (a) In *psae1-3*, the first exon of *PsaE1* gene (At4g28750) is disrupted by an insertion of the pGKB5 T-DNA. (b) The *psae2-1* mutant carry insertion of the pD991-AP3 T-DNA in the first exon of the *PsaE2* gene (At2g20260). The T-DNA insertions are not drawn to scale.

The *psae1-3 psae2-1* double mutant was constructed by crossing the two respective single mutant lines. Homozygous double mutant plants were identified by genotyping F2 progenies obtained after crosses.

### 6.2 Growth of the *psae1-3 psae2-1* double mutant is significantly reduced

The double mutants were able to survive on soil but the growth rate was significantly reduced compared to single mutants and WT plants (Figure 6.2). Additionally, double mutants had pale green leaves that were turning more yellowish during development.

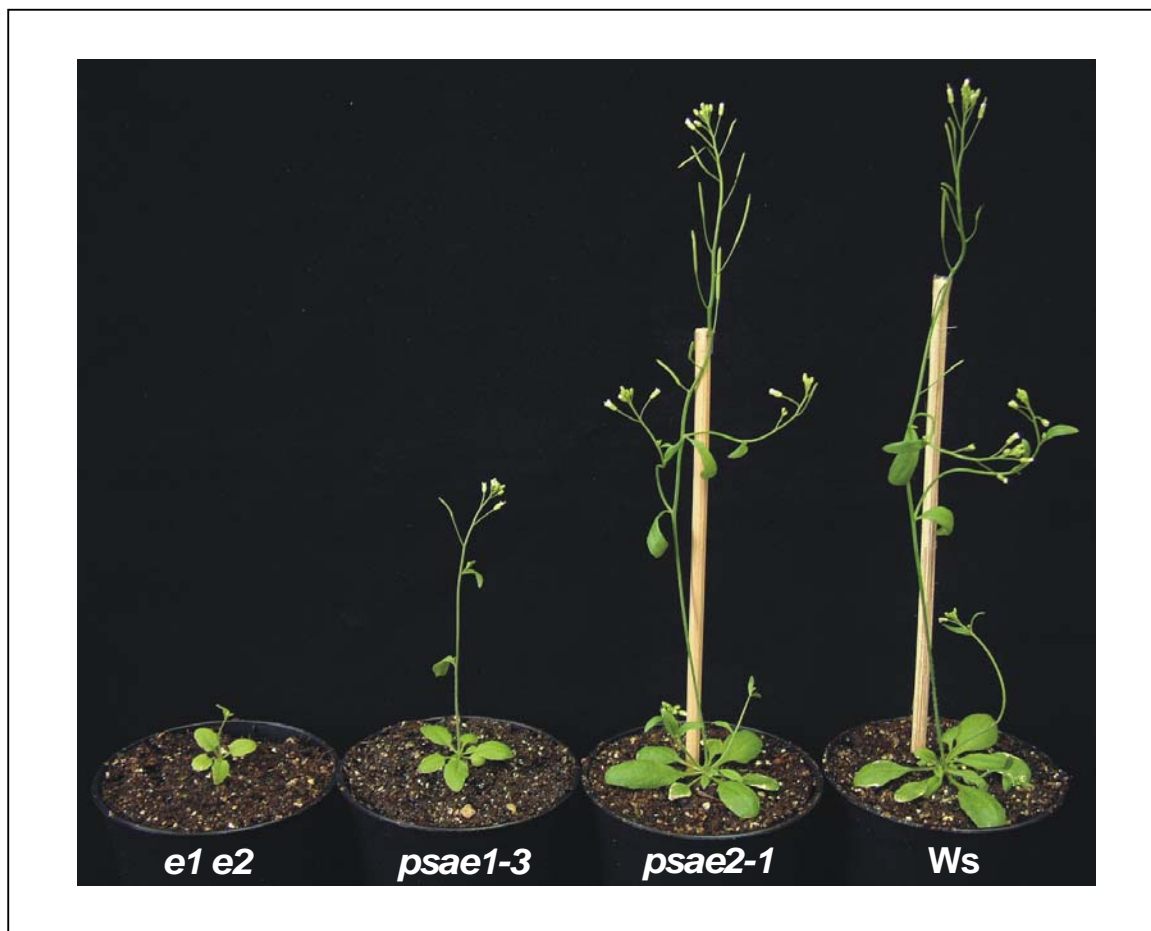


**Figure 6.2**  
Phenotypes of *psae1-3* and *psae2-1* and *psae1-3 psae2-1* double mutants. WT and mutant plants (4 weeks old) were grown in the greenhouse under long-day conditions.

The *psae1-3 psae2-1* double mutant remained very small and exhibited high-chlorophyll fluorescence (hcf) phenotype (Figure 6.3), similar to the phenotype of the *psad1-1 psad2-1* double mutant described previously (see Chapter 3). This indicates that the absence of the PSI-E subunit causes severe alterations in photosynthetic electron flow. In addition, double mutants were photosensitive. The necrosis of the leaves could be observed appearing after a few weeks of growth under green-house conditions. The double mutants were able to produce some seeds, but these failed to germinate.

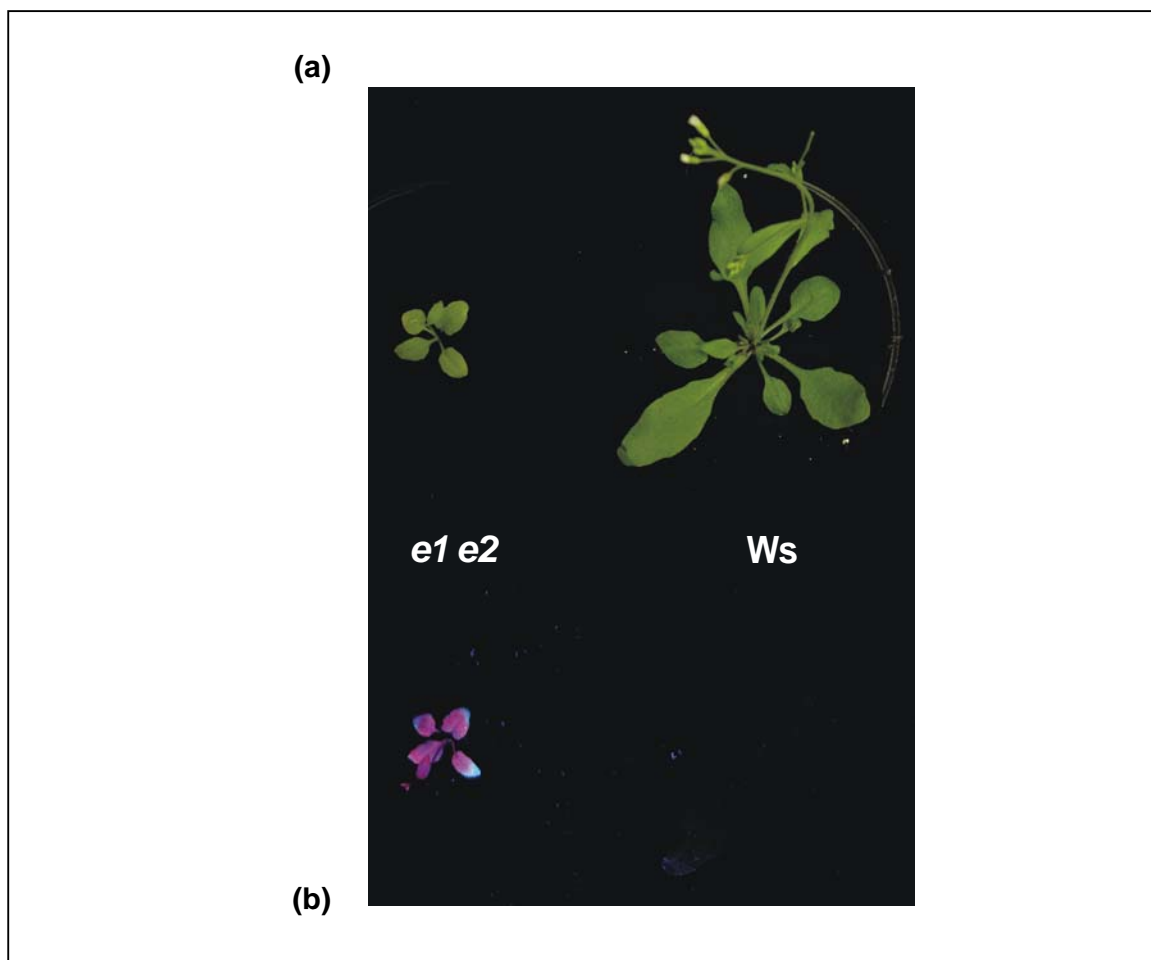


**Figure 6.3**

WT and *psae1-3 psae2-1* double mutant plants (*e1 e2*) grown on soil and illuminated with white light (a) or UV light (b). Plants (4 weeks old) were grown in the greenhouse under long-day conditions.

### 6.3 Accumulation of both *PsaE* transcripts is completely suppressed in *psae1-3 psae2-1* double mutant

Reverse-transcription PCR (RT-PCR) was performed to investigate the presence of *PsaE* transcripts in single and double mutants. Selected primers were complementary to either a sequence conserved between both *PsaE1* and *PsaE2* or a sequence existing only in *PsaE1*. RT-PCR analyses indicated that accumulation of *PsaE1* transcript was completely suppressed in *psae1-3* mutants (Figure 6.4b). When the primer combination specific for both transcripts was used, the presence of *PsaE1* transcript in *psae2-1* mutants and *PsaE2* transcript in *psae1-3* plants was detected.

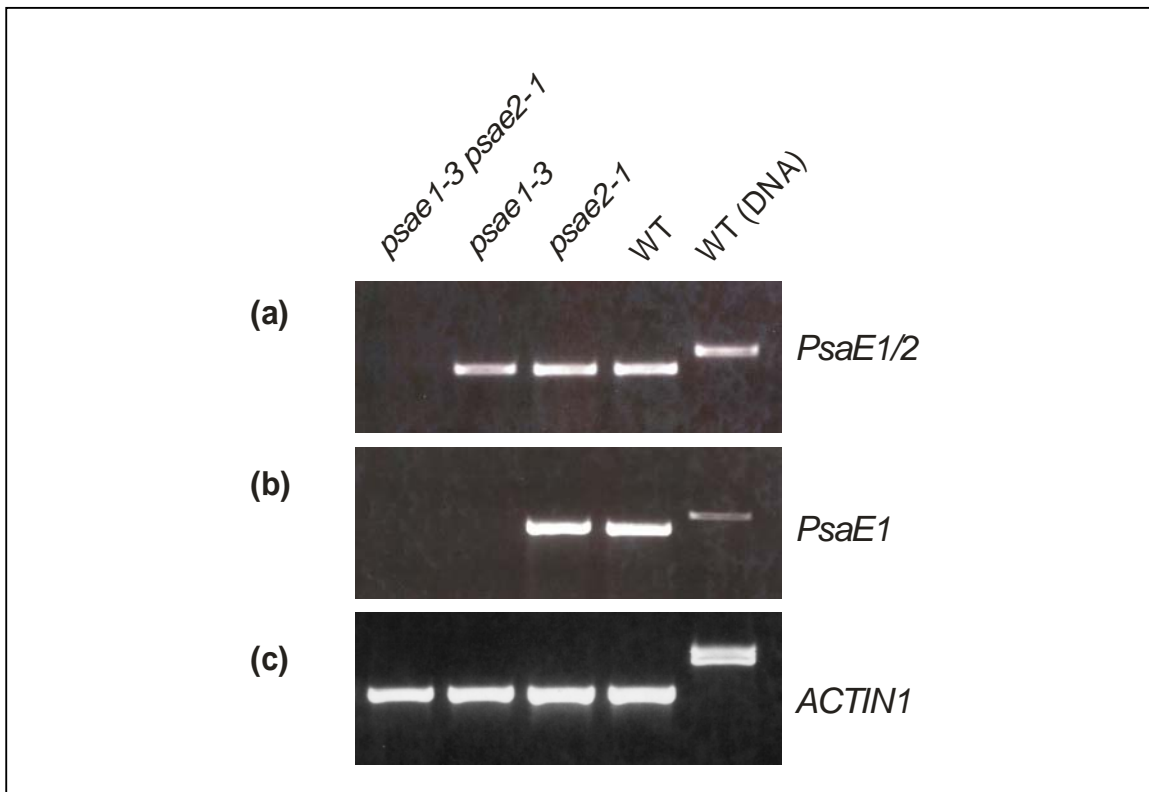


**Figure 6.4**

Detection of *PsaE* mRNA in mutant and WT plants. Detection of *PsaE* transcripts by RT-PCR. Products obtained after PCR of 30 cycles with primers recognizing both *PsaE* transcripts (*PsaE1/2-248/257s* and *PsaE1/2-395/404as*) (a), with primers recognizing only the *PsaE1* transcript (*PsaE1/2-248/257s* and *PsaE1-53499as*) (b) and control primers for the *ACTIN1* gene (c) were analysed on a 2.0% agarose gel. As a control, PCR with genomic WT-DNA was performed. The difference in size of the *ACTIN1* WT (DNA) band is due to the presence of two introns in the genomic amplicon.



Using both combinations of primers we were able to confirm the complete lack of *PsaE* transcript in the *psae1-3 psae2-1* double mutant (Figure 6.4a, b). As a control, RT-PCR with the *ACTINI*- specific primers was performed. The difference in size of the *ACTINI* WT (DNA) band is because of the presence of two introns in the genomic amplicon (Figure 6.4 c).

#### 6.4 PSI-E does not accumulate in *psae1-3 psae2-1* double mutant

Western analyses of thylakoids demonstrated that level of PSI-E subunit was significantly reduced in *psae1-3* mutant, while no alteration was observed in *psae2-1* as compared to WT plants. Accumulation of PSI-E was completely suppressed in the *psae1-3 psae2-1* double mutant (Figure 6.5b).

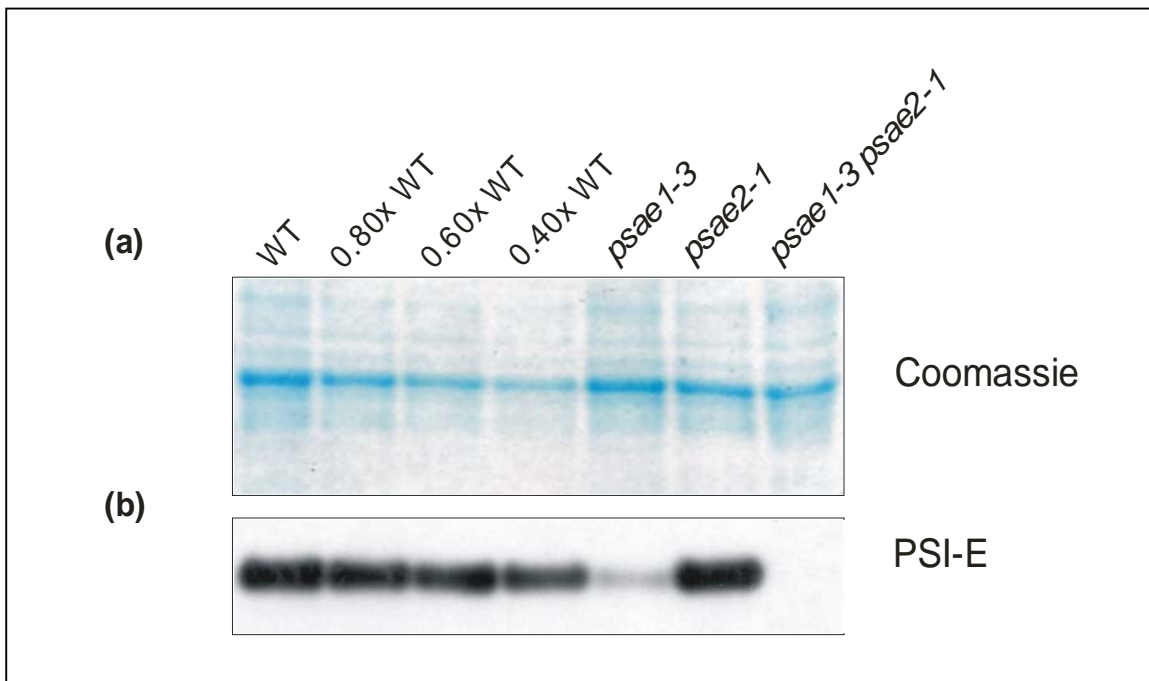


**Figure 6.5**

Immunoblot analysis of *psae* single and double mutants, as well as WT control. Aliquots of thylakoid proteins corresponding to 5  $\mu\text{g}$  of chlorophyll were loaded in each lane, and decreasing amounts of WT proteins were added to lanes 0.8x, 0.6x and 0.4x WT. Accurate loading was confirmed by staining SDS-PAGE with Coomassie (a). Filter was immunolabelled with antibodies raised against PSI-E (b). In the case of the *psae1-3* single mutant and *psae1-3 psae2-1* double mutant, because of its reduced chlorophyll content, relatively more proteins were loaded.

## DISCUSSION

The consequences of a mutation in the *PsaE1*, which is one of the genes coding for PSI-E subunit, were intensively studied by Varotto *et al.* (2000) and Pesaresi *et al.* (2002). The phenotype of *Arabidopsis* plants lacking PSI-E1 includes a light-green pigmentation, delayed growth and alterations in photosynthetic electron flow in both PSII and PSI. Western analyses demonstrated that a significant reduction in the amount of the three extrinsic subunits PSI-E, -C and -D existed in the *psae1* mutant.

During this work, the biological consequences of a lack of both *PsaE* genes have been investigated. The *psae1-3 psae2-1* double mutants were generated and characterized. The complete lack of both *PsaE* transcript and PSI-E protein in the *psae1-3 psae2-1* double mutants was confirmed. *Arabidopsis* plants missing the PSI-E subunit showed a severe phenotype including significant reduction in plant size and pale green leaf pigmentation, which is turning more yellowish during development. The *psae1-3 psae2-1* double mutant remains very small and exhibits the *hcf* phenotype observed before in the *psad1-1 psad2-1* double mutant plants. But even though the absence of the PSI-E subunit most probably causes severe alterations in photosynthetic electron flow as conducted from the phenotype, *psae1-3 psae2-1* double mutant are able to grow under normal photoautotrophic conditions. Anyhow, the observed phenotype is severe and after a few weeks of growth under green-house conditions necrosis of leaves could be observed, which indicates that this double mutant is photosensitive. Plants lacking the PSI-E subunit are able to produce some seeds, but these fail to germinate.

In contrast, cyanobacterial mutants lacking PSI-E do not obviously differ in growth rate from wild type when grown under normal photoautotrophic conditions (Chitnis *et al.*, 1989; Zhao *et al.*, 1993). However, it was shown that fast electron transfer between PsaC and the soluble electron acceptor was impaired when PSI-E was missing (Rousseau *et al.*, 1993). Moreover, the PSI-E-less membranes were severely deficient in ferredoxin-mediated NADP<sup>+</sup> photoreduction (Xu *et al.*, 1994). It was suggested that the PSI-E subunit might be involved in cyclic electron flow. Subsequently, more careful physiological investigations revealed that the growth rate of

cyanobacterial mutants lacking PSI-E was reduced as compared to the wild-type strain under low-light or low-CO<sub>2</sub> conditions (Zhao *et al.*, 1993). Some possibilities were suggested in order to explain the normal growth of cyanobacterial PSI-E-less mutant strains under photoautotrophic conditions (Xu *et al.*, 1994). Firstly, the ability of flavodoxin to accept electrons from PSI in the absence of PSI-E could explain the observed normal growth. Secondly, the small amount of ferredoxin-mediated NADP<sup>+</sup> photoreduction activity that was detected in the PSI-E-less mutants could be sufficient to support growth. Finally, there might be an undetected electron transfer protein that plays a role in electron flow in cyanobacteria.

Concerning these data and the fact that plants lacking PSI-E exhibit a significantly increased chlorophyll fluorescence phenotype, complete spectroscopic measurement should be performed, including chlorophyll fluorescence induction, the absorbance kinetics of P700 and state transition.

Further biochemical and physiological studies are necessary in order to understand the biological consequences of a complete lack of PSI-E subunit and its importance for photosynthesis in plants. The open question is if other PSI subunits can compensate the absence of PSI-E. This interesting possibility that one or more of the remaining PSI subunits can perform the function of the lacking proteins was already studied in cyanobacteria. The biochemical activities and organization of PSI in single- and multiple-mutant strains were compared (Xu *et al.*, 1994). Interestingly, these different multiple-mutant strains grew normally under photoautotrophic conditions with no obvious alterations in photosynthetic electron flow as compared to wild-type strain. It was demonstrated that the loss of PSI-E, -F, -J, and -L or their loss in several combinations did not change the photochemical activity of individual photosystems. In contrast, all strains lacking functional PSI-D were shown to grow slower as compared to WT. Moreover, double mutants lacking both PSI-D and PSI-E could hardly grow under photoautotrophic conditions. It was suggested that the absence of significant defects in some of the above mentioned multiple-mutant strains could be due to the compensatory changes in the PSI organization (Xu *et al.*, 1994). On the other hand, PSI isolated from the multiple-mutant strains were stable assembled, they lacked the deleted subunits but the remaining subunits were present in normal amounts.

In *Arabidopsis*, both subunits PSI-D and PSI-E are involved in the binding of ferredoxin. Also both of them are encoded by two functional genes and contain the N-terminal extensions that are specific for eukaryotes. Moreover, several similarities in physiological and biochemical properties exist between *Arabidopsis* plants lacking PSI-D1 and PSI-E1. Taken together these data, the PSI-D subunit could be the one that perform the function of the lacking PSI-E subunit in plants. In contrary to this hypothesis is decreased amount of PSI-D1 protein in *psae1* single mutant. Immunoblot analysis testing level of all PSI polypeptides, in particular PS-D1 and PSI-D2 in *psae1-3 psae2-1* double mutant, might proof helpful in answering those open questions remaining, concerning functions of the subunits located on the stromal side of PSI.

## **SUMMARY**

Although photosynthesis has been intensively studied, many open questions remain, which still need to be answered. The aim of this thesis was to further investigate the PSI complex, which in the course of the light reaction of photosynthesis catalyzes the light-induced transfer of electrons from plastocyanin on the lumenal side to ferredoxin on the stromal side. In this thesis emphasis was put on the reducing side of PSI, so-called stromal ridge of PSI, which is composed of the subunits D, E and C. Functional analyses of *Arabidopsis* plants carrying disrupted genes for PSI-E and PSI-D subunits were performed. Analyzing PSI-D, it was shown that of the two genes coding for this subunit only a mutation in PSI-D1 led to a general alteration in the polypeptide composition of PSI and thus also in the photosynthetic electron flow. The characterization of *psad1-1 psad2-1* double mutant indicated that PSI-D is necessary for the stability of PSI in *Arabidopsis*. A complete lack of the D subunit led to seedling lethality under photoautotrophic conditions. The instability of *Arabidopsis* PSI without PSI-D can be explained either by an increase in degradation of the incomplete PSI complex or by downregulation of the synthesis of PSI subunits. In contrast, *Arabidopsis* plants lacking the PSI-E subunit were able to grow under photoautotrophic conditions. However, they showed severe phenotype including a significant reduction in size and pale green pigmentation, which was turning more yellowish during development. The *psae1-3 psae2-1* double mutant exhibited a high-chlorophyll fluorescence phenotype, which had already been observed in the *psad1-1 psad2-1* double mutant. This indicates that photosynthetic electron flow is severely altered also in *Arabidopsis* plants lacking PSI-E subunit. Further spectroscopic, biochemical and physiological studies are in progress in order to understand the biological consequences of a complete lack of PSI-E subunit and its importance for photosynthesis in plants. An unexpected feature observed in both *psad1-1* and *psae1-3* single mutants, was a significantly increased level of thylakoid protein phosphorylation and therefore the presence of some new phosphopeptides that could not be detected in WT. A striking feature was that even the level of PSI phosphorylation was affected by these mutations. The only PSI phosphopeptide detected so far had been the PSI-D1 protein. Regarding the complementation analysis performed in this thesis it seems that phosphorylation of PSI-D1 does not play a key function in the PSI. Anyhow, it can not be excluded that this phosphorylation might play a role, if plants are grown under particular environmental conditions, not tested in this work. Mass spectrometry

techniques and methods of proteomics allowed the successful identification and analysis of one previously unknown phosphoprotein Lhca4. This was the first light-harvesting protein outside of LHCII to be phosphorylated. However, a distinct role for Lhca4 phosphorylation remains unknown. Further studies are needed in order to elucidate the cause and consequences of Lhca4 phosphorylation and to get further insight into the implication of a high level of thylakoid protein phosphorylation as observed in *psad1-1* and *psae1-3* mutants.

## **ZUSAMMENFASSUNG**

Obwohl Photosynthese bereits in der Wissenschaft detaillierter untersucht wurde, bleiben noch viele Fragen offen, die zu beantworten sind. Ziel dieser Arbeit war eine vertiefte Analyse des Photosystems I (PSI), das während der Lichtreaktion den Elektronentransfer vom luminal gelegenen Plastocyanin zum stromal gelegenen Ferredoxin katalysiert. Im Vordergrund dieser Arbeit stand die reduzierende Seite von PSI, die sog. stromal ridge. Diese besteht aus den Untereinheiten D, E und C. Hierzu wurden Analysen an transgenen Arabidopsispflanzen durchgeführt, bei denen die Expression der funktionalen Gene, die für die PSI-Untereinheiten E und D kodieren, unterdrückt war. Während der Untersuchungen von PSI-D zeigte sich, dass nur das Fehlen von PSI-D1 zu einer beträchtlichen Veränderung der Polypeptidzusammensetzung von PSI, wie auch des photosynthetischen Elektronenflusses führt. Die Charakteristik der Doppelmutanten *psad1-1 psad2-1* ließ erkennen, dass PSI-D für die Stabilität von PSI in *Arabidopsis* notwendig ist. Das vollständige Fehlen der Untereinheit D führte zur Letalität der Keimlinge unter photoautrophen Bedingungen. Für die Instabilität von PSI ohne die PSI-D-Untereinheit konnte entweder durch einen Anstieg der Degradationsrate des unvollständigen PSI oder durch eine herunterregulierte Synthese der Untereinheiten von PSI ursächlich sein. Im Gegensatz dazu waren Arabidopsispflanzen ohne die Untereinheit PSI-E in der Lage unter photoautrophen Bedingungen zu wachsen. Jedoch wiesen diese Pflanzen einen stark veränderten Phänotyp auf. Dieser war gekennzeichnet durch eine beachtliche Reduktion des Wachses und der Pigmentation. Diese *psae*-Mutanten werden im Laufe ihrer Entwicklung gelb. Wie auch die Doppelmutante *psad1-1 psad2-1* zeigte auch die Doppelmutante *psae1-3 psae2-1* eine erhöhte Chlorophyllfluoreszenz. Dies deutete darauf hin, dass der photosynthetische Elektronenfluss auch in Arabidopsispflanzen ohne die Untereinheit PSI-E stark gestört ist. Weitere spektroskopische, biochemische und physiologische Untersuchungen wurden durchgeführt um die biologischen Konsequenzen des vollständigen Fehlens der Untereinheit PSI-E zu verstehen und seine Bedeutung für die Photosynthese zu erkennen. Gemeinsam für beide Mutanten *psad1* und *psae1-3* ist eine erhebliche Zunahme der Phosphorylierung von Proteinen der Thylakoidmembran. Darüber hinaus konnten in den Mutanten *psad1* und *psae1-3* neben dem bereits bekannten Phosphopeptid PSI-D1 weitere, bislang unbekannte Phosphopeptide in der PSI-Fraktion nachgewiesen werden. Auf Grund von

Komplementationsanalysen konnte angenommen werden, dass die PSI-D1 Phosphorylierung unter den getesteten Bedingungen keine Schlüsselrolle einnimmt. Weiterhin ungeklärt blieb, ob die Phosphorylierung dieses Proteins eine Rolle unter speziellen Wachstumsbedingungen spielen könnte. Massenspektrometrie-Techniken und Proteomics-Methoden erlaubten die erfolgreiche Identifizierung und die Analyse des bislang unbekanntes Phosphoproteins Lhca4. Dieses Protein ist das erste phosphorylierte Protein eines Lichtsammelkomplexes außerhalb LHCI. Die Funktion von Lhca4-Phosphorylierung ist noch unbekannt. Weitere Untersuchungen sind notwendig, um die Funktion Lhca4-Phosphorylierung zu erklären und die Ursache der erhöhten Phosphorylierung der anderen Proteine der Thylakoidmembran der Mutanten *psad1* und *psae1-3* zu analysieren.



---

**A**

- Abdallah, F., Salamini, F., Leister, D. (2000) A prediction of the size and evolutionary origin of the proteome of chloroplasts of *Arabidopsis*. *Trends Plant Sci.* **5**, 141-142.
- Albertsson, P.A. (1995) The structure and function of the chloroplast photosynthetic membrane, a model for the domain organization. *Photosynth. Res.* **46**, 141-149.
- Allen, J.F., Bennett, J. (1981) Photosynthetic protein phosphorylation in intact chloroplasts: Inhibition by DCMU and by the onset of CO<sub>2</sub> fixation. *FEBS Lett.* **123**, 67-70.
- Allen, J.F. (1992) Protein phosphorylation in regulation of photosynthesis. *Biochim. Biophys. Acta* **1098**, 275-335.
- Allen, J.F. and Forsberg, J. (2001) Molecular recognition in thylakoid structure and function. *Trends Plant Sci.* **6**, 317-26.
- Alonso, J.M., Stepanova, A.N., Leisse, T.J. *et al.* (2003) Genome-wide insertional mutagenesis of *Arabidopsis thaliana*. *Science* **301**, 653–657.
- Andersen, B., Koch, B., Scheller, H.V. (1992) Structural and functional analysis of the reducing side of photosystem I. *Physiol.Plant.* **84**, 154–161.
- Andersson, J., Wentworth, M., Walters, R.G., Howard, C.A., Ruban, A.V., Horton, P., Jansson, S. (2003) Absence of the Lhcb1 and Lhcb2 proteins of the light-harvesting complex of photosystem II effects on photosynthesis, grana stacking and fitness. *Plant J.* **35**, 350-61.
- Antonkine, M.L., Jordan, P., Fromme, P., Krauß, N., Golbeck, J.H., Stehlik, D. (2003) Assembly of Protein Subunits within the Stromal Ridge of Photosystem I. Structural Changes between Unbound and Sequentially PS I-bound Polypeptides and Correlated Changes of the Magnetic Properties of the Terminal Iron Sulfur Clusters. *J. Mol. Biol.* **327**, 671-697.
- Arabidopsis Genome Initiative. (2000) Analysis of the genome sequence of the flowering plant *Arabidopsis thaliana*. *Nature* **408**, 796-815.

---

**B**

- Baena-González, E., Barbato, R., and Aro, E.-M. (1999) *Planta* **208**, 196-204.
- Bailey, S., Walters, R.G., Jansson, S., Horton, P. (2001) Acclimation of *Arabidopsis thaliana* to the light environment: the existence of separate low light and high light responses. *Planta* **213**, 794-801.
- Bassi, R., dal Belin Peruffo, A., Barbato, R. and Ghisi, R. (1985) Differences in chlorophyll-protein complexes and composition of polypeptides between thylakoids from bundle sheaths and mesophyll cells in maize. *Eur. J. Biochem.* **146**, 589–595.
- Bellafiore, S., Barneche, F., Peltier, G., Rochaix, J.D. (2005) State transitions and light adaptation require chloroplast thylakoid protein kinase STN7. *Nature* **433**, 892-5.
- Ben-Shem, A., Frolow, F., Nelson, N. (2003) Crystal structure of plant photosystem I. *Nature* **426**, 630-5.
- Bennett, J. (1977) Phosphorylation of chloroplast membrane polypeptides. *Nature (London)* **269**, 344-346.
- Bennett, J. (1980) Chloroplast phosphoproteins. Evidence for a thylakoidbound phosphoprotein phosphatase. *Eur. J. Biochem.* **104**, 85–89.
- Bennett, J. (1991) Protein phosphorylation in green plant chloroplasts. *Annu. Rev. Plant Physiol. Plant Mol. Biol.* **42**, 281–311.
- Bergantino, E., Dainese, P., Cerovic, Z., Sechi, S., Bassi, R. (1995) A post-translational modification of the photosystem II subunit CP29 protects maize from cold stress. *J. Biol. Chem.* **275**, 8474-81.
- Bergantino, E., Sandonà, D., Cugini, D., Bassi, R. (1998) The Photosystem II subunit CP29 can be phosphorylated in both C3 and C4 plants as suggested by sequence analysis. *Plant Mol Biol* **36**, 11–22.
- Blanc, G., Hokamp, K. and Wolfe, K.H. (2003) A recent polyploidy superimposed on older large-scale duplications in the *Arabidopsis* genome. *Genome Res.* **13**, 137–144.
- Bottin, H., Hanley, J. and Lagoutte, B. (2001) Role of acidic amino acid residues of PsaD subunit on limiting the affinity of photosystem I for ferredoxin. *Biochem. Biophys. Res. Commun.* **287**, 833–836.

- 
- Bradbury, M., Baker, N.R. (1981) Analysis of the slow phases of the in vivo chlorophyll fluorescence induction curve. Changes in the redox state of photosystem II electron acceptors and fluorescence emission from photosystems I and II. *Biochim. Biophys. Acta* **635**, 542–551.

## C

- Carlberg, I., Rintamäki, E., Aro, E.-M., Andersson, B. (1999) Thylakoid protein phosphorylation and the thiol redox state. *Biochemistry* **38**, 3197–3204.
- Carlberg, I. *et al.* (2003) A novel plant protein undergoing lightinduced phosphorylation and release from the photosynthetic thylakoid membranes. *Proc. Natl. Acad. Sci. U.S. A.* **100**, 757–762.
- Chitnis, P.R., Reilly, P.A. and Nelson, N. (1989) Insertional inactivation of the gene encoding subunit II of photosystem I from the cyanobacterium *Synechocystis* sp. PCC 6803. *J. Biol. Chem.* **264**, 18381–18385.
- Chitnis, P.R., Reilly, P.A., Miedel, M.C., Nelson N. (1989) Structure and targeted mutagenesis of the gene encoding 8-kDa subunit of photosystem I from the cyanobacterium *Synechocystis* sp. PCC 6803, *J. Biol. Chem.* **264**, 18374-18380.
- Chitnis, P.R., Nelson, N., (1992a) Assembly of two subunits of the cyanobacterial photosystem I on the n-side of thylakoid membranes. *Plant Physiol* **99**, 239-246.
- Chitnis, V.P. and Chitnis, P.R. (1993) PsaL subunit is required for the formation of photosystem I trimers in the cyanobacterium *Synechocystis* sp. PCC 6803. *FEBS Lett.* **336**, 330-334.
- Chitnis, V.P., Ke, A. and Chitnis, P.R. (1997) The PsaD subunit of photosystem I. Mutations in the basic domain reduce the level of PsaD in the membranes. *Plant Physiol.* **115**, 1699-1705.
- Clough, S.J. and Bent, A.F. (1998) Floral dip: a simplified method for *Agrobacterium*-mediated transformation of *Arabidopsis thaliana*. *Plant J.* **16**, 735-743.
- Cohen, Y., Steppuhn, J., Herrmann, R. G., Yalovsky, S., and Nechushtai, R. (1992) Insertion and assembly of the precursor of subunit II into the photosystem I complex may precede its processing. *EMBO J.* **11**, 79-85.

- 
- Cohen, Y., Nelson, N., Chitnis, P.R., Nechustai, R. (1995) The carboxyl-terminal region of the spinach PsaD subunit contains information for its specific assembly into plant thylakoids. *Photosynth Res* **44**, 157-164.
  - Croce, R., Breton, J., Bassi, R. (1996) Conformational changes induced by phosphorylation in the CP29 subunit of photosystem II. *Biochemistry*. **35**, 11142-8.
  - Croce, R., Morosinotto, T., Casteletti, S., Breton, J., Bassi, R. (2002) The Lhca antenna complexes of higher plants photosystem I, *Biochim. Biophys. Acta* **1556**, 29-40.

## D

- Danon, A., Mayfield, S. P. (1994) *Science* **266**, 1717–1719.
- Dekker, J. P. and Boekema, E. J. (2005) Supramolecular organization of thylakoid membrane proteins in green plants. *Biochim Biophys Acta*. **706**, 12-39.
- Devereux, J., Haeblerli, P. and Smithies, O. (1984) A comprehensive set of sequence analysis programs for the VAX. *Nucl. Acids Res.* **12**, 387–395.
- Douglas S.E., (1998) Plastid evolution: origins, diversity, trends. *Curr. Opin. Genet. Dev.* **8**, 655-661.
- Durrant, J.R. *et al.* (1995) A multimer model for P680, the primary electron- donor of photosystem-II. *Proc. Natl. Acad. Sci. U. S. A.* **92**, 4798–4802.

## E

- Emanuelsson, O., Nielsen, H., Brunak, S. and von Heijne, G. (2000) Predicting subcellular localization of proteins based on their N-terminal amino acid sequence. *J. Mol.Biol.* **300**, 1005-1016.

## F

- Färber, A., Young, A.J., Ruban, A.V., Horton, P. and Jahns, P. (1997) Dynamics of xanthophyll-cycle activity in different antenna subcomplexes in the photosynthetic membranes of higher plants: the relationship between zeaxanthin conversion and nonphotochemical fluorescence quenching. *Plant Physiol.* **115**, 1609–1618.

- 
- Foyer, C.H. (1985) Stromal protein phosphorylation in spinach (*Spinacia oleracea*) chloroplasts. *Biochem J.* **231**, 97-103.

## G

- Ganeteg, U., Klimmek, F., Jansson, S. (2004) Lhca5-an LHC-type protein associated with photosystem I. *Plant Mol Biol.* **54**, 641-51.
- Garcia Vescovi, E. and Lucero, H.A. (1990) Phosphorylation of serine residues in endogenous proteins of thylakoids and subthylakoid particles in the dark under nonreducing conditions. *Biochim Biophys Acta* **1018**, 23-28.
- Genty, B., Briantais, J.M., Baker, N.R. (1989) The relationship between the quantum yield of photosynthetic electron-transport and quenching of chlorophyll fluorescence. *Biochim. Biophys. Acta* **990**, 87-92.
- Gross, E. (1993) Plastocyanin-structure and function. *Photosynth. Res.* **37**, 103-116.

## H

- Haldrup, A. et al. (2001) Balance of power: a view of the mechanism of photosynthetic state transitions. *Trends Plant Sci.* **6**, 301-305.
- Haldrup, A., Naver, H. and Scheller, H.V. (1999) The interaction between plastocyanin and photosystem I is inefficient in transgenic *Arabidopsis* plants lacking the PSI-N subunit of photosystem I. *Plant J.* **17**, 689-698.
- Haldrup, A., Simpson, D.J. and Scheller, H.V. (2000) Down-regulation of the PSI-F subunit of photosystem I (PSI) in *Arabidopsis thaliana*. The PSI-F subunit is essential for photoautotrophic growth and contributes to antenna function. *J. Biol. Chem.* **275**, 31211-31218.
- Haldrup, A., Lunde, C. and Scheller, H.V. (2003) Plants lacking the PSI-D subunit of photosystem I suffer severe photoinhibition, have unstable photosystem I complexes and altered redox homeostasis in the chloroplast stroma. *J. Biol. Chem.* **278**, 33276-33283.
- Hankamer, B., Barber, J., Boekema, E.J. (1997) Structure and membrane organization of photosystem II in green plants. *Annu. Rev. Plant Physiol. Plant Mol. Biol.* **48**, 641-671.

- 
- Hankamer, B., Morris, E.P., Barber, J. (1998) Revealing the structure of the oxygen-evolving core dimer of photosystem II by cryoelectron crystallography. *Nat. Struct. Biol.* **6**, 560–564.
  - Hanley, J., Setif, P., Bottin, H. and Lagoutte, B. (1996) Mutagenesis of photosystem I in the region of the ferredoxin cross-linking site: modifications of positively charged amino acids. *Biochemistry* **35**, 8563–8571.
  - Hansson, M., Vener, A.V. (2003) Identification of Three Previously Unknown *in Vivo* Protein Phosphorylation Sites in Thylakoid Membranes of *Arabidopsis thaliana*. *Molecular & Cellular Proteomics* **2**, 550-559.
  - Haworth, P., Watson, J.L., Arntzen, C.J. (1983) The detection, isolation and characterization of a light-harvesting complex which is specifically associated with photosystem I. *Biochim. Biophys. Acta* **724**, 151-158.
  - Heathcote, P., Fyfe, P.K., Jones, M.R. (2002) Reaction centres: the structure and evolution of biological solar power. *Trends Biochem Sci.* **27**, 79-87.
  - Hieter, P., Boguski, M. (1997) Functional Genomics: It's All How You Read It. *Science* **278**, 601-602.
  - Hoyer-Hansen, G., Bassi, R., Honberg, L.S. and Simpson, D.J. (1988) Immunological characterization of chlorophyll *a/b*-binding proteins of barley thylakoids. *Planta* **173**, 12–21.
  - Horton, H. (2003) Principles of Biochemistry 3rd Edition. *Prentice Hall*.

## J

- Jahns, P., Graf, M., Munekage, Y., Shikanai, T. (2002) Single point mutation in the Rieske iron-sulfur subunit of cytochrome *b6/f* leads to an altered pH dependence of plastoquinol oxidation in *Arabidopsis*. *FEBS Lett.* **519**, 99-102.
- Jansson, S. (1994) The light harvesting chlorophyll *a/b* binding proteins. *Biochim Biophys Acta* **1184**, 1-19.
- Jansson, S., Andersen, B. and Scheller, H. V. (1996). Nearest-neighbor analysis of higher plant photosystem I holocomplex. *Plant Physiol.* **112**, 409-420.

- 
- Jansson, S. (1999) A guide to the Lhc genes and their relatives in *Arabidopsis*. *Trends Plant Sci.* **4**, 236–240.
  - Jensen, P.E., Gilpin, M., Knoetzel, J. and Scheller, H.V. (2000) The PSI-K subunit of photosystem I is involved in the interaction between light-harvesting complex I and the photosystem I reaction center core. *J. Biol. Chem.* **275**, 24701–24708.
  - Jensen, P.E., Rosgaard, L., Knoetzel, J. and Scheller, H.V. (2002) Photosystem I activity is increased in the absence of the PSI-G subunit. *J. Biol. Chem.* **277**, 2798–2803.
  - Jordan, P., Fromme, P., Witt, H.T., Klukas, O., Saenger, W. and Krauss, N. (2001) Three-dimensional structure of cyanobacterial photosystem I at 2.5 Å resolution. *Nature* **411**, 909–917.

## K

- Kamiya, N., Shen, J.R. (2003) Crystal structure of oxygen-evolving photosystem II from *Thermosynechococcus vulcanus* at 3.7-angstrom resolution. *Proc. Natl. Acad. Sci. U. S. A.* **100**, 98–103.
- Kitmitto, A., Holzenburg, A. and Ford, R.C. (1997) Two-dimensional crystals of photosystem I in higher plant grana margins. *J. Biol. Chem.* **272**, 19497–19501.
- Klukas, O., Schubert, W.D., Jordan, P., Krauss, N., Fromme, P., Witt, H.T. and Saenger, W. (1999) Photosystem I, an improved model of the stromal subunits PsaC, PsaD, and PsaE. *J. Biol. Chem.* **274**, 7351–7360.
- Knoetzel, J., Mant, A., Haldrup, A., Jensen, P.E. and Scheller, H.V. (2002) PSI-O, a new 10-kDa subunit of eukaryotic photosystem I. *FEBS Lett.* **510**, 145–148.
- Koncz, C., Mayerhofer, R., Koncz-Kalman, Z., Nawrath, C., Reiss, B., Redei, G.P., Schell J. Isolation of a gene encoding a novel chloroplast protein by T-DNA tagging in *Arabidopsis thaliana*, *Embo J.* **9**, 1337-1346.
- Krisan, P.J., Young, J.C., Sussman, M.R. (1999) T-DNA as an insertional mutagen in *Arabidopsis*. *Plant Cell* **11**, 2283-2290.

- 
- Kruij, J., Chitnis, P.R., Lagoutte, B., Rogner, M. and Boekema, E.J. (1997) Structural organization of the major subunits in cyanobacterial photosystem I. Localization of subunits PsaC, -D, -E, -F, and -J. *J. Biol. Chem.* **272**, 17061–17069.
  - Kurisu, G., Zhang, H., Smith, J.L. and Cramer, W.A. (2003) Structure of the cytochrome *b* (6) *f* complex of oxygenic photosynthesis: tuning the cavity. *Science* **302**, 1009–1014.
  - Kurth, J., Varotto, C., Pesaresi, P., Biehl, A., Richly, E., Salamini, F. and Leister, D. (2002) Gene-sequence-tag expression analyses of 1,800 genes related to chloroplast functions. *Planta* **215**, 101–109.

## L

- Lagoutte, B., Hanley, J. and Bottin, H. (2001) Multiple functions for the C terminus of the PsaD subunit in the cyanobacterial photosystem I complex. *Plant Physiol.* **126**, 307–316.
- Leister, D., Varotto, C., Pesaresi, P., Niwergall, A. and Salamini, F. (1999) Large-scale evaluation of plant growth in *Arabidopsis thaliana* by non-invasive image analysis. *Plant Physiol. Biochem.* **37**, 671–678.
- Link, A.J., Eng, J., Schieltz, D.M., Carmack, E., Mize, J.Z., Morris, D.R., Garvik, M.B., Yates, J.R.III (1999) Direct analysis of protein complexes using mass spectrometry. *Nat Biotechnol.* **17**, 676–82.
- Lunde, C., Jensen, P.E., Haldrup, A., Knoetzel, J. and Scheller, H.V. (2000) The PSI-H subunit of photosystem I is essential for state transitions in plant photosynthesis. *Nature* **408**, 613–615.

## M

- Maiwald, D., Dietzmann, A., Jahns, P., Pesaresi, P., Joliot, P., Joliot, A., Levin, J.Z., Salamini, F. and Leister, D. (2003) Knock-out of the genes coding for the Rieske protein and the ATP-synthase  $\delta$ -subunit of *Arabidopsis thaliana*. Effects on photosynthesis, thylakoid protein composition and nuclear chloroplast gene expression. *Plant Physiol.* **133**, 191–202.
- Mannan, R.M., Pakrasi, H.B. and Sonoike, K. (1994) The PsaC protein is necessary for the stable association of the PsaD, PsaE, and PsaL proteins in the photosystem I complex: analysis of a cyanobacterial mutant strain. *Arch. Biochem. Biophys.* **315**, 68–73.
- Maxwell, K., Johnson, G.N. (2000) Chlorophyll fluorescence—a practical guide. *J Exp. Bot.* **345**, 659–68.



- 
- Meinke, D.W., Cherry, J.M., Dean, C., Rounsley, S.D., Koornneef, M. (1998) *Arabidopsis thaliana*: a model plant for genome analysis. *Science* **282**, 679-82.
  - Meissner, R.C., Jin, H., Cominelli, E., Denekamp, M., Fuertes, A., Greco, R., Kranz, H.D., Penfield, S., Petroni, K., Urzainqui, A. (1999) Function search in a large transcription factor gene family in *arabidopsis*. Assessing the potential of reverse genetics to identify insertional mutations in r2r3 *myb* genes. *Plant Cell* **11**, 1827-1840.
  - Merati, G. and Zanetti, G. (1987) Chemical cross-linking of ferredoxin to spinach thylakoids –evidence for two independent binding-sites of ferredoxin to the membrane. *FEBS Lett.* **215**, 37–40.
  - Meurer, J., Meierhoff, K. and Westhoff, P. (1996) Isolation of high-chlorophyll fluorescence mutants of *Arabidopsis thaliana* and their characterization by spectroscopy, immunoblotting and Northern hybridization. *Planta* **198**, 385–396.
  - Meurer, J., Plucken, H., Kowallik, K.V., Westhoff, P. (1998) A nuclear-encoded protein of prokaryotic origin is essential for the stability of photosystem II in *Arabidopsis thaliana*. *Embo J.* **17**, 5286-97.
  - Michel, H., Bennett, J. (1987) Identification of the phosphorylation site of an 8.3 kDa protein from Photosystem II of spinach. *FEBS Lett.* **212**, 103-108.
  - Michel, H., Bennett, J. (1989) Use of synthetic peptides to study the substrate specificity of a thylakoid protein kinases. *FEBS Lett.* **254**, 165-170.
  - Minai, L., Cohen, Y., Chitnis, P. R., and Nechushtai, R. (1996) The precursor of PsaD assembles into the photosystem I complex in two steps. *Proc. Natl. Acad. Sci. U. S. A.* **93**, 6338-6342.
  - Minai, L., Fish, A., Darash-Yahana, M., Verchovsky, L., Nechushtai, R. (2001) The assembly of the PsaD subunit into the membranal photosystem I complex occurs via an exchange mechanism. *Biochemistry* **40**, 12754–12760.

## N

- Naver, H., Scott, M.P., Andersen, B., Moller, B.L. and Scheller, H.V. (1995) Reconstitution of barley photosystem I reveals that the N-terminus of the PSI-D subunit is essential for tight binding of PSI-C. *Physiol. Plant.* **95**, 19–26.

- 
- Naver, H., Haldrup, A. and Scheller, H.V. (1999) Cosuppression of photosystem I subunit PSI-H in *Arabidopsis thaliana*. Efficient electron transfer and stability of photosystem I is dependent upon the PSI-H subunit. *J. Biol. Chem.* **274**, 10784–10789.
  - Nielsen, V.S., Scheller, H.V. and Moller, B.L. (1996) The photosystem I mutant *viridis-zb*<sup>63</sup> of barley (*Hordeum vulgare*) contains low amounts of active but unstable photosystem I. *Physiol. Plant.* **98**, 637–644.
  - Nugent, J. (2001) Photosynthetic water oxidation. *Biochim. Biophys. Acta* **503**, 1.

## P

- Parinov, S., Sevugan, M., De, Y., Yang, W.C., Kumaran, M., Sundaresan V. (1999) Analysis of flanking sequences from *Dissociation* insertion lines. A database for reverse genetics in *Arabidopsis*. *Plant Cell* **11**, 2263-2270.
- Park, Y.I., Chow, W.S., Anderson, J.M. (1997) Antenna size dependency of photoinactivation of Photosystem II in light-acclimated pea leaves. *Plant Physiol* **115**, 151–157.
- Pesaresi, P., Varotto, C., Richly, E., Kurth, J., Salamini, F. and Leister, D. (2001) Functional genomics of *Arabidopsis thaliana* photosynthesis. *Plant Physiol. Biochem.* **39**, 285-294.
- Pesaresi, P., Varotto, C., Meurer, J., Jahns, P., Salamini, F. and Leister, D. (2001) Knock-out of the plastid ribosomal protein L11 in *Arabidopsis*: effects on mRNA translation and photosynthesis. *Plant J.* **27**, 179–189.
- Pesaresi, P., Lunde, C., Jahns, P. *et al.* (2002) A stable LHCII-PSI aggregate and suppression of photosynthetic state transitions in the *psae1-1* mutant of *Arabidopsis thaliana*. *Planta* **215**, 940–948.
- Pesaresi, P., Gardner, N.A., Masiero, S., Dietzmann, A., Eichacker, L., Wickner, R., Salamini, F. and Leister, D. (2003a) Cytoplasmic N-terminal protein acetylation is required for efficient photosynthesis in *Arabidopsis*. *Plant Cell* **15**, 1817–1832.
- Pesaresi, P., Varotto, C., Richly, E., Leßnick, A., Salamini, F. and Leister, D. (2003b) Protein-protein and protein-function relationships in *Arabidopsis* photosystem I: cluster analysis of PSI polypeptide levels and photosynthetic parameters in PSI mutants. *J. Plant Physiol.* **160**, 17–22.

---

**R**

- Richly, E., Dietzmann, A., Biehl, A., Kurth, J., Laloi, C., Apel, K., Salamini, F. and Leister, D. (2003) Co-variations in the nuclear chloroplast transcriptome reveal a regulatory master switch. *EMBO Rep.* **4**, 491–498.
- Richmond, T., Somerville, S. (2000) Chasing the dream: plant EST microarrays. *Curr Opin Plant Biol.* **3**, 108-16.
- Rintamäki, E., Salonen, M., Suoranta, U.M., Carlberg, I., Andersson, B., Aro, E.M. (1997) Phosphorylation of Light-harvesting Complex II and Photosystem II Core Proteins Shows Different Irradiance-dependent Regulation *in Vivo*. APPLICATION OF PHOSPHOTHREONINE ANTIBODIES TO ANALYSIS OF THYLAKOID PHOSPHOPROTEINS. *J. Biol. Chem.* **272**, 30476-30482.
- Rintamäi, E., Martinsuo, P., Pursiheimo, S., and Aro, E.-M. (2000) Cooperative regulation of light-harvesting complex II phosphorylation via the plastoquinol and ferredoxin-thioredoxin system in chloroplasts. *Proc. Natl. Acad. Sci. U. S. A.* **97**, 11644–11649.
- Rousseau, F., Setif, P., Lagoutte, B. (1993) Evidence for the involvement of PSI-E subunit in the reduction of ferredoxin by photosystem I, *Embo J.* **12**, 1755-1765.
- Rutherford, A.W. and Faller, P. (2001) The heart of photosynthesis in glorious 3D. *Trends Biochem. Sci.* **26**, 341–344.
- Rutherford, A.W. and Krieger-Liszky, A. (2001) Herbicide-induced oxidative stress In photosystem II. *Trends Biochem. Sci.* **26**, 648–653.

**S**

- Sambrook, J., Fritsch, E.F. and Maniatis, T. (1989) *Molecular Cloning: a Laboratory Manual*, 2nd edn. Cold Spring Harbor: Cold Spring Harbor Laboratory Press.
- Scheller, H.V., Jensen, P.E., Haldrup, A., Lunde, C. and Knoetzel, J. (2001) Role of subunits in eukaryotic photosystem I. *Biochim. Biophys. Acta* **1507**, 41-60.
- Scheller, H.V., Jensen, P.E., Haldrup, A., Lunde, C., Knoetzel, J. (2001) Role of subunits in eukaryotic Photosystem I. *Biochimica et Biophysica Acta (BBA)-Bioenergetics* **1507**, 41-60.

- 
- Schmid, V. H. R., Cammarata, K. V., Bruns, B. U. and Schmidt, G. W. (1997). In vitro reconstitution of the photosystem I light-harvesting complex LHCI-730: Heterodimerization is required for antenna pigment organization. *Proc. Natl. Acad. Sci. USA* **94**, 7667-7672.
  - Schmid, V.H.R., Paulsen, H., Rupprecht, J. (2002) Identification of N- and C-terminal amino acids of Lhca1 and Lhca4 required for formation of the heterodimeric peripheral photosystem I antenna LHCI-730. *Biochemistry* **41**, 9126–9131.
  - Schreiber, U., Schliwa, U., Bilger, W. (1986) Continuous recording of photochemical and non-photochemicalchlorophyll fluorescence quenching with a new type of modulation fluorometer, *Photosynth. Res.* **10**, 51-62.
  - Soll, J., Bennett, J. (1988) Localization of a 64-kDa phosphoprotein in the lumen between the outer and inner envelopes of pea chloroplasts. *Eur J Biochem.* **175**, 301-7.
  - Somerville, C., Somerville, S. (1999) Plant functional genomics. *Science.* **285**, 380-3.
  - Speulman, E., Metz, P.L., van Arkel, G., te Lintel Hekkert, B., Stiekema, W.J., Pereira, A. (1999) A two-component *enhancer-inhibitor* transposon mutagenesis system for functional analysis of the *arabidopsis* genome. *Plant Cell* **11**, 1853-1866.
  - Staehelin, L. A. and Arntzen, C. J. (1986) Photosynthesis. III. Photosynthetic Membranes and Light Harvesting Systems. *Encyclopedia of Plant Physiology, new series* Vol. **19**, Springer, Berlin.
  - Sveshnikova, N., Soll, J., Schleiff, E. (2000) Toc34 is a preprotein receptor regulated by GTP and phosphorylation. *Proc Natl Acad Sci U S A.* **97**, 4973-8.

## T

- Thompson, J.D., Higgins, D.G. and Gibson, T.J. (1994) CLUSTAL W: improving the sensitivity of progressive multiple sequence alignment through sequence weighting, position-specific gap penalties and weight matrix choice. *Nucl. Acids Res.* **22**, 4673–4680.
- Tullberg, A.; Håkansson, G.; Race, H.L. (1998) A Protein Tyrosine Kinase of Chloroplast Thylakoid Membranes Phosphorylates Light Harvesting Complex II Proteins. *Biochemical and Biophysical Research Communications*, **250**, 617-622.

- 
- Tissier, A.F., Marillonnet, S., Klimyuk, V., Patel, K., Torres, M.A., Murphy, G. and Jones, J.D. (1999) Multiple independent defective *Suppressor-mutator* transposon insertions in *Arabidopsis*: a tool for functional genomics. *Plant Cell* **11**, 1841–1852.

## U

- Usami, S., Hiroharu, B., Ito, Y., Nishihama, R., Machida, Y. (1995) Cutting activates a 46-kilodalton kinase in plants. *Proc Natl Acad Sci USA*. **92**, 8660–8664.

## V

- Varotto, C., Pesaresi, P., Meurer, J., Oelmuller, R., Steiner-Lange, S., Salamini, F. and Leister, D. (2000a) Disruption of the *Arabidopsis* photosystem I gene *psaE1* affects photosynthesis and impairs growth. *Plant J.* **22**, 115–124.
- Varotto, C., Pesaresi, P., Maiwald, D., Kurth, J., Salamini, F. and Leister, D. (2000b) Identification of photosynthetic mutants of *Arabidopsis* by automatic screening for altered effective quantum yield of photosystem 2. *Photosynthetica* **38**, 497–504.
- Varotto, C., Pesaresi, P., Jahns, P., Leßnick, A., Tizzano, M., Schiavon, F., Salamini, F. and Leister, D. (2002a) Single and double knock-outs of the genes for photosystem I subunits PSI-G, -K and -H of *Arabidopsis thaliana*: effects on PSI composition, photosynthetic electron flow and state transitions. *Plant Physiol.* **129**, 616–624.
- Varotto, C., Maiwald, D., Pesaresi, P., Jahns, P., Salamini, F. and Leister, D. (2002b) The metal ion transporter IRT1 is necessary for iron homeostasis and efficient photosynthesis in *Arabidopsis thaliana*. *Plant J.* **31**, 589–599.
- Vener, A. V., Van Kan, P. J., Gal, A., Andersson, B., and Ohad, I. (1995) Activation/deactivation cycle of redox-controlled thylakoid protein phosphorylation. Role of plastoquinol bound to the reduced cytochrome bf complex. *J. Biol. Chem.* **270**, 25225–25232.
- Vener, A. V., Van Kan, P. J. M., Rich, P. R., Ohad, I., and Andersson, B. (1997) Plastoquinol at the quinol oxidation site of reduced cytochrome bf mediates signal transduction between light and protein phosphorylation: Thylakoid protein kinase deactivation by a single-turnover flash. *Proc. Natl. Acad. Sci. U. S. A.* **94**, 1585–1590.

- 
- Vener, A. V., Harms, A., Sussman, M. R., and Vierstra, R. D. (2001) Mass spectrometric resolution of reversible protein phosphorylation in photosynthetic membranes of *Arabidopsis thaliana*. *J. Biol. Chem.* **276**, 6959–6966.

## W

- Weber, N., Strotmann, H. (1993) On the function of subunit PsaE in chloroplast Photosystem I. *Biochim Biophys Acta.* **1143**, 204-10.
- Weigel, M., Varotto, C., Pesaresi, P., Finazzi, G., Rappaport, F., Salamini, F. and Leister, D. (2003) Plastocyanin is indispensable for photosynthetic electron flow in *Arabidopsis thaliana*. *J. Biol. Chem.* **278**, 31286–31289.
- Wu, C.C., MacCoss, M.J., Howell, K.E., Yates, J.R.III (2003) A method for the comprehensive proteomic analysis of membrane proteins. *Nat Biotechnol.* **21**, 532-538.

## X

- Xu, Q., Jung, Y.S., Chitnis, V.P., Guikema, J.A., Golbeck, J.H. and Chitnis, P.R. (1994) Mutational analysis of photosystem I polypeptides in *Synechocystis* sp. PCC6803. Subunit requirements for reduction of NADP<sup>+</sup> mediated by ferredoxin and flavodoxin. *J. Biol. Chem.* **269**, 21512–21518.

## Y

- Yakushevskaya, A. E., Jensen, P. E., Keegstra, W., Roon, H., Scheller, H. V., Boekema, E. J., Dekker, J. P. (2001) Supermolecular organization of photosystem II and its associated light-harvesting antenna in *Arabidopsis thaliana*. *Eup.Journ. Bioch.* **268**, 6020-2001.
- Yamamoto, Y., Tsuji, H. and Obokata, J. (1993) Structure and expression of a nuclear gene for the PSI-D subunit of photosystem I in *Nicotiana glauca*. *Plant Mol.Biol.* **22**, 985–994.
- Yu, J., Smart, L.B., Jung, Y.S., Golbeck, J. and McIntosh, L. (1995) Absence of PsaC subunit allows assembly of photosystem I core but prevents the binding of PsaD and PsaE in *Synechocystis* sp. PCC6803. *Plant Mol. Biol.* **29**, 331–342.

---

**Z**

- Zer, H., Vink, M., Keren, N., Dilly-Hartwig, H. G., Paulsen, H., Herrmann, R. G., Andersson, B., and Ohad, I. (1999) Regulation of thylakoid protein phosphorylation at the substrate level: reversible light-induced conformational changes expose the phosphorylation site of the light-harvesting complex II. *Proc. Natl. Acad. Sci. U. S. A.* **96**, 8277–8282.
- Zer, H., Ohad, I. (2003) Light, redox state, thylakoid-protein phosphorylation and signaling gene expression. *Trends Biochem Sci.* **28**, 467-70.
- Zer, H., Vink, M., Shochat, S., Herrmann, R. G., Andersson, B., and Ohad, I. (2003) Light affects the accessibility of the thylakoid light harvesting complex II (LHCII) phosphorylation site to the membrane protein kinase(s). *Biochemistry* **42**, 728–738.
- Zhang, H., Goodman, H.M., Jansson, S. (1997) Antisense inhibition of the photosystem I antenna protein Lhca4 in *Arabidopsis thaliana*. *Plant Physiol.* **115**, 1525-1531.
- Zhao, J., Snyder, W.B., Mühlhoff, U., Rhiel, E., Warren, P.V., Golbeck, J.H., Bryant, D.A. (1993) Cloning and characterization of the *psaE* gene of the cyanobacterium *Synechococcus* sp. PCC 7002: characterization of a *psaE* mutant and overproduction of the protein in *Escherichia coli*. *Mol. Microbiol.* **9**, 183–194.
- Zilber, A.L. and Malkin, R. (1988) Ferredoxin cross-links to a 22-kD subunit of photosystem I. *Plant Physiol.* **88**, 810–814.
- Zouni, H.T., Witt, J., Kern, P., Fromme, N., Krauss, W. Saenger, Orth, P. (2001) Crystal structure of photosystem II from *Synechococcus elongatus* at 3.8 angstrom resolution. *Nature* **409**, 739–743.

## **APPENDIX**

### **ERKLÄRUNG**

“Ich versichere, dass ich die von mir vorgelegte Dissertation selbständig angefertigt, die benutzten Quellen und Hilfsmittel vollständig angegeben und die Stellen der Arbeit – einschließlich Tabellen, Karten und Abbildungen –, die anderen Werken im Wortlaut oder dem Sinn nach entnommen sind, in jedem Einzelfall als Entlehnung kenntlich gemacht habe; dass diese Dissertation noch keiner anderen Fakultät oder Universität zur Prüfung vorgelegen hat; dass sie – abgesehen von unten angegebenen Teilpublikationen – noch nicht veröffentlicht worden ist sowie, dass ich eine solche Veröffentlichung vor Abschluss des Promotionsverfahrens nicht vornehmen werde.

Die Bestimmungen dieser Promotionsordnung sind mir bekannt. Die von mir vorgelegte Dissertation ist von Prof. Dr. Francesco Salamini betreut worden.”

Köln, den 16.05.2005

Anna Ihnatowicz

### **Teilpublikationen**

Ihnatowicz, A., Pesaresi, P., Varotto, C., Richly, E., Schneider, A., Jahns, P., Salamini, F., Leister, D. (2004) Mutants of photosystem I subunit D of *Arabidopsis thaliana*: effects on photosynthesis, photosystem I stability and expression of nuclear genes for chloroplast functions. *Plant J.* **37**, 839-852.



---

## **LEBENS LAUF**

### **Name**

Anna Ihnatowicz

### **Adresse**

Max-Planck-Institut für Züchtungsforschung  
Carl-von-Linné-Weg 10  
D-50829 Köln  
Tel: +49 (0) 221 5062 426  
Fax: +49 (0) 221 5062 413  
E-Mail: ihnat@mpiz-koeln.mpg.de

### **Geburtsdatum und -ort**

08.02.1977, Danzig (Gdańsk)  
Polen

### **Nationalität**

polnisch

### **Ausbildung**

1984-1992	Grundschule Nr. 45 in Danzig
1992-1996	Gymnasium Nr. III in Danzig
1996	Abitur
1996-2001	Biologiestudium an der Universität zu Danzig, Spezialisierung: Molekularbiologie, Thema der Diplomarbeit: "Analysis of intraspecies variability of <i>Melanelia fuliginosa</i> (Fr. ex Duby) Essl. on the DNA level".
26.06.2001	Diplomprüfung
01.03.2002	Beginn der Doktorarbeit am Max-Planck-Institut für Züchtungsforschung in Köln, Abteilung Prof. Dr. Francesco Salamini, Arbeitsgruppe Dr. Dario Leister.

### **Publikationen**

Ihnatowicz, A., Pesaresi, P., Varotto, C., Richly, E., Schneider, A., Jahns, P., Salamini, F., Leister, D. (2004) Mutants of photosystem I subunit D of *Arabidopsis thaliana*: effects on photosynthesis, photosystem I stability and expression of nuclear genes for chloroplast functions. *Plant J.* **37**, 839-852.

## **ACKNOWLEDGEMENTS**

First of all I would like to express my gratitude to Prof. Dr. F. Salamini for providing me the opportunity to work in his department at the Max-Planck-Institut für Züchtungsforschung and Prof. Dr. U.I. Flügge for providing the DFG fellowship for this Ph.D. and giving me the great possibility to be a member of the Graduate Training Program: “Molecular Analysis of Development Processes”.

I would like to thank and to express my appreciation to my group leader and supervisor PD Dr. Dario Leister for supporting me during my Ph.D. and for gathering such a great working group and successful projects.

Many, many thanks to my entire group: Alex, Angie, Barbara, Beatrice, Christos, Claudio, Daniela, Erik, Giovanni, Ivo, Joachim, Martin, Paolo, Ricardo, Ute and Vera. It was a real pleasure to work with you. I would like to mention Angie, Claudio, Martin and Paolo who were helping me a lot at the beginning of my Ph.D.

Big thanks to Angie, Alex and Erik for the DNA array analysis, as well as to Claudio and Erik for isolating some of the mutant lines used in this work. I also would like to thank Christos for the good cooperation concerning mass spectroscopic analysis. Special thanks go to Ute for the great help in correcting my English.

I would like to thank also external collaborators for their valuable help: Dr. Peter Jahns for HPLC analysis and Dr. Dirk Wolters for MS analysis.

Huge thanks goes to Łuki. Thank you for all the support you gave me during the last years.